A few issues in turbulence and how to cope with them using computers

Annick Pouquet, NCAR

Alex Alexakis[!], Julien Baerenzung[&], Marc-Etienne Brachet[!], Jonathan Pietarila-Graham[&&], Aimé Fournier, Darryl Holm[@], Giorgio Krstulovic[*], Ed Lee[#], Bill Matthaeus[%], Pablo Mininni^, Jean-François Pinton!!, Hélène Politano, Yannick Ponty*, Duane Rosenberg, Amrik Sen & Josh Stawarz*

! &!! ENS, Paris and Lyon
& MPI, Postdam
&& LANL
@ Imperial College & LANL
** Observatoire de Nice*
 # U. Leuwen
% Bartol, U. Delaware,
^ and Universidad de Buenos Aires

CU Boulder, July 2011 , pouquet@ucar.edu

Happy Bastille day

GENERAL OUTLINE for LECTURES

Physical complexity of flows on Earth and beyond
Vorticity and helicity dynamics
Kinematics of tensors and methodology
Exact laws, structures and different energy spectra in MHD?
Complexity of phenomenology: beyond Kolmogorov

****

Weak turbulence and beyond, towards strong turbulence with closures

****

II – Some results for MHD *and for rotation*

II - Modeling: why and how
II - The Lagrangian averaging model, for MHD and perhaps for fluids

II - Adaptive mesh refinement with spectral accuracy
II - Application to the dynamo problem at low magnetic Prandtl number

A Few Issues in Turbulence:

In search of a small parameter

A Few Issues in Turbulence:

In search of a small parameter

The theoretically solvable case of weak/wave turbulence

A Few Issues in Turbulence:

In search of a small parameter

The theoretically solvable case of weak/wave turbulence

But is it useful?

Conditions & methodology for weak/wave turbulence

- $\partial_t u = \mathcal{L}_x u + \epsilon\, \mathcal{N}_x(u,u)$

$$\epsilon = 0 \quad \Longrightarrow \quad \hat{u}(\mathbf{k},t) = \hat{u}_0(\mathbf{k}) e^{-i\omega_k t} \qquad \text{wave of frequency } \omega_k$$

- $\epsilon \ll 1 \rightarrow \exists$ two different time scales:

$$\hat{u}(\mathbf{k},t) = a(\mathbf{k},t) e^{-i\omega_k t}$$

$$\Longrightarrow \quad \begin{cases} \text{Fast variation in time of } e^{-i\omega_k t} \\ \\ \text{Slow variation of } a(\mathbf{k},t) \textit{ through wave coupling} \end{cases}$$

- $\exists$ resonances $\rightarrow$ "kinetic" equations

For 2^{nd} order moments

$\rightarrow$ rigorous closure of the statistical problem

Conditions & methodology for weak/wave turbulence

- $\partial_t u = \mathcal{L}_x u + \epsilon\, \mathcal{N}_x(u,u)$

$$\epsilon = 0 \quad \Longrightarrow \quad \hat{u}(\mathbf{k},t) = \hat{u}_0(\mathbf{k}) e^{-i\omega_k t}$$

wave of frequency ω_k

- $\epsilon \ll 1 \rightarrow \exists$ two different time scales:

$$\hat{u}(\mathbf{k},t) = a(\mathbf{k},t) e^{-i\omega_k t}$$

$$\Longrightarrow \begin{cases} \text{Fast variation in time of } e^{-i\omega_k t} \\ \\ \text{Slow variation of } a(\mathbf{k},t) \textit{ through wave coupling} \end{cases}$$

unless ω(k)=0,
e.g. for $k_{para}=0$ …

- $\exists$ resonances $\rightarrow$ "kinetic" equations

For 2nd order moments

$\rightarrow$ rigorous closure of the statistical problem

$$\frac{\partial u}{\partial t} = \mathcal{L}_x u + \varepsilon \mathcal{N}_x(u; u)$$

with $\varepsilon << 1$

Fourier: $A(k,t) = \int e^{ik.x} u(x,t) dx$
$\omega(k)$ frequency associated with the linear operator
$H(m,n)$ the Fourier representation of the non-linear operator :

Fourier formulation

$$[\partial_t + i\omega(k)] A(k,t) = \varepsilon \int_{-\infty}^{\infty} H(m,n) A(m,t) A(n,t) \delta(k-m-n) dm dn$$

$\delta_{kmn} = \delta(k-m-n)$ and $d_{mn} = dmdn$ and $H_{mn} = H(m,n)$, $\omega_k = \omega(k)$
$A(k,t) = a_k e^{i\omega(k)t}$

and interaction representation

$$\frac{\partial a_k}{\partial t} = \varepsilon \int H_{mn} a_m a_n e^{i(-\omega_k + \omega_m + \omega_n)t} \delta_{kmn} d_{mn}$$

Perform an ϵ–expansion

$$a_\ell = a_{0,\ell} + \varepsilon a_{1,\ell} + \varepsilon^2 a_{2,\ell} + \ldots$$

and solve order by order iteratively.

Note that $a_{0,\ell}$ is constant.

$$a_{1,\ell} = \int H_{mn} a_{0,m} a_{0,n} \Delta(\omega_{\ell,mn}) \delta(\omega_{\ell,mn}) d_{mn} \quad .$$

with

$$\omega_{\ell,mn} = \omega(\ell) - \omega(m) - \omega(n)$$

$$\Delta(\omega_{\ell,mn}) = \int_0^t \exp\left[it\omega_{\ell,mn}\right] dt = \frac{\exp\left[i\omega_{\ell,mn}\right] - 1}{i\omega_{\ell,mn}}$$

Resonance occurs for $\omega_{\ell,mn} = 0$.

Expand in small parameter, solve at lowest order and iterate

The closure at second order

As is standard in similar computations for ODE's (see for example, Bender & Orszag, 1978, Chapter II) the terms $\delta q_0^{(N)}/\delta T_2$ are chosen to remove secularities. The last step is to realize that since

$$\varepsilon = \tau_\omega/\tau_{NL} << 1$$

and since we wish to average over many wave periods, we have to evaluate integrals of the form

$$lim_{t\to\infty} \int f(k)\Delta(k,t)dk$$

where

$$\Delta(k) = \int_0^t e^{i\omega(k)t}dt$$

contains the time–dependence, and ω(k) (*i.e.* the dispersion relation) is the link with the (linearized) physical problem. We now use the Lemma:

$$lim_{t\to\infty} \int f(k)\Delta(k,t)dk = \pi f(0) + iP_C \int \frac{f(k)}{k}dk$$

where P_C stands for the Cauchy Principal Value integral. In other words, what we are really doing here is to replace

$$lim_{t\to\infty} \int \frac{sin\omega t}{\omega}$$

by $\pi\delta(\omega)$.

This allows you to perform the closure

Fundamental steps in the development

- A closure problem and the problem of cumulants :

$$\partial_t < a_j a_{j'} > = < a_j a_{j'} a_{j''} >$$

$$\partial_t < a_j a_{j'} a_{j''} > = < a_j a_{j'} a_{j''} a_{j'''} >$$

$$\equiv \sum < a_j a_{j'} > < a_{j''} a_{j'''} > + < a_j a_{j'} a_{j''} a_{j'''} >_C$$

cumulant

r small ϵ, one finds that there is no **contribution** at lowest order of the 4th order cumulants

$\rightarrow$ resulting equations "like" the random phase approximation

- It is different from Eddy Damped Quasi Normal Markovian (EDQNM) models where

$$< a_j a_{j'} a_{j''} a_{j'''} >_C = -\mu_m < a_j a_{j'} a_{j''} >$$

with μ_m a characteristic rate

Closure:

No contribution at lowest order of 4^{th} order cumulants

Traditional Closure schemes

$$< a_j a_{j'} a_{j''} a_{j'''} >_C = -\mu_m < a_j a_{j'} a_{j''} >$$

$\mu_m = 0$ (Quasi Normal approximation, Ogura; Millioshikov, mid 40's; Chandrasekhar, mid 50's) leads to negative energy spectra (lack of realisability)

$\mu_m = \mu_0, \neq 0 \ \forall k \quad \rightarrow$ energy spectrum $E(k) \sim k^{-2}$ (MRCM) *(and shocks ...)*

$\mu_m = \omega_{int}(k) \quad \rightarrow$ energy spectrum $E(k) \sim k^{-5/3}$

$\mu_m = \omega_{int}(k) + \omega_A(k) \rightarrow$ energy spectrum $E(k) \sim k^{-3/2}$

Eddy Damped Quasi Normal Markovian Model Or EDQNM

anisotropic DIA (Nakayama, 1999): $E(k) \sim k_\perp^{-3/2}$

- Compute μ_m from an auxiliary problem: Test Field Model (Kraichnan)
- Weak turbulence does it naturally

Traditional Closure schemes

$$< a_j a_{j'} a_{j''} a_{j'''} >_C = -\mu_m < a_j a_{j'} a_{j''} >$$

$\mu_m = 0$ (Quasi Normal approximation, Ogura; Millioshikov, mid 40's; Chandrasekhar, mid 50's) leads to negative energy spectra (lack of realisability)

$\mu_m = k^i \mu_0, \neq 0 \; \forall t$ $\rightarrow$ energy spectrum $E(k) \sim k^{-2}$ for i=1
(MRCM) *(and shocks ...)*

$\mu_m = \omega_{int}(k)$ $\rightarrow$ energy spectrum $E(k) \sim k^{-5/3}$

$\mu_m = \omega_{int}(k) + \omega_A(k)$ $\rightarrow$ energy spectrum $E(k) \sim k^{-3/2}$

anisotropic DIA (Nakayama, 1999): $E(k) \sim k_\perp^{-3/2}$

Eddy
Damped
Quasi
Normal
Markovian
Model
Or
EDQNM

- Compute μ_m from an auxiliary problem: Test Field Model (Kraichnan)
- Weak turbulence does it naturally

Closure ad hoc hypothesis *vs*. weak turbulence theory, & how they meet:

$$\partial_t < a_j a_{j'} a_{j''} > = < a_j a_{j'} a_{j''} a_{j'''} > \qquad or \qquad \partial_t T_3 = Q_4 = \sum E_2^2 + Q_{4,C}$$

$$\equiv \sum < a_j a_{j'} >< a_{j''} a_{j'''} > + < a_j a_{j'} a_{j''} a_{j'''} >_C$$

Now, the EDQNM stipulates that the relaxation of triple correlation involves the characteristic times of the problem:

$$Q_{4,C} = -\mu_m T_3$$

with

$$\mu_m = \tau_{NL}^{-1} + \tau_{wave}^{-1}$$

And now take the limit of $\tau_{wave} \rightarrow 0$

Henceforth, the fourth order cumulant in the limit of fast waves in the EDQNM goes to zero as well

$$\boxed{Q_{4,C} \rightarrow 0}$$

Thus, one may say that the EDQNM closure and the theory of weak turbulence are compatible in that limit.

Resulting equations of the simplified dynamics, in the weak turbulence regime, for MHD for all second-order moments, including helicity

Note: equations are anisotropic, with expressions in terms of k_{perp} and $k_{//}$

$$
\begin{aligned}
\partial_t e^s(\mathbf{k}) = \frac{\pi\varepsilon^2}{b_0}\int \Bigg[& \left(L_\perp^2 - \frac{X^2}{k^2}\right)\Psi^s(\mathbf{L}) - \left(k_\perp^2 - \frac{X^2}{L^2}\right)\Psi^s(\mathbf{k}) \\
& + \left(L_\perp^2 L^2 - \frac{k_\parallel^2 W^2}{k^2}\right)\Phi^s(\mathbf{L}) - \left(k_\perp^2 k^2 - \frac{k_\parallel^2 Y^2}{L^2}\right)\Phi^s(\mathbf{k}) \\
& + \frac{k_\parallel XY}{L^2} I^s(\mathbf{k}) - \frac{k_\parallel XW}{k^2} I^s(\mathbf{L}) \Bigg] Q_k^{-s}(\boldsymbol{\kappa})\delta(\kappa_\parallel)\delta_{\mathbf{k},\boldsymbol{\kappa}\mathbf{L}}\, d_{\boldsymbol{\kappa}\mathbf{L}},
\end{aligned} \tag{26}
$$

$$
\begin{aligned}
\partial_t[k_\perp^2 k^2 \Phi^s(\mathbf{k})] = \frac{\pi\varepsilon^2}{b_0}\int \Bigg\{ & k_\parallel^2 X^2 \left[\frac{\Psi^s(\mathbf{L})}{k_\perp^2 k^2} - \frac{\Phi^s(\mathbf{k})}{L_\perp^2}\right] \\
& + (k_\parallel^2 Z + k_\perp^2 L_\perp^2)^2 \left[\frac{\Phi^s(\mathbf{L})}{k_\perp^2 k^2} - \frac{\Phi^s(\mathbf{k})}{L_\perp^2 L^2}\right] + \frac{k_\parallel X}{k_\perp^2 k^2}(k_\parallel^2 Z + k_\perp^2 L_\perp^2) I^s(\mathbf{L}) \\
& + \frac{k_\parallel XY}{2L^2} I^s(\mathbf{k}) \Bigg\} Q_k^{-s}(\boldsymbol{\kappa})\delta(\kappa_\parallel)\delta_{\mathbf{k},\boldsymbol{\kappa}\mathbf{L}} d_{\boldsymbol{\kappa}\mathbf{L}} \\
& - \frac{\varepsilon^2}{b_0} s R^s(\mathbf{k}) \mathscr{P}\int \frac{X}{2\kappa_\parallel L^2}(k_\parallel Z - L_\parallel k_\perp^2) Q_k^{-s}(\boldsymbol{\kappa})\delta_{\mathbf{k},\boldsymbol{\kappa}\mathbf{L}} d_{\boldsymbol{\kappa}\mathbf{L}},
\end{aligned} \tag{27}
$$

$$
\begin{aligned}
\partial_t\left[k_\perp^2 R^s(\mathbf{k})\right] = -\frac{\pi\varepsilon}{b_0}\int \Bigg\{ & L_\perp^2 \frac{Z + k_\parallel^2}{k^2} R^s(\mathbf{L}) \\
& + \frac{k_\perp^2}{2}\left[1 + \frac{(Z + k_\parallel^2)^2}{k^2 L^2}\right] R^s(\mathbf{k}) \Bigg\} Q_k^{-s}(\boldsymbol{\kappa})\delta(\kappa_\parallel)\delta_{\mathbf{k},\boldsymbol{\kappa}\mathbf{L}} d_{\boldsymbol{\kappa}\mathbf{L}} \\
& + \frac{\varepsilon^2}{b_0} s\mathscr{P}\int \Bigg\{ 2X(k_\parallel Z - L_\parallel k_\perp^2)[\Psi^s(\mathbf{k}) + k^2\Phi^s(\mathbf{k})] \\
& + \left[(k_\parallel Z - L_\parallel k_\perp^2)^2 - k^2 X^2\right] I^s(\mathbf{k}) \Bigg\} \frac{Q_k^{-s}(\boldsymbol{\kappa})}{2\kappa_\parallel k^2 L^2}\delta_{\mathbf{k},\boldsymbol{\kappa}\mathbf{L}} d_{\boldsymbol{\kappa}\mathbf{L}},
\end{aligned} \tag{28}
$$

$$
\begin{aligned}
\partial_t[k_\perp^2 k^2 I^s(\mathbf{k})] = \frac{\pi\varepsilon^2}{b_0}\int\Bigg\{&\left[L_\perp^2 Z + \frac{k_\parallel^2}{k_\perp^2}(Z^2 - X^2)\right] I^s(\mathbf{L}) \\
&+\left(\frac{k_\parallel^2 Y^2}{2L^2} - k_\perp^2 k^2 + \frac{k^2 X^2}{2L^2}\right) I^s(\mathbf{k}) + \frac{k_\parallel XY}{L^2}[\Psi^s(\mathbf{k}) + k^2\Phi^s(\mathbf{k})] \\
&+\frac{2k_\parallel X}{k_\perp^2}[Z\Psi^s(\mathbf{L}) - (k_\parallel^2 Z + k_\perp^2 L_\perp^2)\Phi^s(\mathbf{L})]\Bigg\} Q_k^{-s}(\boldsymbol{\kappa})\delta(\kappa_\parallel)\delta_{\mathbf{k},\kappa\mathbf{L}} d_{\kappa\mathbf{L}} \\
&-\frac{\varepsilon^2}{b_0} s R^s(\mathbf{k}) \mathscr{P}\int \frac{1}{2\kappa_\parallel L^2}\left[(k_\parallel Z - L_\parallel k_\perp^2)^2 - k^2X^2\right] Q_k^{-s}(\boldsymbol{\kappa})\delta_{\mathbf{k},\kappa\mathbf{L}} d_{\kappa\mathbf{L}}
\end{aligned}
\quad (2
$$

with

$$
\delta_{\mathbf{k},\kappa\mathbf{L}} = \delta(\mathbf{L} + \boldsymbol{\kappa} - \mathbf{k}),
$$

$$
d_{\kappa\mathbf{L}} = d\boldsymbol{\kappa}\, d\mathbf{L},
$$

and

$$
\begin{aligned}
Q_k^{-s}(\boldsymbol{\kappa}) &= k_m k_p\, q_{p\ m}^{-s-s}(\boldsymbol{\kappa}) \\
&= X^2\Psi^{-s}(\boldsymbol{\kappa}) + X(k_\parallel \kappa_\perp^2 - \kappa_\parallel Y) I^{-s}(\boldsymbol{\kappa}) + (\kappa_\parallel Y - k_\parallel \kappa_\perp^2)^2 \phi^{-s}(\boldsymbol{\kappa}).
\end{aligned} \quad (30)
$$

Note that Q_k^{-s} does not involve the spectral densities $R^s(\mathbf{k})$, because of the symmetry properties of the equations. The geometrical coefficients appearing in the kinetic equations are

$$
X = (\mathbf{k}_\perp \times \boldsymbol{\kappa}_\perp)_z = k_\perp \kappa_\perp \sin\theta, \quad (31a)
$$

$$
Y = \mathbf{k}_\perp \cdot \boldsymbol{\kappa}_\perp = k_\perp \kappa_\perp \cos\theta, \quad (31b)
$$

$$
\begin{aligned}
Z = \mathbf{k}_\perp \cdot \mathbf{L}_\perp &= k_\perp^2 - k_\perp \kappa_\perp \cos\theta \\
&= k_\perp^2 - Y,
\end{aligned} \quad (31c)
$$

$$
\begin{aligned}
W = \boldsymbol{\kappa}_\perp \cdot \mathbf{L}_\perp &= k_\perp^2 - L_\perp^2 - k_\perp \kappa_\perp \cos\theta \\
&= Z - L_\perp^2,
\end{aligned} \quad (31d)
$$

where θ is the angle between $\mathbf{k}_\perp$ and $\boldsymbol{\kappa}_\perp$, and with

$$
d\boldsymbol{\kappa}_\perp = \kappa_\perp d\kappa_\perp d\theta = \frac{L_\perp}{k_\perp \sin\theta}\, d\kappa_\perp dL_\perp, \quad (32)
$$

$$
\cos\theta = \frac{\kappa_\perp^2 + k_\perp^2 - L_\perp^2}{2\kappa_\perp k_\perp}. \quad (33)
$$

In (27)–(29), $\mathscr{P}\int$ means the Cauchy principal value of the integral in question.

(**simplified** MHD, page 2)

Galtier et al., J. Plasma Phys. 2000

$$
\begin{aligned}
\partial_t[k_\perp^2 k^2 I^s(\mathbf{k})] = \frac{\pi\varepsilon^2}{b_0}\int\Bigg\{&\left[L_\perp^2 Z + \frac{k_\parallel^2}{k_\perp^2}(Z^2 - X^2)\right] I^s(\mathbf{L}) \\
&+\left(\frac{k_\parallel^2 Y^2}{2L^2} - k_\perp^2 k^2 + \frac{k^2 X^2}{2L^2}\right) I^s(\mathbf{k}) + \frac{k_\parallel XY}{L^2}[\Psi^s(\mathbf{k}) + k^2\Phi^s(\mathbf{k})] \\
&+\frac{2k_\parallel X}{k_\perp^2}[Z\Psi^s(\mathbf{L}) - (k_\parallel^2 Z + k_\perp^2 L_\perp^2)\Phi^s(\mathbf{L})]\Bigg\} Q_k^{-s}(\boldsymbol{\kappa})\delta(\kappa_\parallel)\delta_{\mathbf{k},\kappa\mathbf{L}}\, d_{\kappa\mathbf{L}} \\
&-\frac{\varepsilon^2}{b_0} s R^s(\mathbf{k}) \mathscr{P}\int \frac{1}{2\kappa_\parallel L^2}\left[(k_\parallel Z - L_\parallel k_\perp^2)^2 - k^2 X^2\right] Q_k^{-s}(\boldsymbol{\kappa})\delta_{\mathbf{k},\kappa\mathbf{L}}\, d_{\kappa\mathbf{L}}
\end{aligned}
\quad (2
$$

with

$$
\delta_{\mathbf{k},\kappa\mathbf{L}} = \delta(\mathbf{L} + \boldsymbol{\kappa} - \mathbf{k}),
$$

$$
d_{\kappa\mathbf{L}} = d\boldsymbol{\kappa}\, d\mathbf{L},
$$

and

$$
\begin{aligned}
Q_k^{-s}(\boldsymbol{\kappa}) &= k_m k_p\, q_{p\,m}^{-s-s}(\boldsymbol{\kappa}) \\
&= X^2\Psi^{-s}(\boldsymbol{\kappa}) + X(k_\parallel\kappa_\perp^2 - \kappa_\parallel Y)I^{-s}(\boldsymbol{\kappa}) + (\kappa_\parallel Y - k_\parallel\kappa_\perp^2)^2\phi^{-s}(\boldsymbol{\kappa}).
\end{aligned}
\quad (30)
$$

Note that Q_k^{-s} does not involve the spectral densities $R^s(\mathbf{k})$, because of the symmetry properties of the equations. The geometrical coefficients appearing in the kinetic equations are

$$
X = (\mathbf{k}_\perp \times \boldsymbol{\kappa}_\perp)_z = k_\perp\kappa_\perp \sin\theta, \quad (31a)
$$

$$
Y = \mathbf{k}_\perp \cdot \boldsymbol{\kappa}_\perp = k_\perp\kappa_\perp \cos\theta, \quad (31b)
$$

$$
\begin{aligned}
Z = \mathbf{k}_\perp \cdot \mathbf{L}_\perp &= k_\perp^2 - k_\perp\kappa_\perp \cos\theta \\
&= k_\perp^2 - Y,
\end{aligned}
\quad (31c)
$$

$$
\begin{aligned}
W = \boldsymbol{\kappa}_\perp \cdot \mathbf{L}_\perp &= k_\perp^2 - L_\perp^2 - k_\perp\kappa_\perp\cos\theta \\
&= Z - L_\perp^2,
\end{aligned}
\quad (31d)
$$

where θ is the angle between $\mathbf{k}_\perp$ and $\boldsymbol{\kappa}_\perp$, and with

$$
d\boldsymbol{\kappa}_\perp = \kappa_\perp d\kappa_\perp d\theta = \frac{L_\perp}{k_\perp \sin\theta}\, d\kappa_\perp dL_\perp, \quad (32)
$$

$$
\cos\theta = \frac{\kappa_\perp^2 + k_\perp^2 - L_\perp^2}{2\kappa_\perp k_\perp}. \quad (33)
$$

In (27)–(29), $\mathscr{P}\int$ means the Cauchy principal value of the integral in question.

(**simplified** MHD, page 2)

Question:

Why can one call this set of equations a ``**simplified**'' dynamics for MHD?

Galtier et al., J. Plasma Phys. 2000

Further simplification: 2D MHD limit

s=±1, $E_{\pm} = v^2 + b^2 \pm 2\mathbf{v}.\mathbf{b}$

Resulting equation for energy spectrum $E^s(\mathbf{k}) = (k_\perp^2/k_z^2) q^s(\mathbf{k})$, with $\mathcal{D}_{k\kappa L} = \delta(\kappa_\parallel)\, \delta_{\mathbf{k},\boldsymbol{\kappa}\mathbf{L}}\, d\boldsymbol{\kappa} d\mathbf{L}$

$$\partial_t E^s(\mathbf{k}) = \frac{\pi\epsilon^2}{b_0} \int \frac{(\mathbf{k}_\perp \cdot \mathbf{L}_\perp)^2 (\mathbf{k} \times \boldsymbol{\kappa})_\parallel^2}{k_\perp^2 L_\perp^2 \kappa_\perp^2} E^{-s}(\boldsymbol{\kappa}) [E^s(\mathbf{L}) - E^s(\mathbf{k})]\, \mathcal{D}_{k\kappa L}$$

Simplified version (2D MHD)

s=±1, $E_\pm = v^2+b^2 \pm 2\mathbf{v}.\mathbf{b}$

Resulting equation for energy spectrum $E^s(\mathbf{k}) = (k_\perp^2/k_2^2)q^s(\mathbf{k})$, with $\mathcal{D}_{k\kappa L} = \delta(\kappa_{||})\,\delta_{\mathbf{k},\boldsymbol{\kappa}\mathbf{L}}\,d\boldsymbol{\kappa}d\mathbf{L}$

$$\partial_t E^s(\mathbf{k}) = \frac{\pi\epsilon^2}{b_0}\int \boxed{\frac{(\mathbf{k}_\perp\cdot\mathbf{L}_\perp)^2\,(\mathbf{k}\times\boldsymbol{\kappa})_{||}^2}{k_\perp^2\,L_\perp^2\,\kappa_\perp^2}}\,E^{-s}(\boldsymbol{\kappa})\,[E^s(\mathbf{L}) - E^s(\mathbf{k})]\,\mathcal{D}_{k\kappa L}$$

Geometrical & physical coefficient,
with
k=ϰ+L

Simplified version (2D MHD)

$s = \pm 1$, $E_{\pm} = v^2 + b^2 \pm 2\mathbf{v}.\mathbf{b}$

Resulting equation for energy spectrum $E^s(\mathbf{k}) = (k_\perp^2 / k_z^2) q^s(\mathbf{k})$, with $\mathcal{D}_{k\kappa L} = \delta(\kappa_{\|})\, \delta_{\mathbf{k},\boldsymbol{\kappa}\mathbf{L}}\, d\boldsymbol{\kappa} d\mathbf{L}$

$$\partial_t E^s(\mathbf{k}) = \frac{\pi \epsilon^2}{b_0} \int \frac{(\mathbf{k}_\perp \cdot \mathbf{L}_\perp)^2 (\mathbf{k} \times \boldsymbol{\kappa})_{\|}^2}{k_\perp^2 L_\perp^2 \kappa_\perp^2} E^{-s}(\boldsymbol{\kappa}) [E^s(\mathbf{L}) - E^s(\mathbf{k})]\, \mathcal{D}_{k\kappa L}$$

Geometrical & physical coefficient, with **k=ϰ+L**

Emission term *(eddy noise source)*

Simplified version (2D MHD)

$s = \pm 1$, $E_{\pm} = v^2 + b^2 \pm 2\mathbf{v}.\mathbf{b}$

Resulting equation for energy spectrum $E^s(\mathbf{k}) = (k_\perp^2/k_2^2)q^s(\mathbf{k})$, with $\mathcal{D}_{k\kappa L} = \delta(\kappa_{||})\,\delta_{\mathbf{k},\boldsymbol{\kappa}\mathbf{L}}\,d\boldsymbol{\kappa}d\mathbf{L}$

$$\partial_t E^s(\mathbf{k}) = \frac{\pi\epsilon^2}{b_0}\int \frac{(\mathbf{k}_\perp\cdot\mathbf{L}_\perp)^2\,(\mathbf{k}\times\boldsymbol{\kappa})_{\|}^2}{k_\perp^2\,L_\perp^2\,\kappa_\perp^2}\,E^{-s}(\boldsymbol{\kappa})\,[E^s(\mathbf{L}) - E^s(\mathbf{k})]\,\mathcal{D}_{k\kappa L}$$

Geometrical & physical coefficient,
with
k=ϰ+L

``Emission''

(eddy noise)

"Absorption"

(eddy viscosity)

Simplified version (2D MHD)

s=±1, $E_{\pm} = v^2+b^2 \pm 2\mathbf{v.b}$

Convolution Integral

Resulting equation for energy spectrum $E^s(\mathbf{k}) = (k_\perp^2/k_2^2)q^s(\mathbf{k})$, with $\mathcal{D}_{k\kappa L} = \delta(\kappa_{\|})\, \delta_{\mathbf{k},\boldsymbol{\kappa}\mathbf{L}}\, d\boldsymbol{\kappa} d\mathbf{L}$

$$\partial_t E^s(\mathbf{k}) = \frac{\pi\epsilon^2}{b_0} \int \frac{(\mathbf{k}_\perp \cdot \mathbf{L}_\perp)^2 (\mathbf{k} \times \boldsymbol{\kappa})_{\|}^2}{k_\perp^2 L_\perp^2 \kappa_\perp^2} E^{-s}(\boldsymbol{\kappa}) [E^s(\mathbf{L}) - E^s(\mathbf{k})]\, \mathcal{D}_{k\kappa L}$$

Geometrical & physical coefficient,
with
k=ϰ+L

Emission

(eddy noise)

Absorption

(eddy viscosity)

Galtier et al., Astrophys. J. 2002

Evidence of weak MHD turbulence

with a k_{perp}^{-2} spectrum

- In Reduced MHD computations *(Dmitruk et al., PoP **10**, 2003)*
- In the Jovian magnetosphere *(Saur et al., Astron. Astrophys. **386**, 2002)*

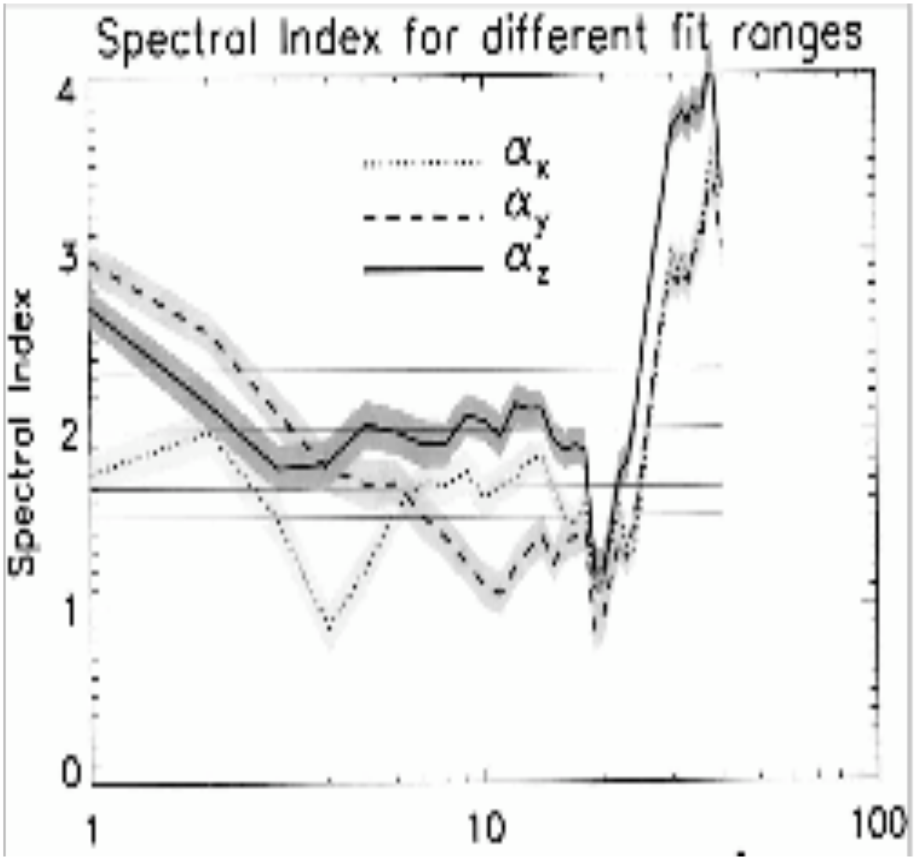

Compensated spectrum

Isotropic phenomenology of turbulence with waves

- Assumption: î $= \tau_W / \tau_{NL} << 1$; transfer time T_{tr} evaluated as

$$\boxed{T_{tr} = T_{NL} / \text{î} = T_{NL} * (T_{NL}/T_W)}$$

with $T_{NL}=l/u_l$ *and* $T_W = 1/\Omega$

- Constant energy flux: $\varepsilon = DE/Dt \sim k*E(k) / T_{tr}$

$$\longrightarrow \quad E(k) \sim [\varepsilon\Omega]^{1/2} k^{-2}$$

(Dubrulle &Valdetarro, 1992; Zhou, 1995)

Structure functions: $<\delta u(l)^p> \sim l^{\zeta p}$, $\boxed{\zeta_p = p/2}$

Isotropic phenomenology of turbulence with waves

- Assumption: î $= \tau_W / \tau_{NL} << 1$; transfer time T_{tr} evaluated as

$T_{tr} = T_{NL}$ / î $= T_{NL} * (T_{NL}/T_W)$ with $T_{NL} = l/u_l$ and $T_W = 1/\Omega$

- Constant energy flux: $\varepsilon = DE/Dt \sim k * E(k) / T_{tr}$

$\longrightarrow$ $E(k) \sim [\varepsilon\Omega]^{1/2} k^{-2}$ *(Dubrulle & Valdetarro, 1992; Zhou, 1995)*

Structure functions: $<\delta u(l)^p> \sim l^{\zeta p}$, $\boxed{\zeta_p = p/2}$

Exercise: MHD: $T_W = l/B_0$, $E(k) \sim [\varepsilon B_0]^{1/2} k^{-3/2}$, $\zeta_p = p/4$

Isotropic phenomenology of turbulence with waves

- Assumption: î $= \tau_W / \tau_{NL} << 1$; transfer time T_{tr} evaluated as

$$\boxed{T_{tr} = T_{NL} / \text{î} = T_{NL}{}^{*} (T_{NL}/T_W)} \qquad \textit{with } T_{NL} = l/u_l \textit{ and } T_W = 1/\Omega$$

- Constant energy flux: $\varepsilon = DE/Dt \sim k^{*}E(k) / T_{tr}$

$$\longrightarrow \quad E(k) \sim [\varepsilon\Omega]^{1/2} k^{-2}$$

(Dubrulle & Valdetarro, 1992; Zhou, 1995)

Structure functions: $<\delta u(l)^p> \sim l^{\zeta p}$, $\boxed{\zeta_p = p/2}$

Exercise: MHD: $T_W = l/B_0$, $E(k) \sim [\varepsilon B_0]^{1/2} k^{-3/2}$, $\zeta_p = p/4$

Anisotropic case: $T_W = l_{para}/B_0$, $E(k_{perp}, k_{para}) \sim [\varepsilon B_0]^{1/2} k_{perp}{}^{-2} k_{para}{}^{-1/2}$

The scaling of
the energy
spectrum at
high enough
rotation rate

can differ from
the classical
Kolmogorov
spectrum,

i.e. $E(k) \neq k^{-5/3}$

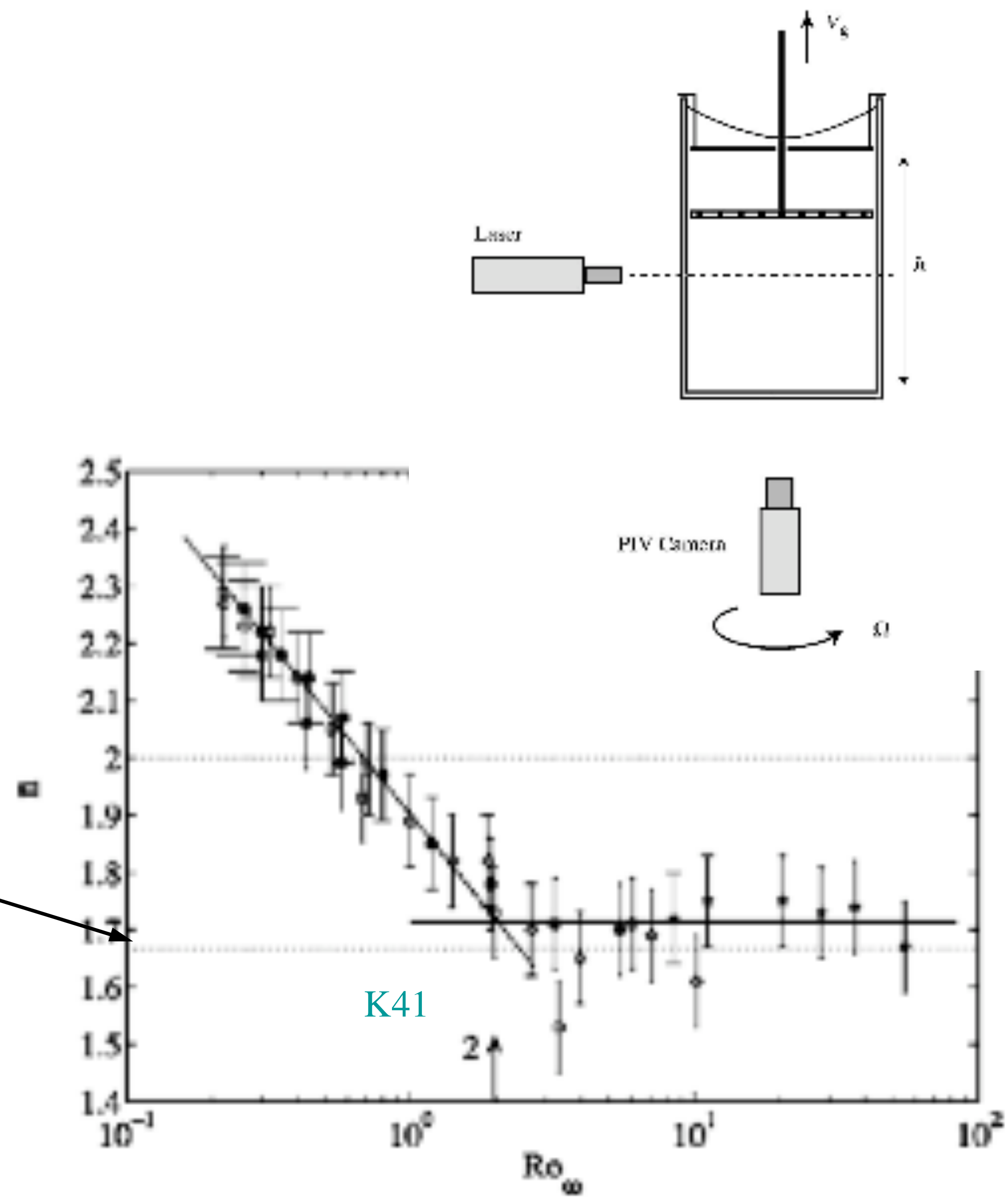

(Morize et al., 2005)

But it does not stop at k^{-2} …

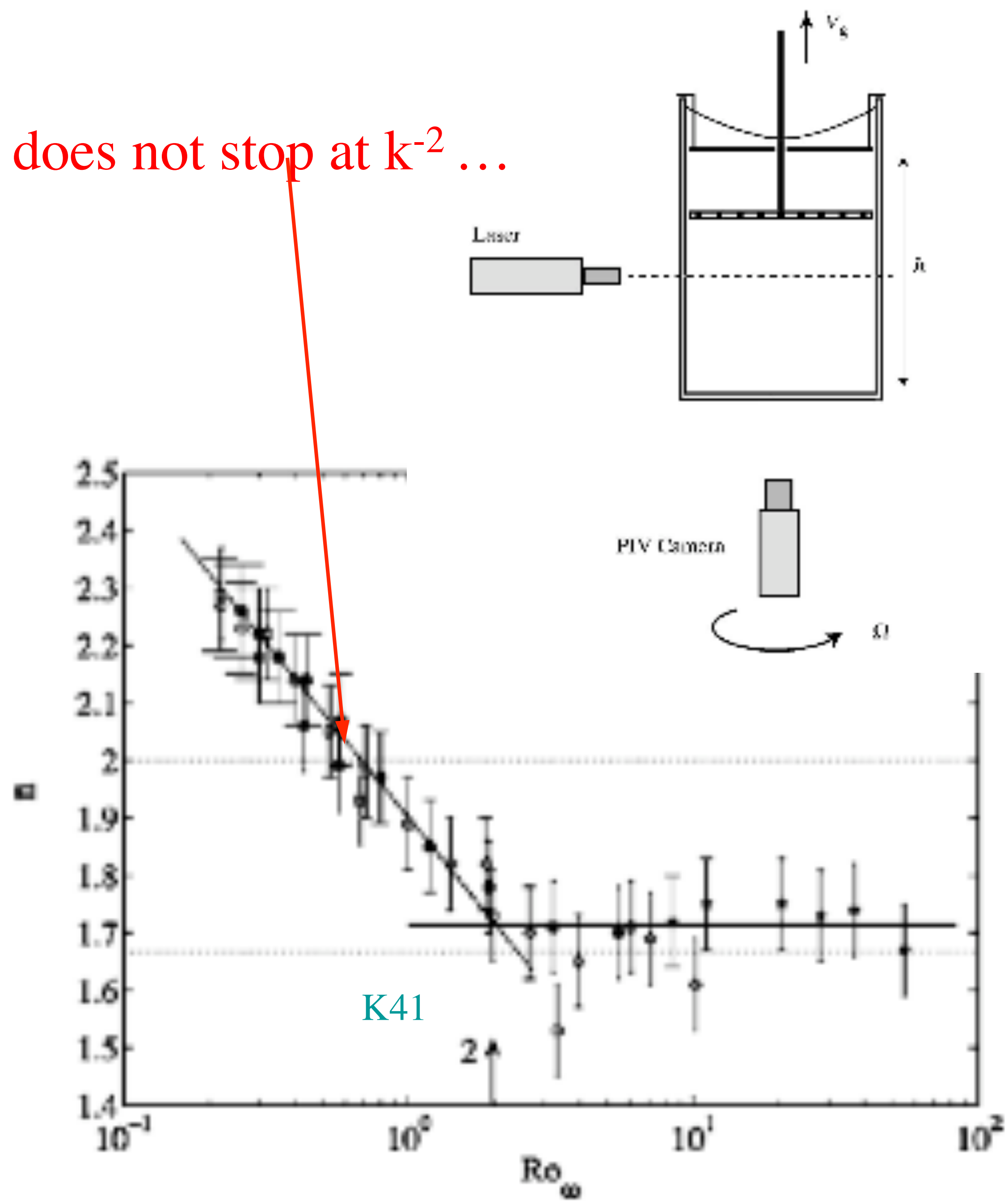

The scaling of the energy spectrum at high enough rotation rate

can differ from the classical Kolmogorov spectrum,

i.e. $E(k) \neq k^{-5/3}$

(Morize et al., 2005)

But it does not stop at k^{-2} …

Is it stopping at ~ 2.3?

The scaling of the energy spectrum at high enough rotation rate

can differ from the classical Kolmogorov spectrum,

i.e. $E(k) \neq k^{-5/3}$

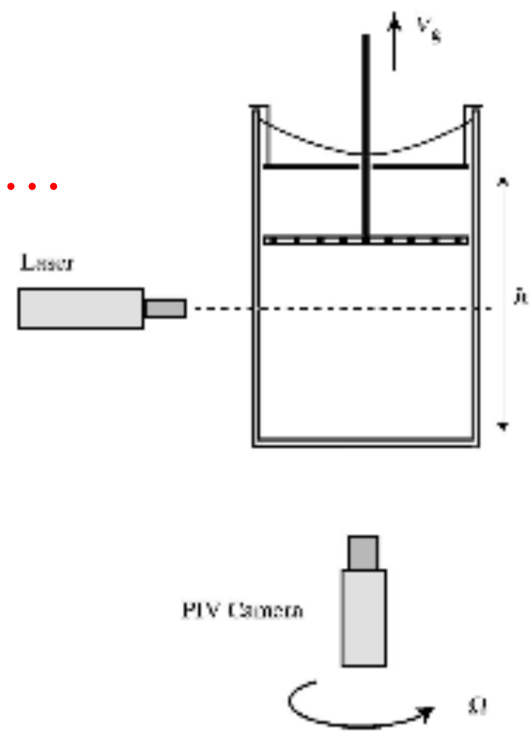

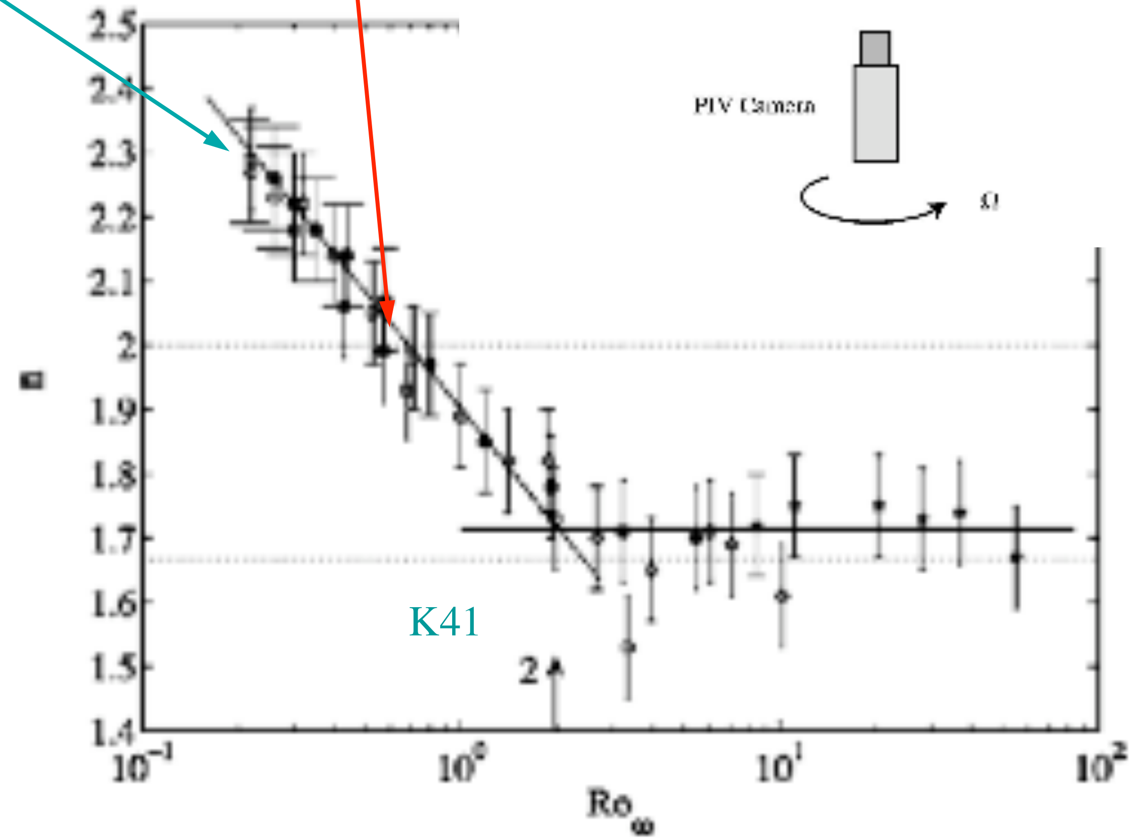

(Morize et al., 2005)

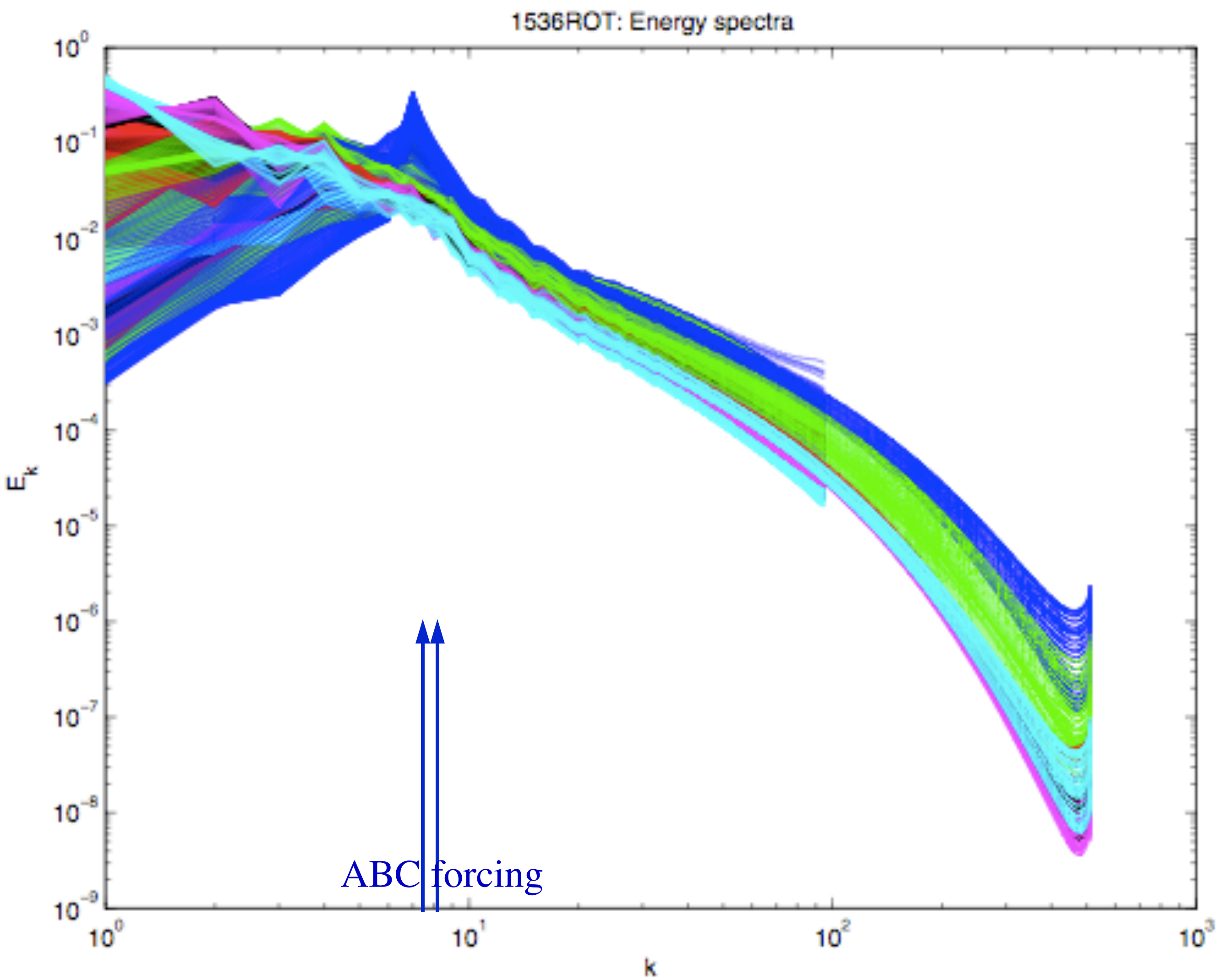

Initial conditions: fully developed non rotating Kolmogorov flow, 1536^3 grid

T=0 to T=30 *, going through dark blue, green, mauve, red, pink, pale blue* *+ LES*

GHOST

- **G**eophysical **H**igh **O**rder **S**uite for **T**urbulence *(Gomez & Mininni)*

- *Community code*
- Pseudo spectral, incompressible Navier-Stokes (including rotation and passive scalar), and magnetic fields (MHD, with or w/o Hall term); it also includes some LES (the alpha model; a helical spectral model)

- The code parallelizes linearly up to 2,000 processors using MPI, and now up to 40,000 processors using hybrid Open-MP / MPI *(Mininni et al. 2011, see arxiv:1003.432)*

- Community Data *(2048^3 forced Navier-Stokes turbulence with and without helicity; 1536^3 and 3072^3 helically forced rotating turbulence; 1536^3 decaying turbulence with a magnetic field, 2048^3 MHD with symmetries) [3D visualization with VAPOR freeware]*

Top view

& side view of

(left) relative helicity

(positive or negative)

&

(right) vorticity

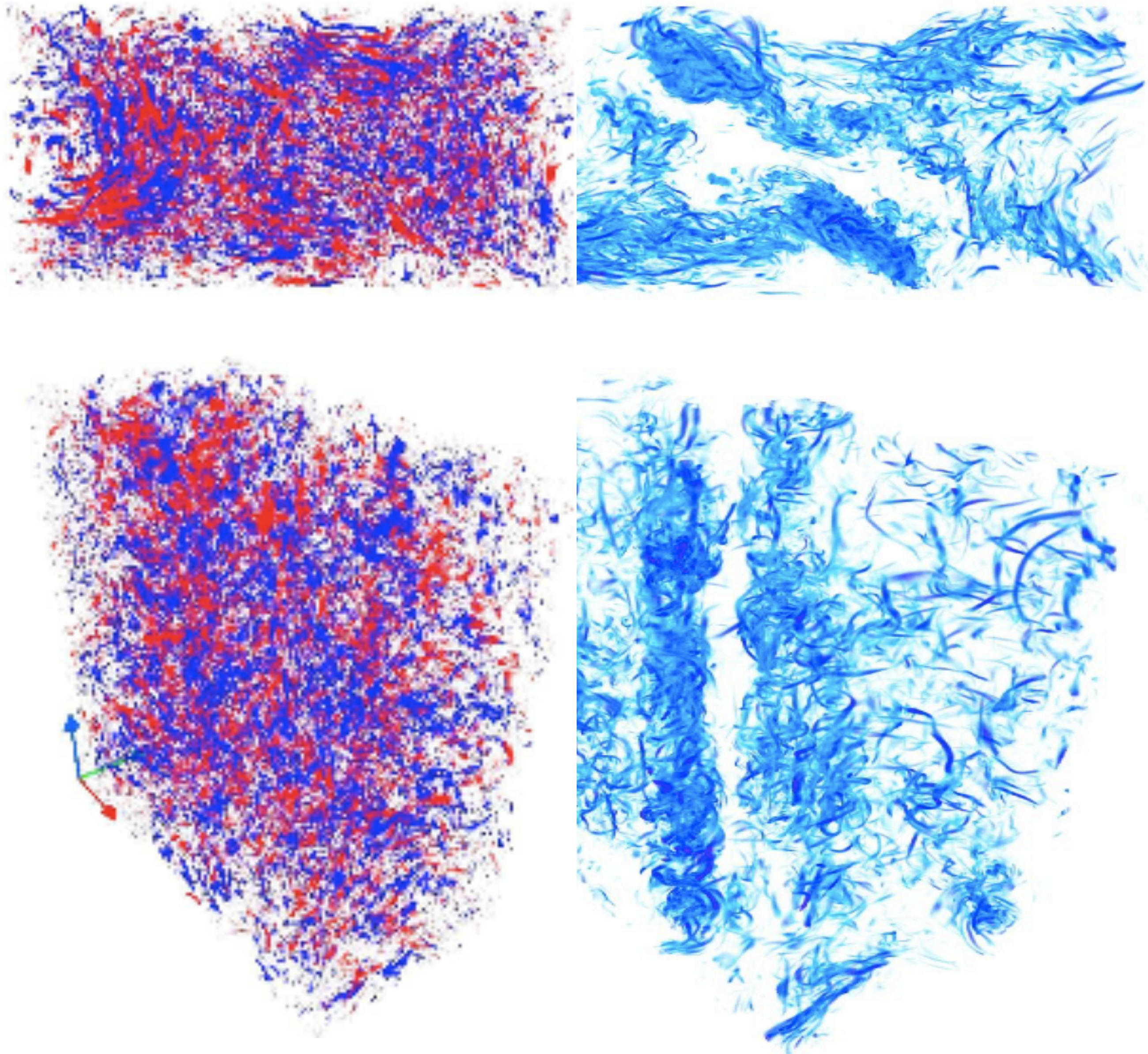

Taylor-Green non-helical forcing, $k_0=4$, 512^3, $Ro=0.35$

Scaling of structure functions in rotating turbulence

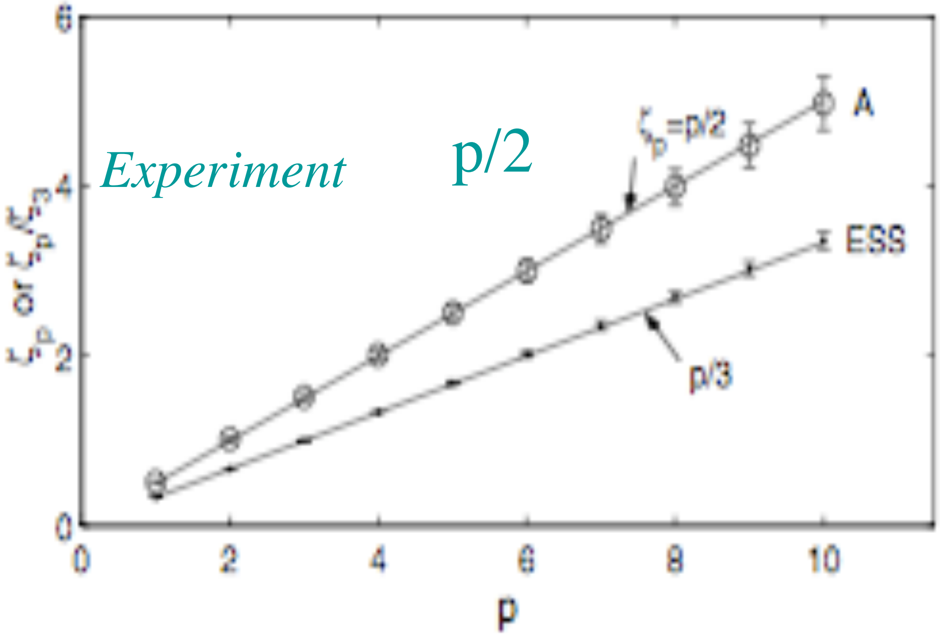

Simand et al., '00; Baroud et al., '02

DNS

As time evolves

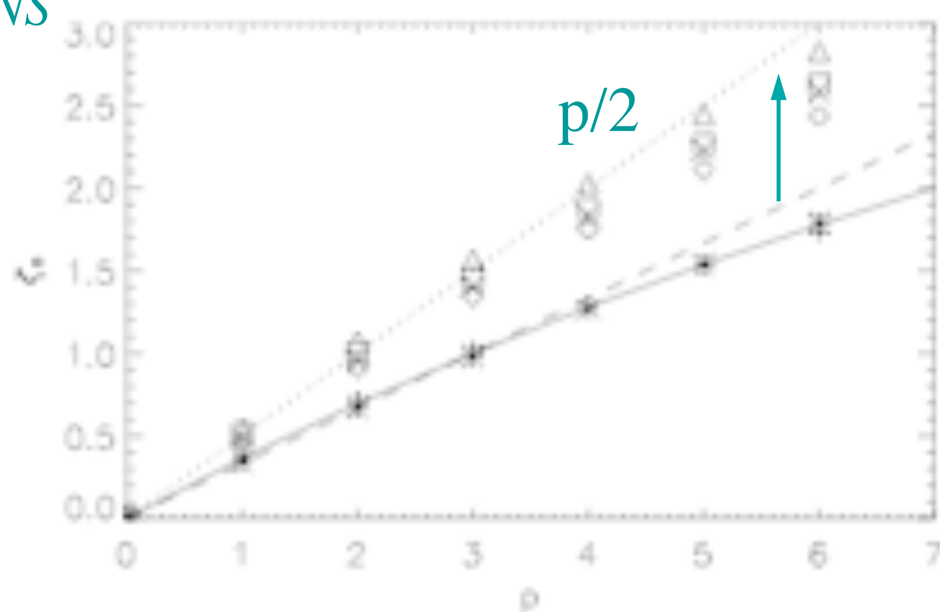

*Mininni+AP, PRE **79***

From Taylor-Green forcing
(globally non helical)

to ABC forcing
(Beltrami flow, fully helical)

for rotating turbulence

With helicity, strong coherent structures form that are organized

Beltrami Core Vortices

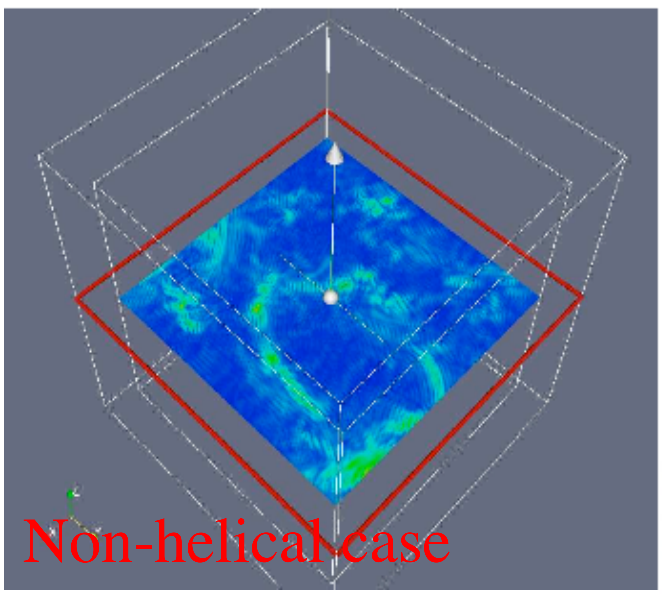

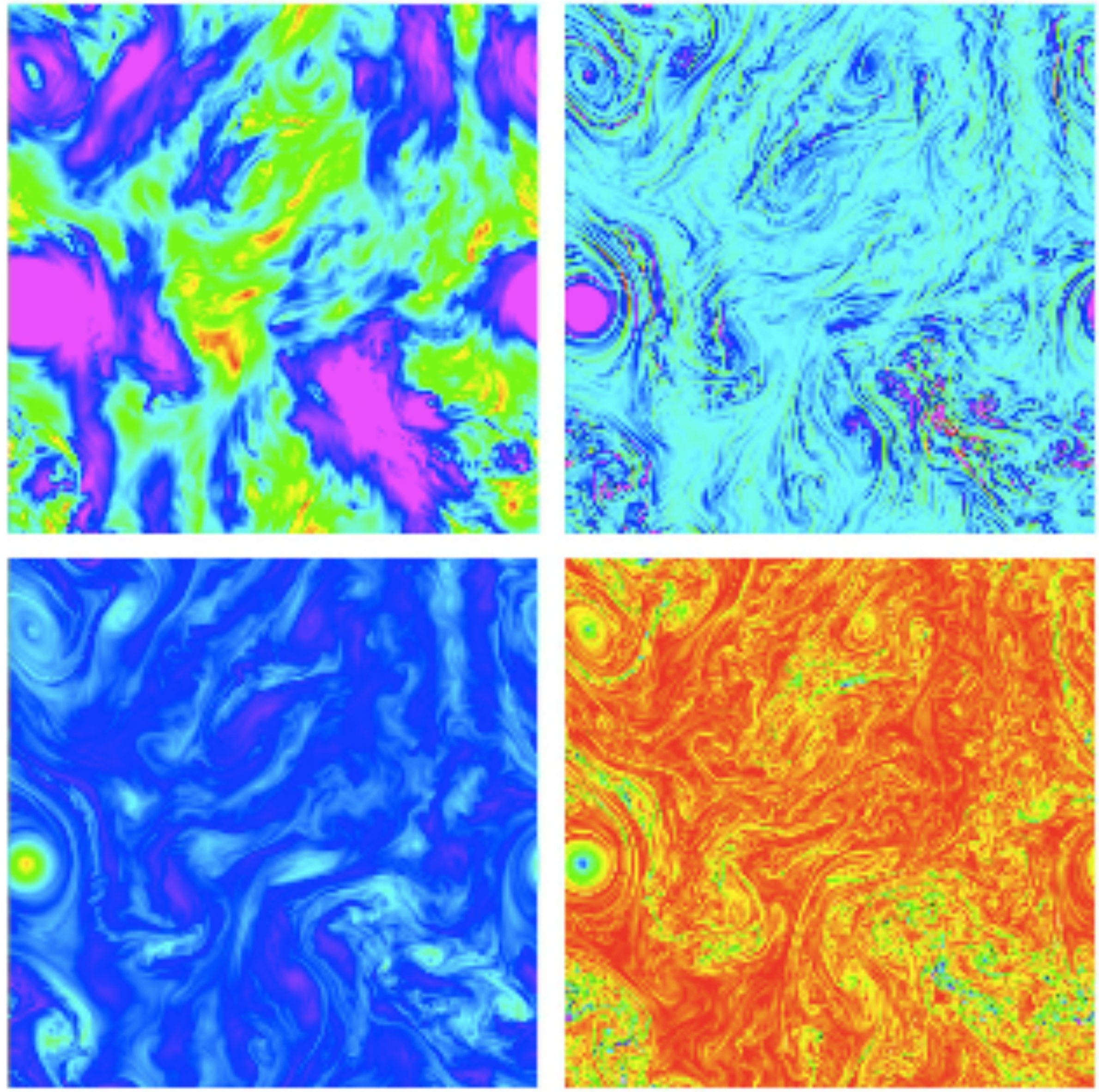

FIG. 9: From top to bottom and from left to right, slices of the energy density, vorticity intensity, z component of the velocity, and helicity density, in run B at $t \approx 30$.

Mininni & AP,
Phys. Fluids 22 (2010)

Zoom on a
Beltrami core
vortex

amidst a tangle
of smaller-scale
vortex filaments

Together with
particle trajectories

1536^3 grid, $k_F=7$,
Re=5100,
Ro=0.06,

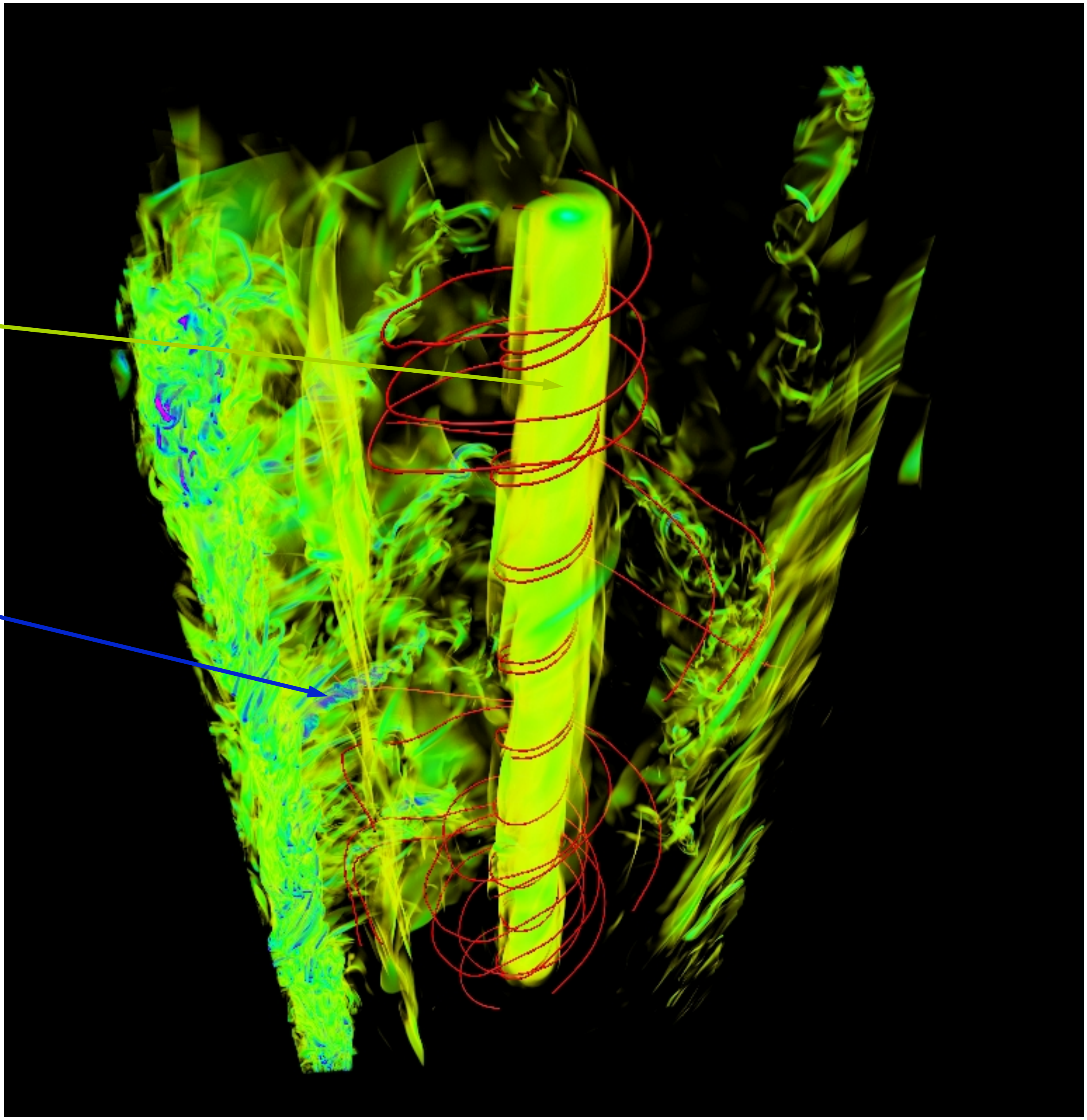

ZOOM on Vorticity:

Beltrami core vortices

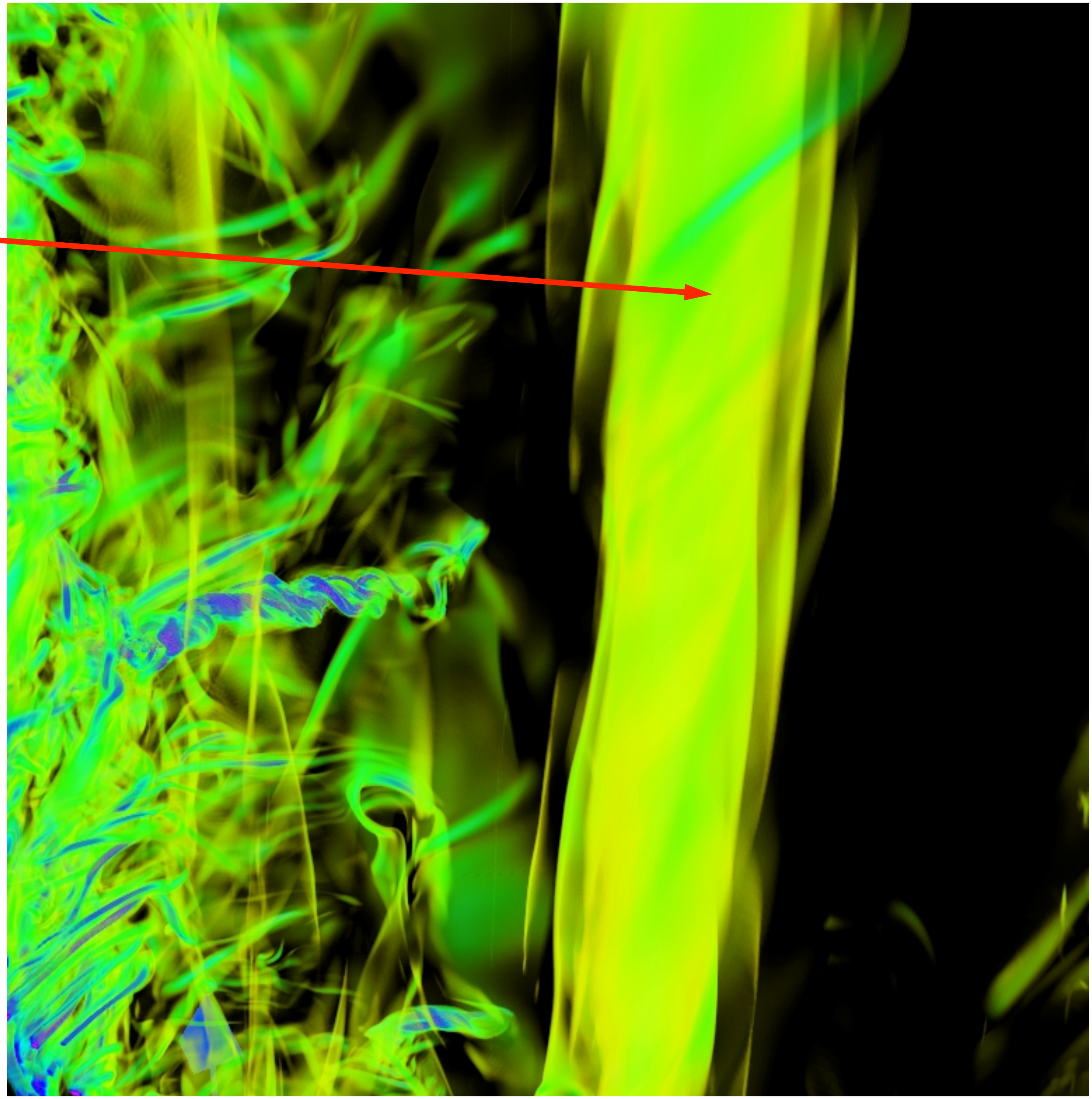

Helical forcing at $k_F=7$

DNS on 1536^3 grid points

Re=5100, Ro=0.06

Updrafts, with H>0

- Mininni & AP, Phys. Fluids 22 (2010)

From Taylor-Green forcing (globally non helical) to ABC forcing
(Beltrami flow, fully helical) for rotating flows

Weakened intermittency in the **direct** energy cascade

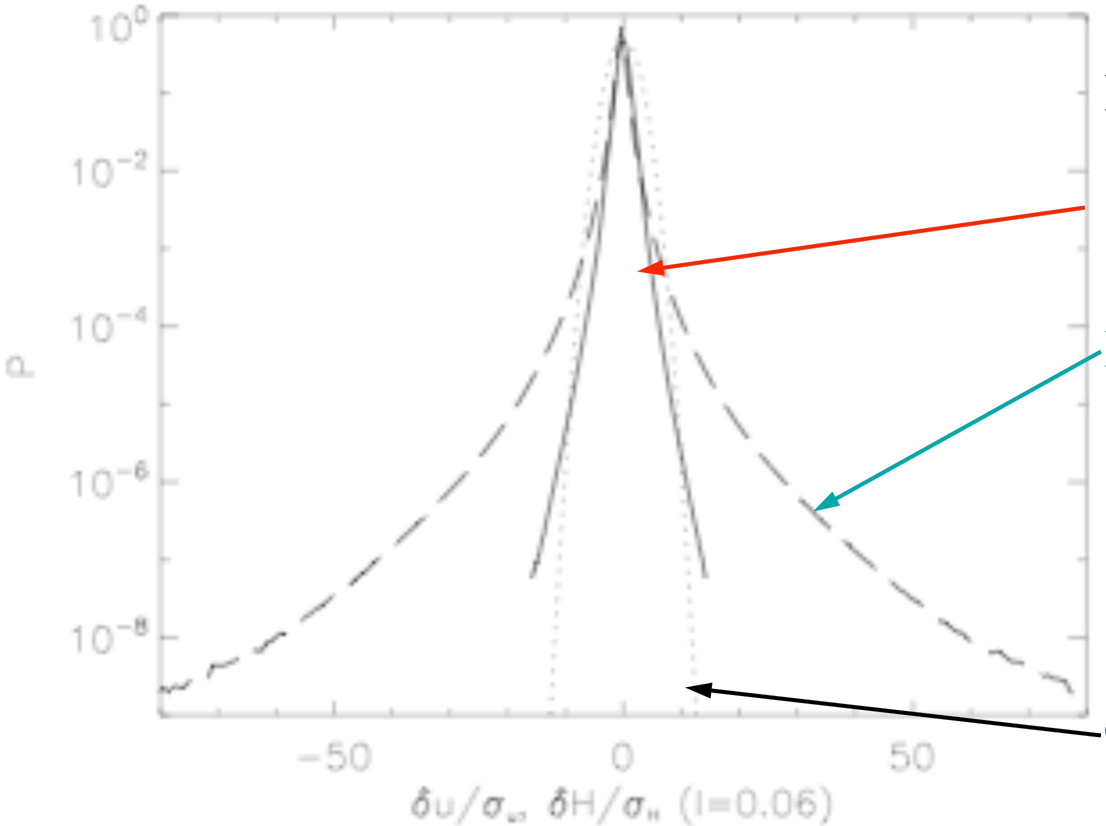

PdF of normalized small scale

Solid: velocity gradients

Dash: helicity gradients

dots: Gaussian

Scaling exponents of structure functions

$<\delta f = f(x+r)-f(x)]^p> \sim r^{\zeta p}$

of velocity

and helicity

$<\delta u^2(l)> \sim l^{1.4}$

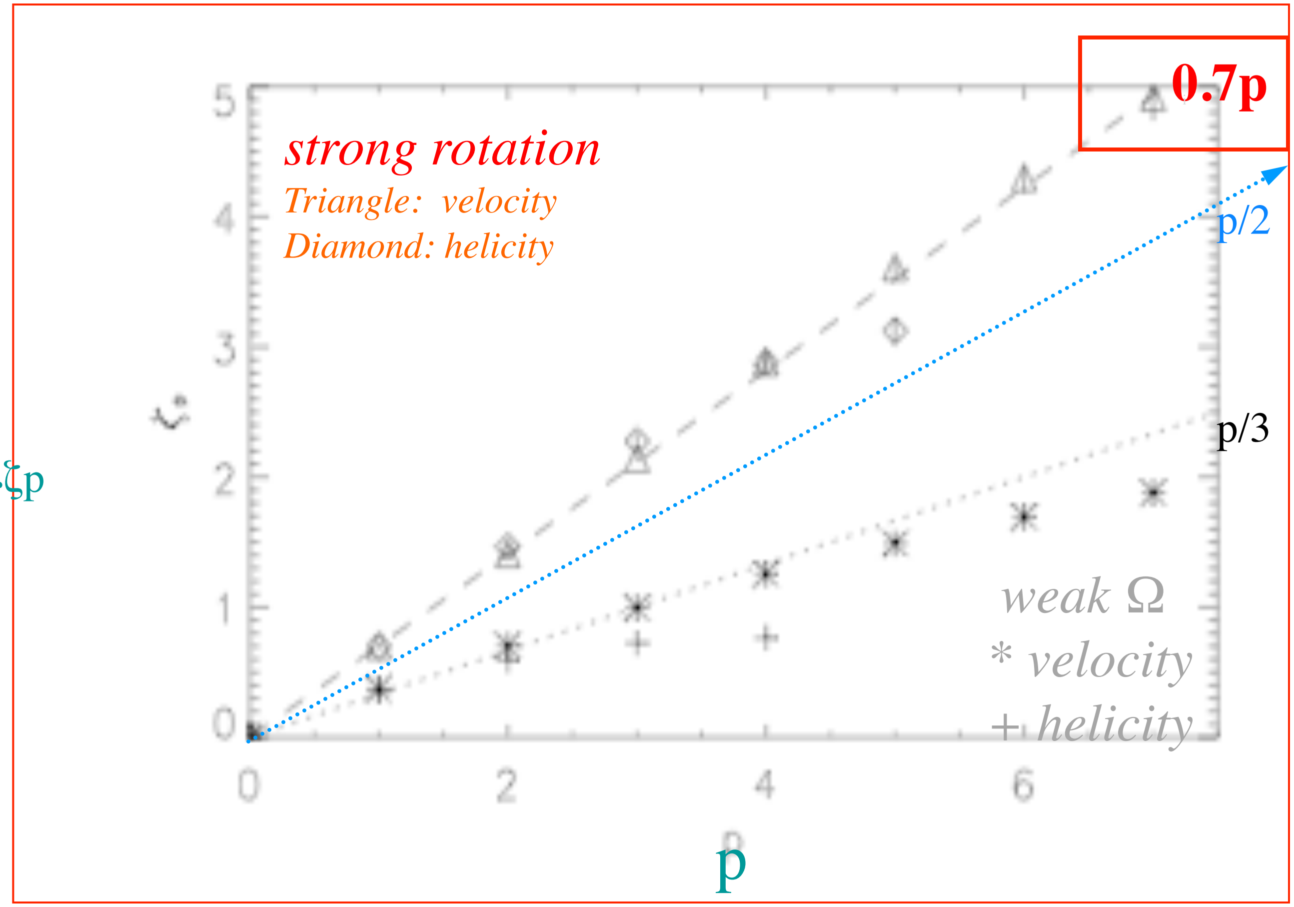

The energy in the direct cascade is **self-similar** for strong rotation,
whereas helicity displays some modicum of intermittency

$\zeta_p = p/2$ for the non-helical case (Simand + '00; Baroud + '02; Mininni & AP '09) not observed here

Scaling exponents of structure functions

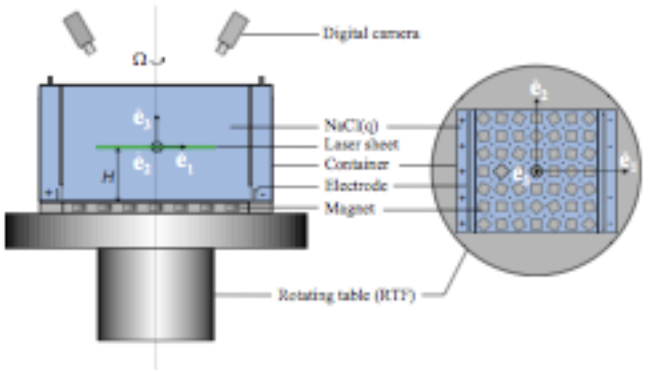

70 cm

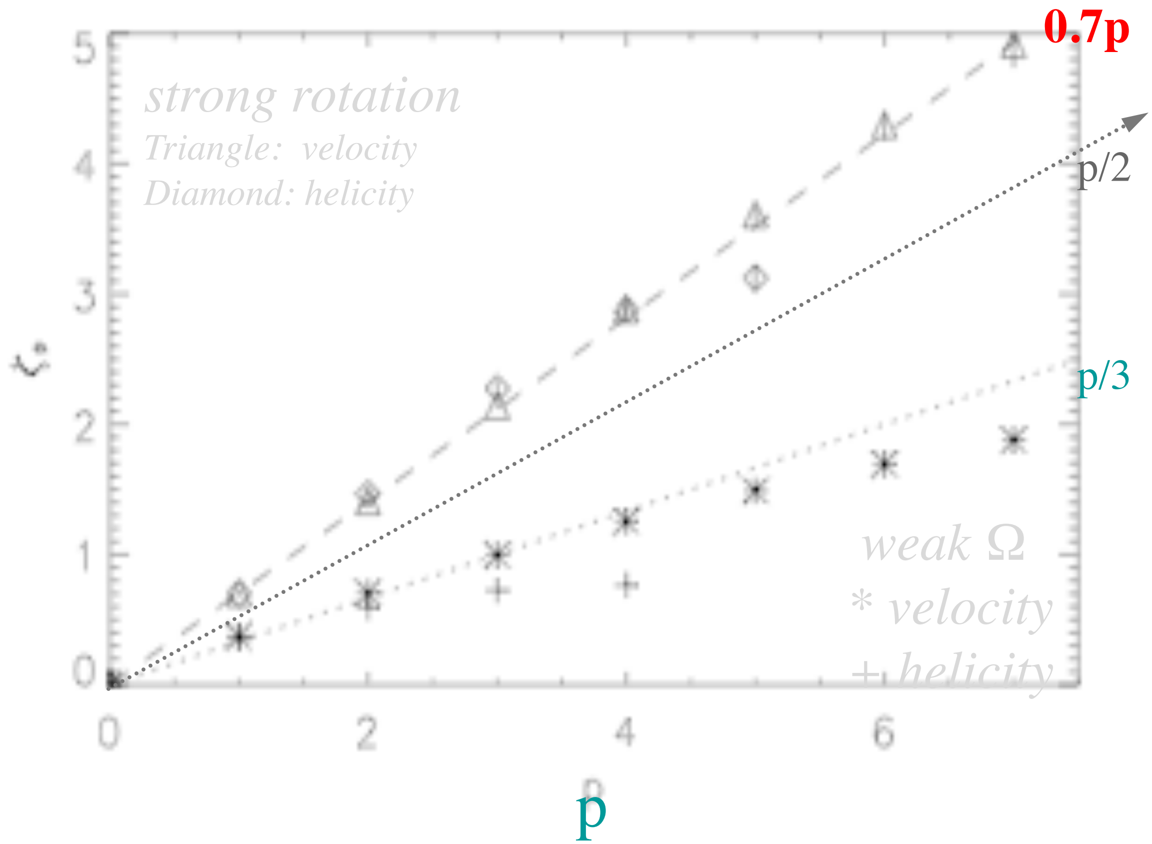

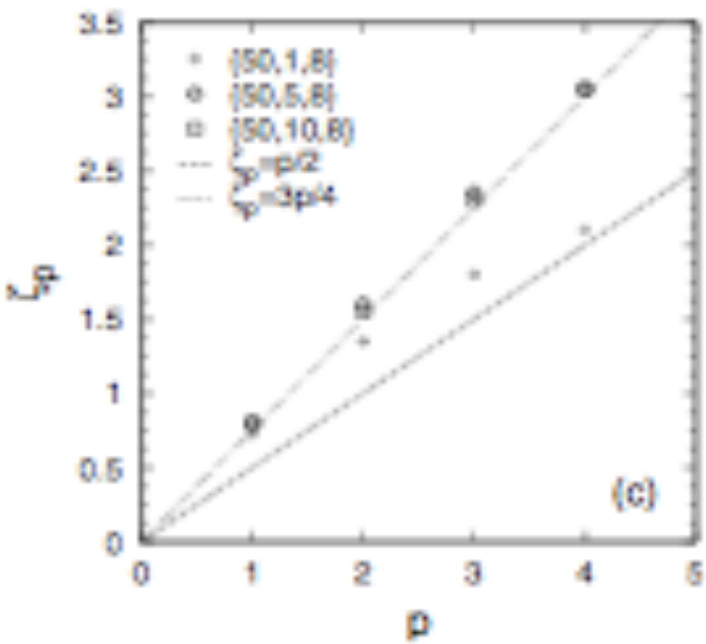

$\zeta_p \sim 3p/4$ at high Ω

experimentally

as well

van Bhokhoven et al. 2009

So, what's happening?

New spectral law for energy and helicity at high rotation

Isotropic phenomenology of turbulence with waves:

- Small parameter: $\hat{\imath} = \tau_W / \tau_{NL}$; transfer time T_{tr} evaluated as:

  $T_{tr} = T_{NL} / \hat{\imath} = T_{NL}{}^* (T_{NL}/T_W)$ *with* $T_{NL}=l/u_l$ *and* $T_W= 1/\Omega$

- Constant helicity flux: $\tilde{\varepsilon} = DH/Dt \sim k^*H(k) / T_{tr}$
- Assume $E(k) \sim k^{-e}$, $H(k) \sim k^{-h}$

→ **e + h = 4** in the helical case with rotation

Assuming maximal helicity [$H(k)=kE(k)$] leads to $e=5/2$
and structure functions: $<\delta u(l)^p> \sim l^{\zeta p}$, $\zeta_p = 3p/4$ *(Mininni & AP, 2009)*

But is maximal helicity a reachable solution?

$$E(k) = E_\Omega + E_K \sim \epsilon^a\, \tilde{\epsilon}^b\, \Omega^f\, k^{-e} + \epsilon^{2/3}\, k^{-5/3}$$

$$H(k) = H_\Omega + H_K \sim \epsilon^c \tilde{\epsilon}^d \Omega^g k^{-h} + \tilde{\epsilon}\epsilon^{-1/3} k^{-5/3}$$

$$\epsilon = dE/dt, \tilde{\epsilon} = dH/dt \quad , \ \mathcal{F}(a,b,c,d,e,f,g) = 0$$

Zeman wavenumber at which $\tau_W = \tau_{NL}$: $k_\Omega \sim \epsilon^\alpha \tilde{\epsilon}^\beta \Omega^\gamma$

Wavenumbers $k_{e,h}$ at which $E_\Omega, H_\Omega = E_K, H_K$

$$k_e \sim \epsilon^\delta\, \tilde{\epsilon}^{\,\phi}\, \Omega^{\frac{3(3a+3e-7)}{3e-5}} \ , \ k_h \sim \epsilon^\psi\, \tilde{\epsilon}^{\,\xi}\, \Omega^{\frac{-3(3a+3e-8)}{3e-7}}$$

$k_\Omega = k_E$ $\rightarrow$ $k_\Omega \sim \epsilon^{-1/2}\, \Omega^{3/2}\, \forall e$ and

$$E_\Omega \sim \epsilon^{\frac{3-e}{2}}\, \Omega^{\frac{3e-5}{2}}\, k^{-e} \qquad (1)$$

$$H_\Omega \sim \epsilon^{\frac{-(3-e)}{2}}\, \tilde{\epsilon}\, \Omega^{\frac{7-3e}{2}}\, k^{-(4-e)} \qquad (2)$$

$\rightarrow \boxed{e \leq 7/3}$ if $k_{e,h,\Omega} \rightarrow \infty$ for $\Omega \rightarrow \infty$

Chakraborty, 2007; Rosenberg et al. 2011

k^x - Compensated spectra for energy (x=e) & helicity (x=h)

1536^3 run

- k_F=7
- Re=5100
- Ro=0.06

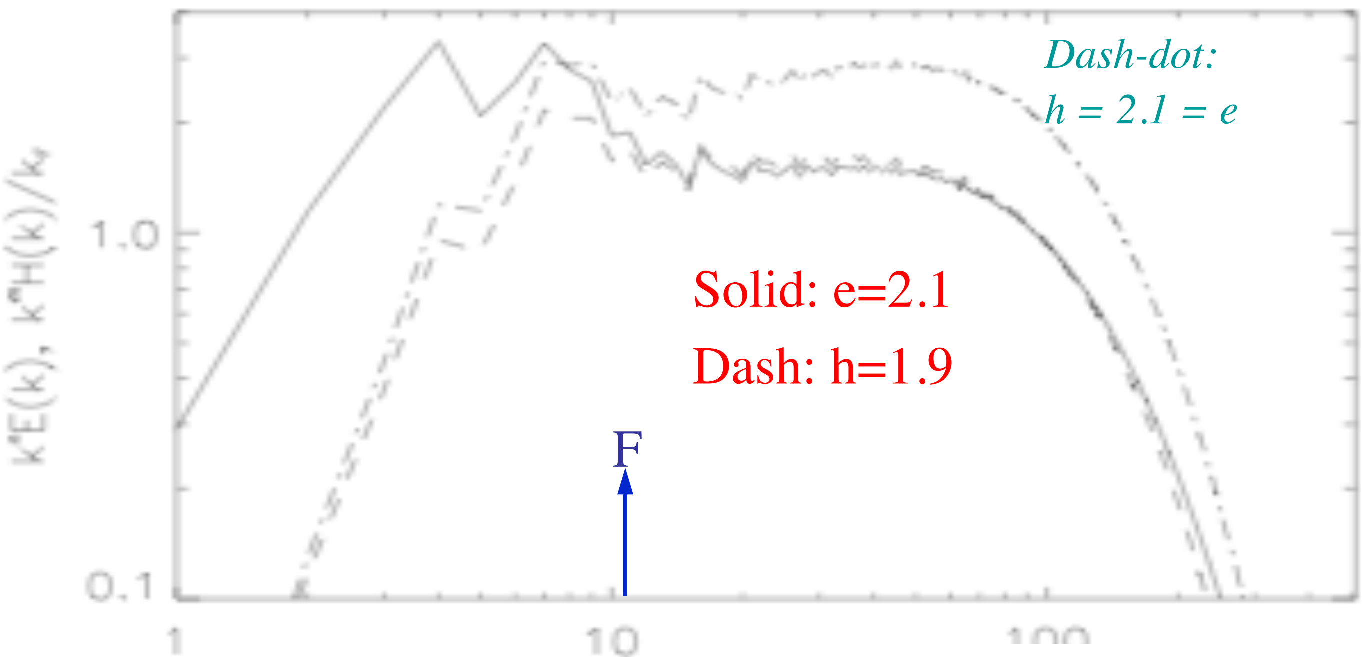

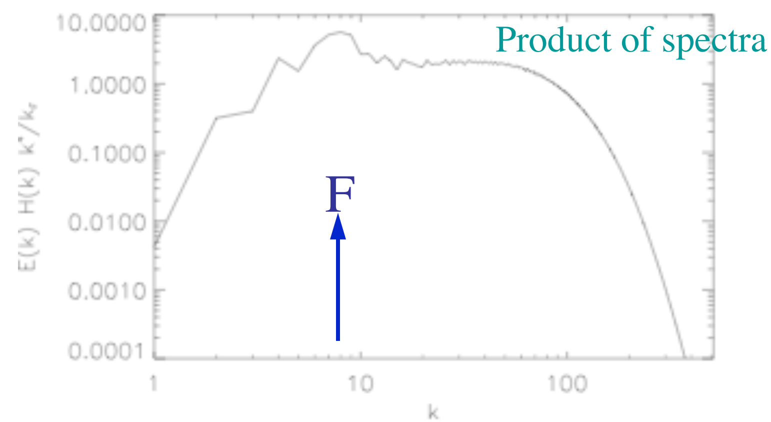

Mininni & AP,
Phys. Fluids 2010

Compensated spectra for the new spectral law:
$k_{perp}^4 E(k)*H(k)/k_F$

k^x - Compensated spectra for energy (x=e) & helicity (x=h)

1536^3 run

- $k_F=7$
- Re=5100
- Ro=0.06

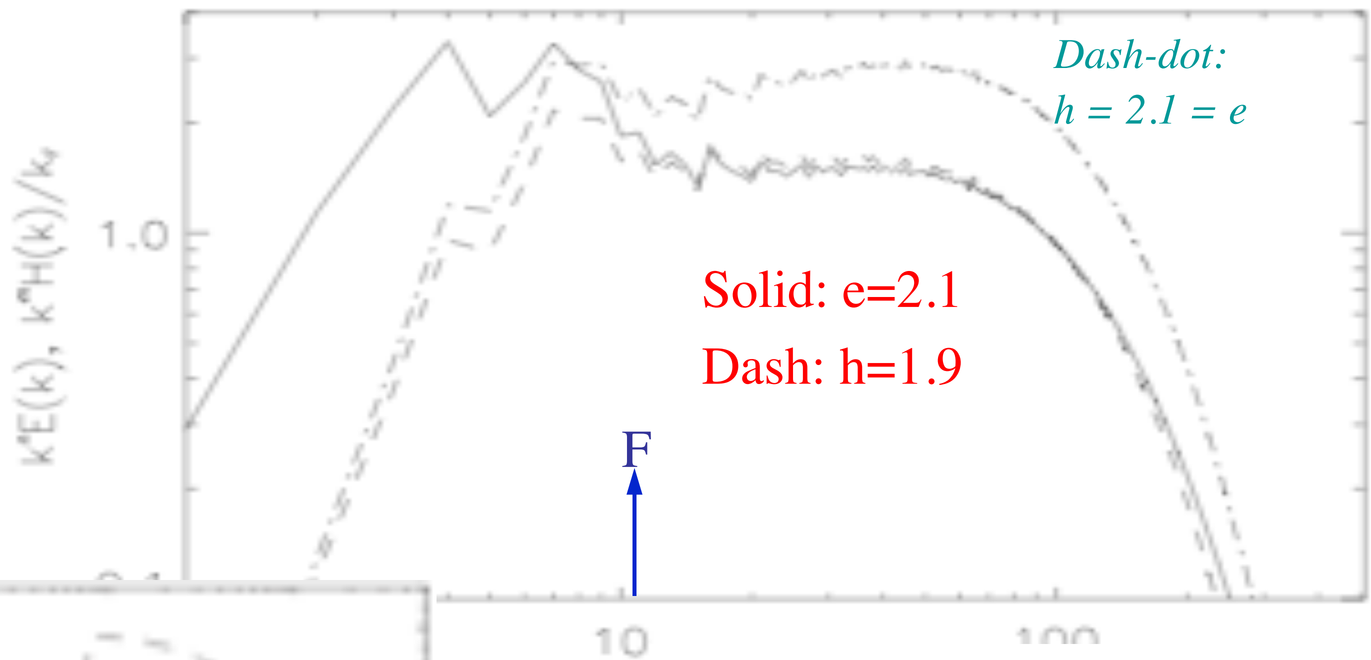

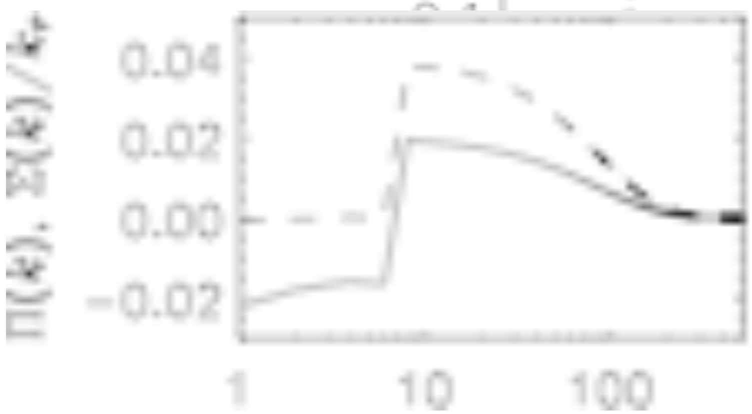

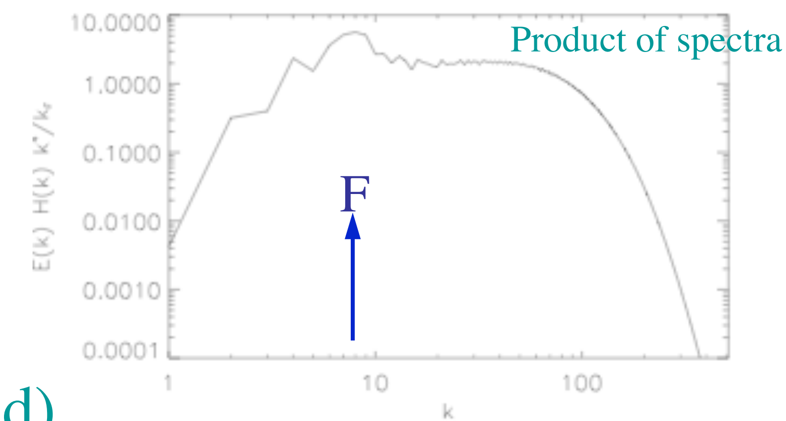

Fluxes of energy (solid)
And helicty (dash)

Mininni & AP,
Phys. Fluids 2010

k^x - Compensated spectra for energy (x=e) & helicity (x=h)

1536^3 run

- k_F=7
- Re=5100
- Ro=0.06

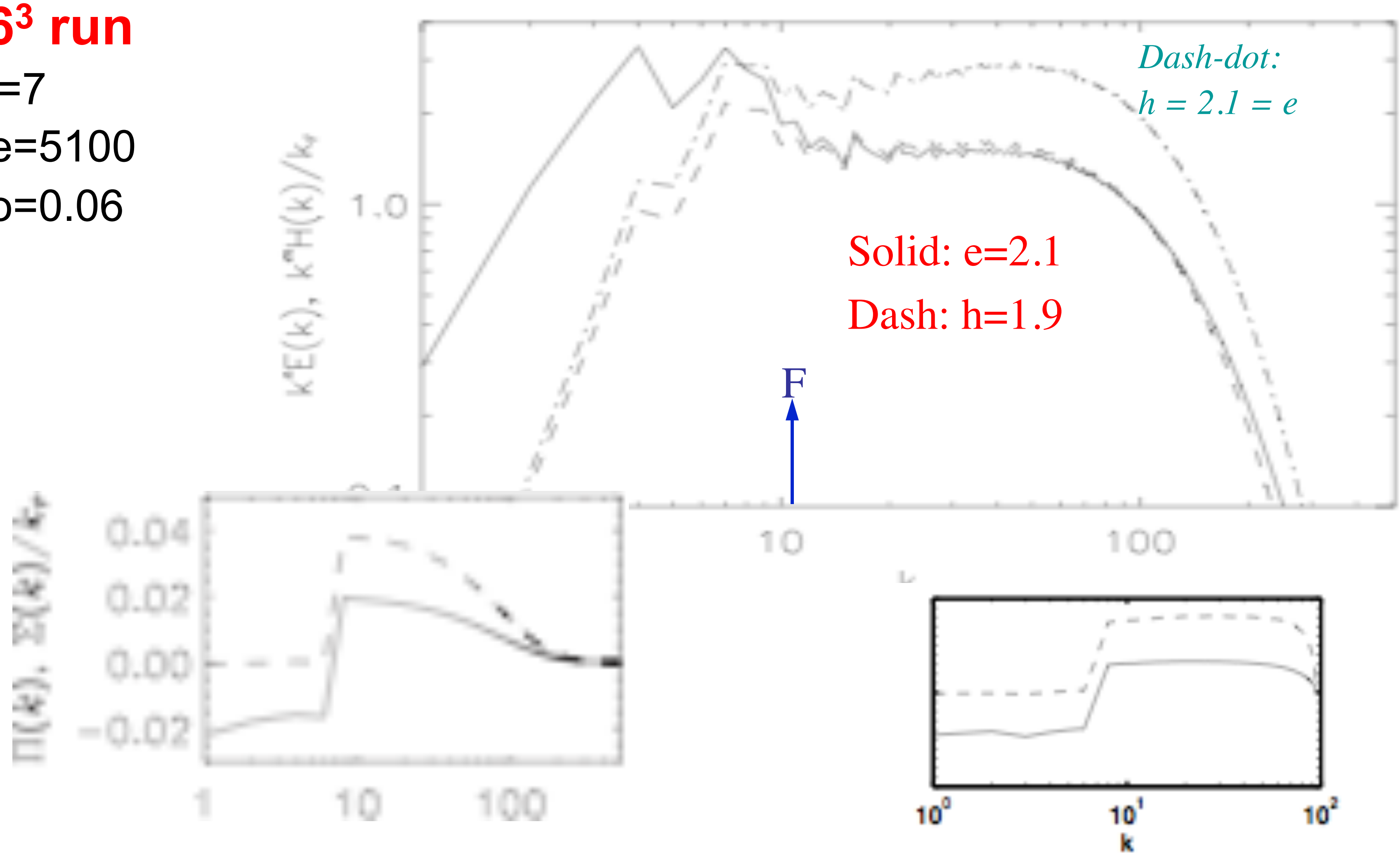

Fluxes of energy (solid)
And helicty (dash)

Mininni & AP,
Phys. Fluids 2010

NORMALIZED RATIO OF HELICITY TO ENERGY TO SMALL SCALES

as a function of rotation

Mininni & AP, Phys. Fluids 2010

- Does the clear self-similarity of the direct cascade of energy in this quasi-2D flow imply conformal invariance, *à la Bernard et al. (2006)*, which these authors found in 2D NS in the inverse energy cascade?

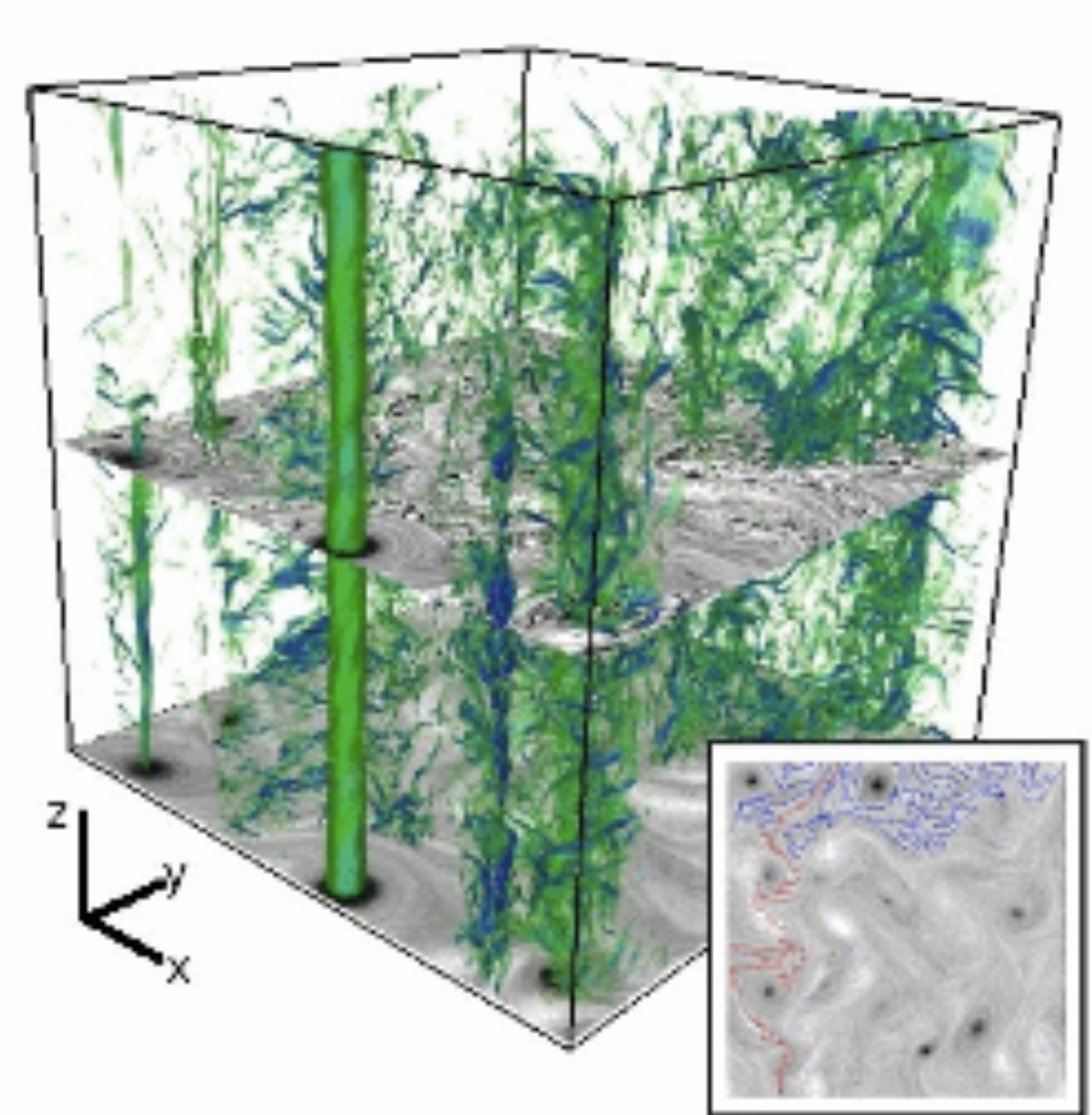

Thalabard et al., PRL to appear, arXiv:1104.1658

Zero vorticity paths in z-averaged field

- Does the clear self-similarity of the direct cascade of energy in this quasi-2D flow imply conformal invariance, à la Bernard et al. (2006), which these authors found in 2D NS in the inverse energy cascade?

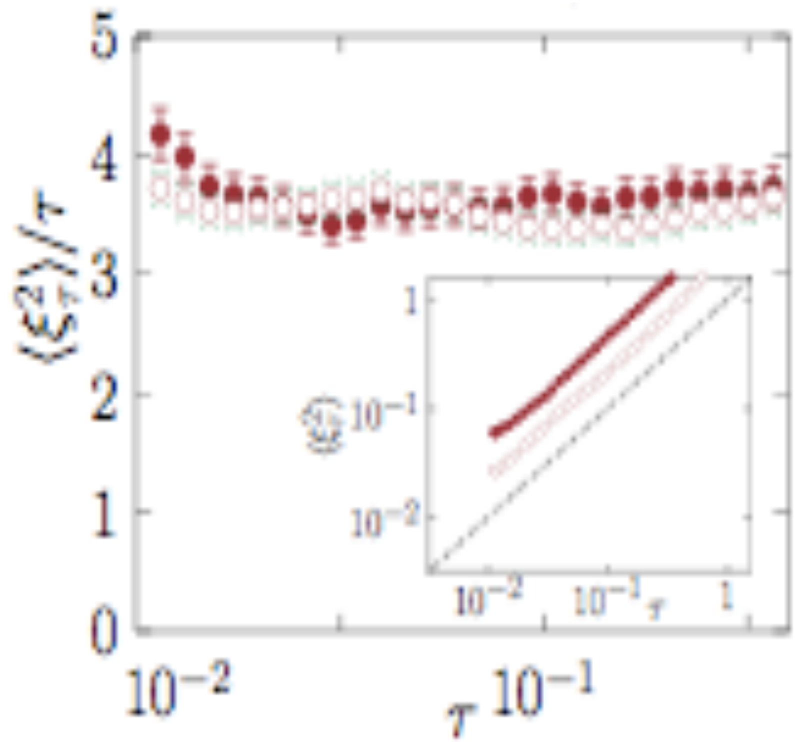

Yes, with $\varkappa = 3.6 \pm 0.1$,

$\varkappa \neq 6$ (2D NS inverse cascade)

Thalabard et al., PRL to appear, arXiv:1104.1658

Going beyond, at higher resolution

- What about recovery of isotropy at small scale beyond what we call the Zeman scale l_Ω at which $T_W = T_{NL} \rightarrow l_\Omega = [\varepsilon/\Omega^3]^{1/2}$
- Large run to resolve the inverse cascade, the wave-modulated anisotropic inertial range, the isotropic inertial range and the dissipation range
- 3072^3 grid points, Tera-grid allocation of 21 million hours on ~ 30,000 proc (i.e., 700 hours of clock time, or 6 weeks)

Return to isotropy in the small scales.

3072^3 grid

Ro ~ 0.07

Re ~ 24000

NSF Tera-grid

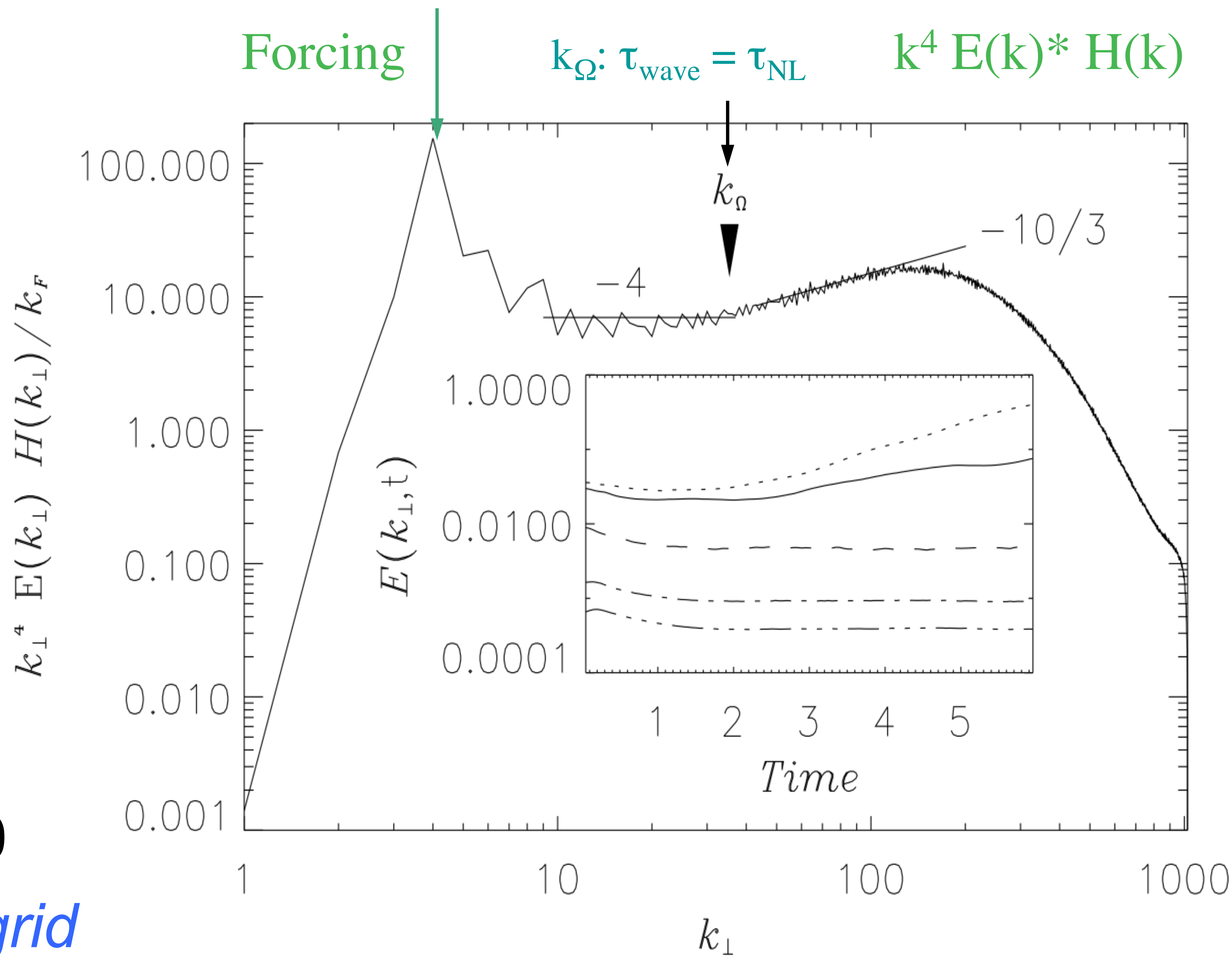

Return to isotropy in the small scales.

3072^3 grid

Ro ~ 0.07

Re ~ 24000

NSF Tera-grid

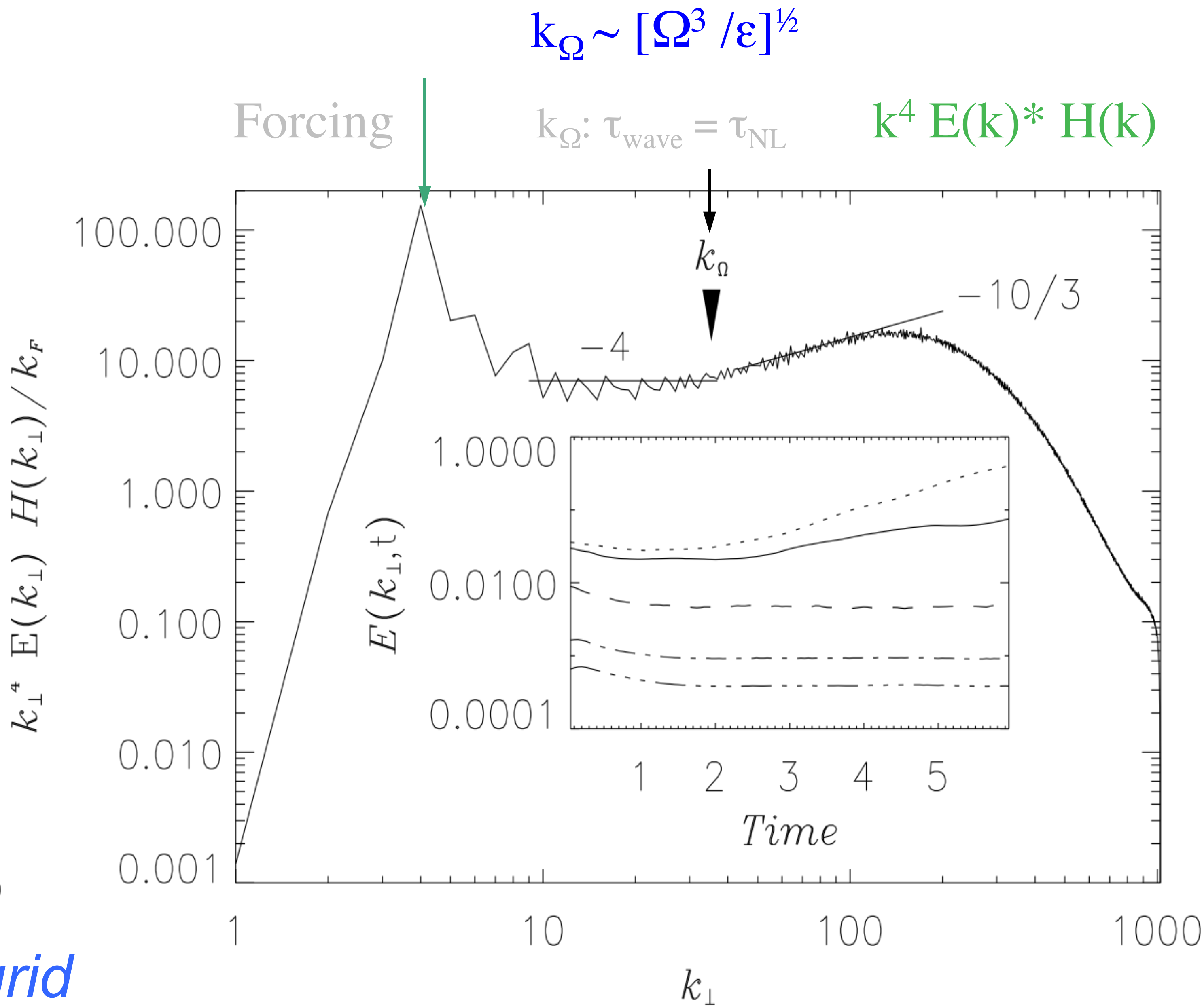

Return to isotropy in the small scales, angular dependence of spectra

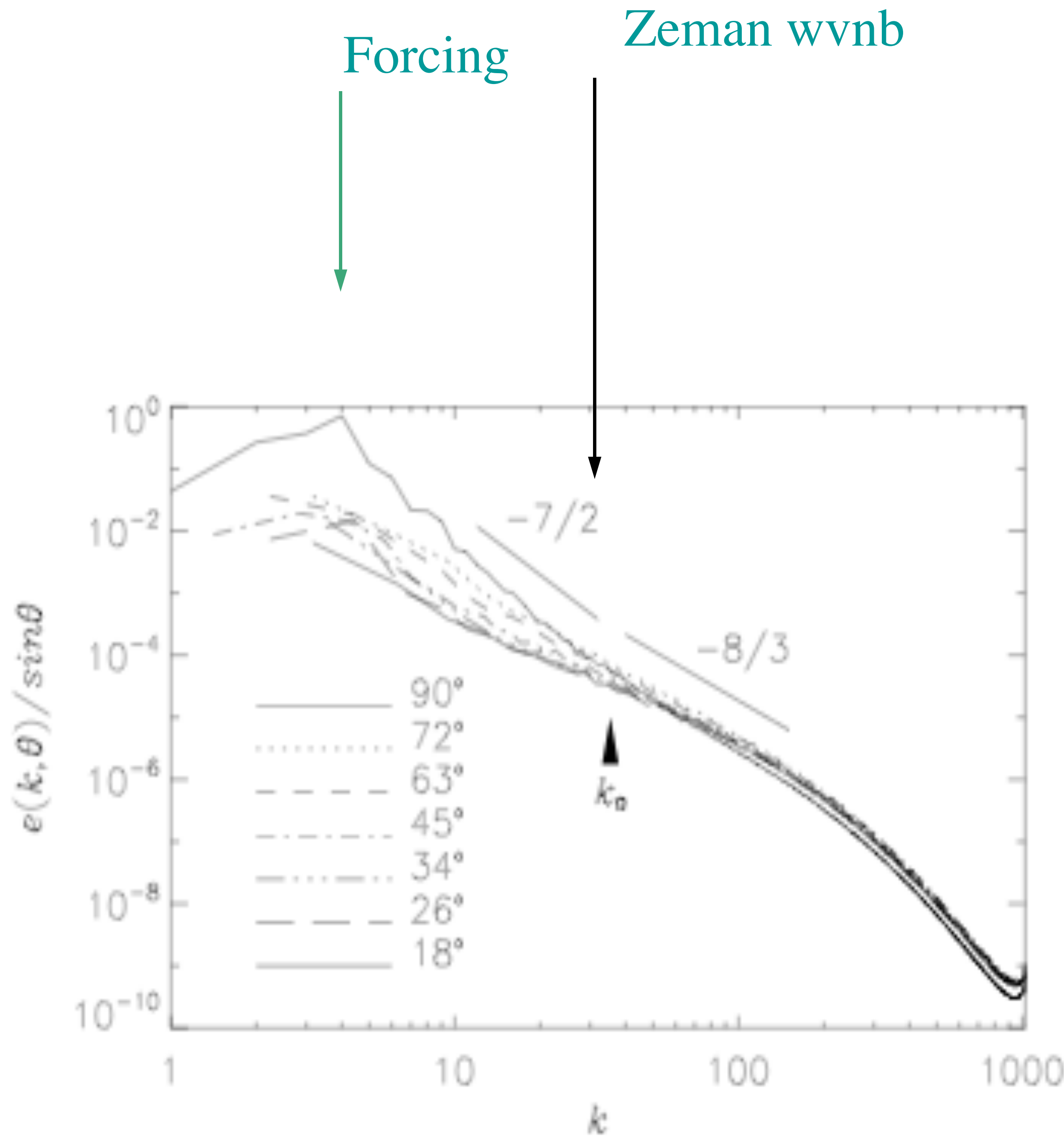

3072^3 grid
Ro ~ 0.07
Re ~ 24000
NSF Tera-grid

Summary of results

- In the presence of helicity and rotation, the direct transfer to small scales is dominated by the helicity cascade and the energy cascade to small scales is quenched because of the inverse cascade

- This provides a ``*small'' parameter* for the problem (the normalized ratio of energy to helicity fluxes), besides the small Rossby number
- The direct energy cascade is non-intermittent and conformal invariant (when properly averaged in the vertical direction). It is also (presumably) different from (i) the non-helical case, and (ii) the (presumably) self-similar inverse cascade of energy to large scales.

- There is a change of inertial index in the small scales from a Kolmogorov law to a law steeper than what is predicted by a wave-induced non-helical model, with a possible breaking of universality and with a possible $e \leq 7/3$, $h \geq 5/3$ limit
- Isotropy recovers at small scale provided the Zeman scale is resolved
- The flow produces strong organized long-lived columnar helical structures, Beltrami Core Vortices, at scales slightly smaller than the injection scale, *with also a growth of structures at large scales*

Some questions

- Can helicity help in interpreting laboratory experiments or atmospheric data?

- Is there experimental evidence for this e+h=4 law?
- Is there experimental evidence for Beltrami Core Vortices?

- What about the large Reynolds number limit?

- How does the dynamics change in terms of the relative alignment between the velocity and the vorticity [relative helicity $\rho(k)=H(k)/kE(k)$]?

Some questions

Does the nature of the imposed forcing at large scale play a role?
(helical or not: yes; random vs. deterministic? 2D vs 3D?)

- What happens locally in space? What structures transfer to small *vs.* large scales? What are the Beltrami Core Vortex structures made of? How do they evolve and interact to lead to both a direct and an inverse cascade?

- Universality?
- Modeling: isotropic vs. anisotropic?
- Need/nature of helical contribution?

- What happens when helicity is neither zero nor maximal globally?

A Few Issues in Turbulence

II – What do we mean by modeling?

Kolmogorov-compensated energy spectra: $k^{5/3}$ E(k)

Navier-Stokes, ABC forcing

Small Kolmogorov $k^{-5/3}$ law
(flat part of the spectrum)

K41 scaling increases in range, as the Reynolds number increases

- **Bottleneck** at dissipation scale

Solid: 2048^3, $R_v = 10^4$, $R_\lambda \sim 1200$
Dash: 1024^3, $R_v=4000$

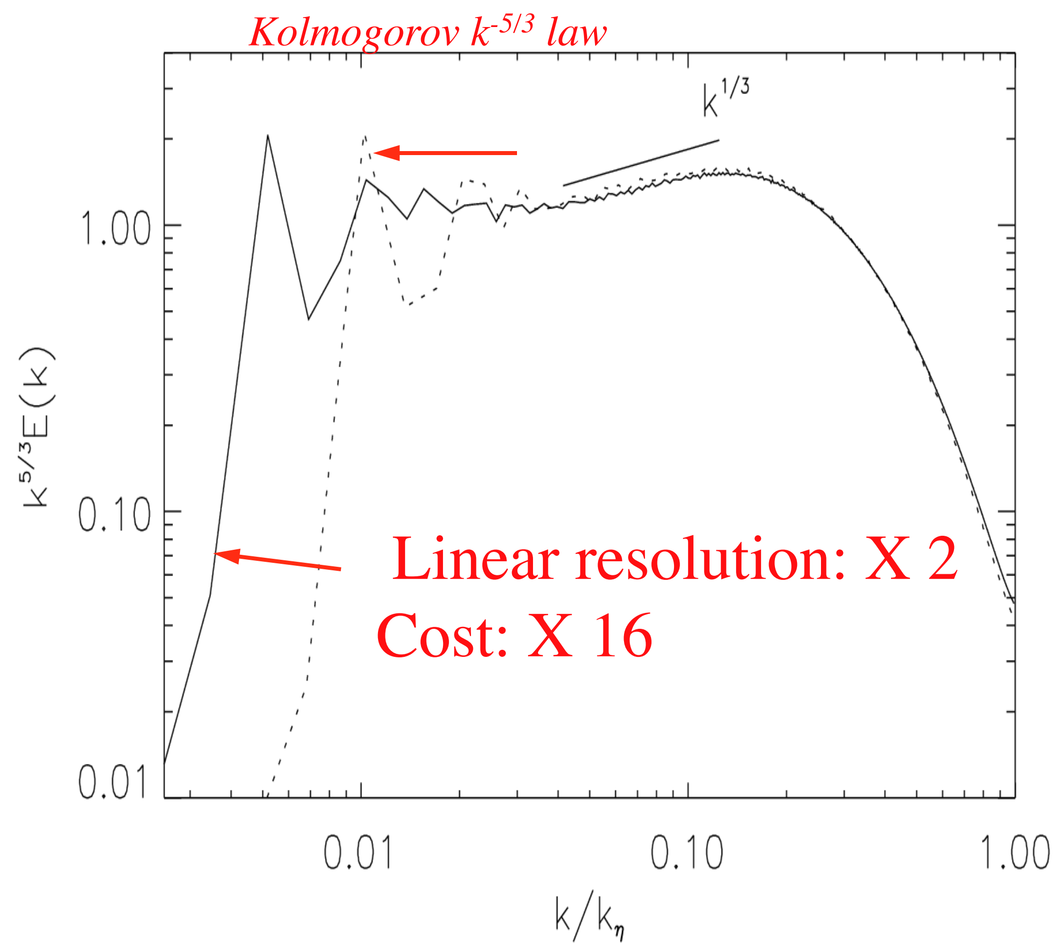

*Mininni et al., Phys. Rev. E **77** (2008)*

Large effort

- Linear number of modes N ~ Reynolds number R_e

  ($N \sim L_0/l_{diss} \sim Re^{3/4}$ for a Kolmogorov spectrum)

- 1D FFT cost is *NlogN*

- Time of computation ~ $T_{diss}/T_{NL} \sim R_e$

- Cost of three-dimensional computation ~ Re^4

  Moore's law: doubling of resolution every 6 years …

4096^3 Navier-Stokes on Earth Simulator:16 Teraflops, 10 TeraBytes

12288^3 (NSF plan): 2 Petaflops, 200 Terabytes, *20MW, \$200M, 10^{5+} CPUs*

Data output, analysis, visualization and storage

There are several ways out

- **Zero**-dimensional models: phenomenology, shell (scalar) models, SOC, …
- **One** dimensional: Burgers equation and its extension to fully compressible flows, MHD flows, kinetic effects (the Hada equation), solitons, …
- **Two**-dimensional problem with either 2 or 3 components (2D2C, 2D3C) and ``thick'' 2D
- Implementing **symmetries** in 3D at all times
- Adaptive mesh refinement (**AMR**)
- Quasi - direct numerical modeling, with **filtering** really
- Eddy viscosity and Large-Eddy Simulations (**LES**)

And combining them

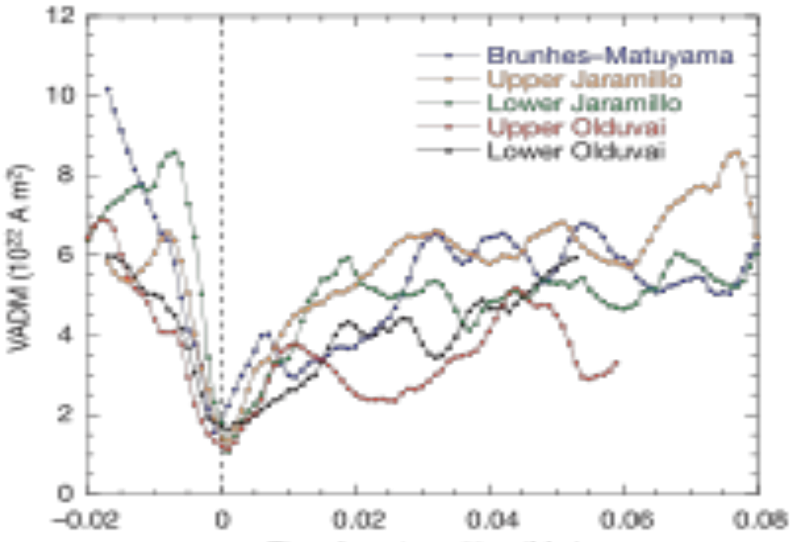

Reversal of the Earth's magnetic field over the last 2Myrs

(Valet, Nature, 2005)

Temporal assymmetry and chaos in reversal processes

Brunhes *Jamarillo* *Matuyama* *Olduvai*

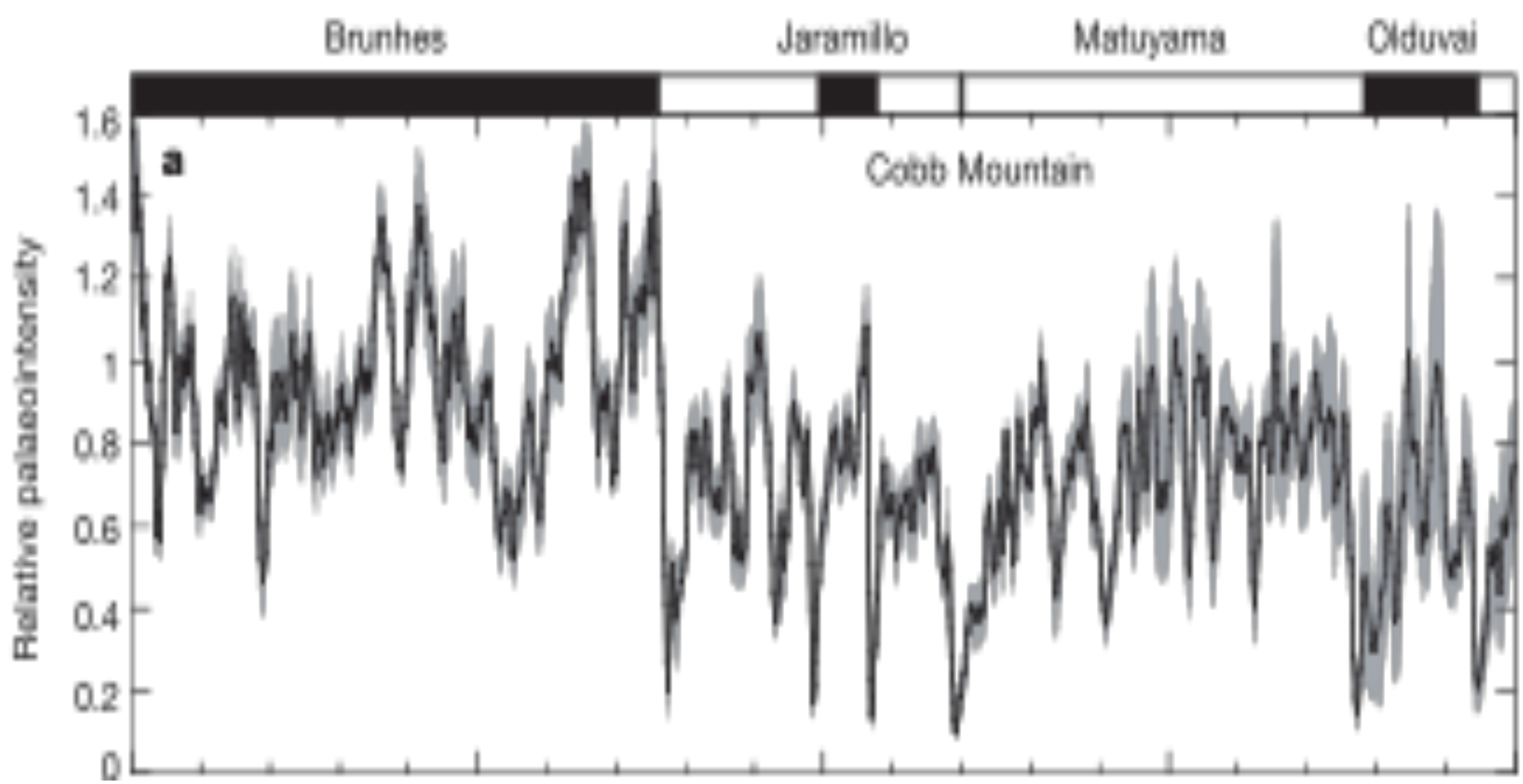

Surface (1 bar) radial magnetic fields for

Jupiter, **Saturne** & **Earth** *versus* **Uranus** & **Neptune**

(16-degree truncation, Sabine Stanley, 2006)

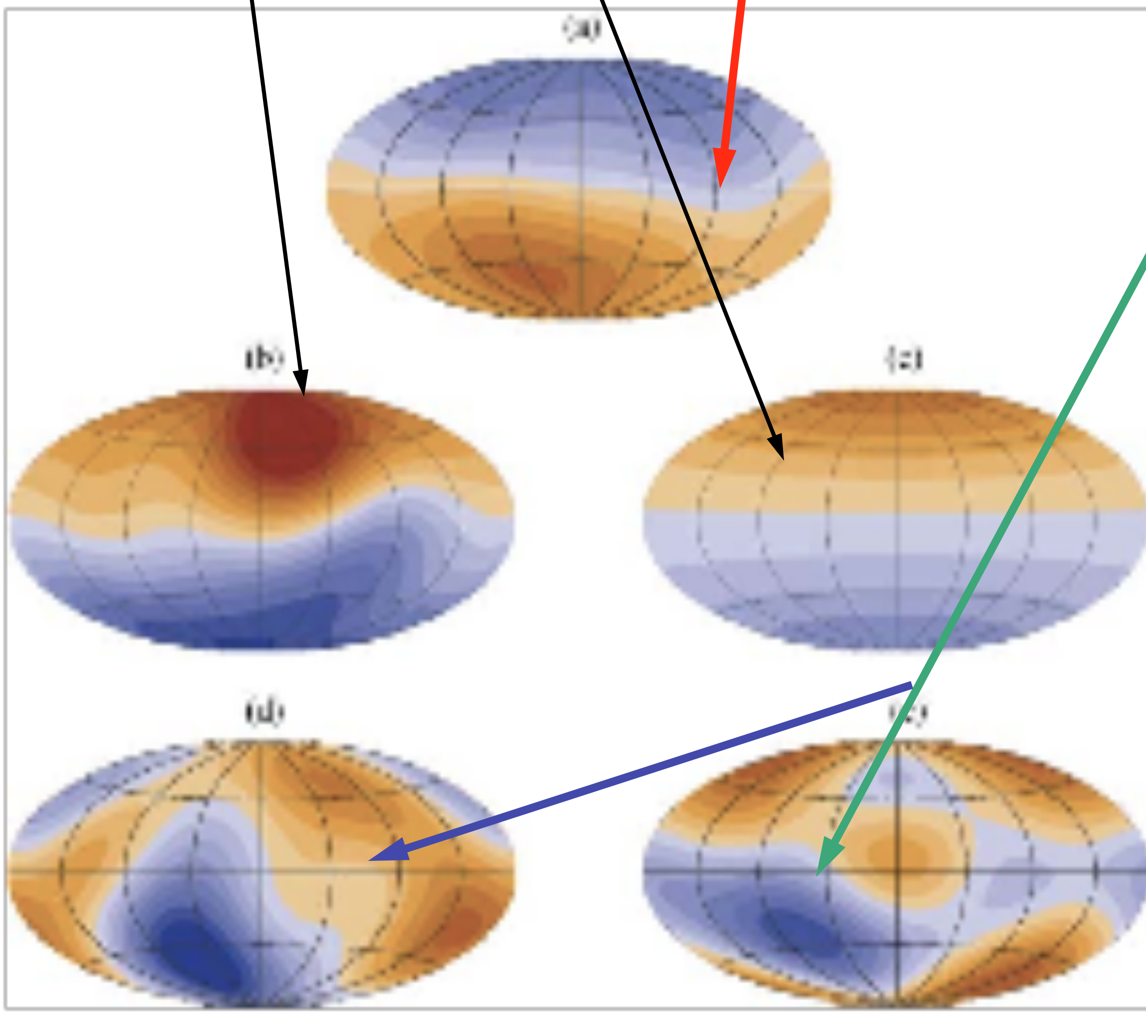

Axially dipolar

Quadrupole ~ dipole

The Taylor-Green flow

$$\mathbf{F} = \begin{bmatrix} \sin(k_0 x)\cos(k_0 y)\cos(k_0 z) \\ -\cos(k_0 x)\sin(k_0 y)\cos(k_0 z) \\ 0 \end{bmatrix}$$

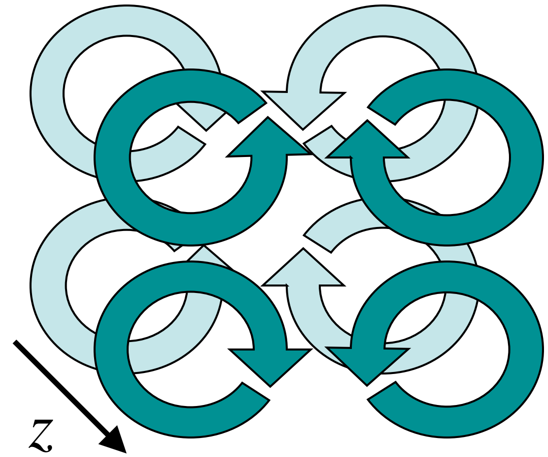

The Taylor-Green flow is a globaly non-helical forcing (Taylor & Green, *Proc. Roy. Soc.* A **151**, 421, 1935).

•The resulting flow shares similarities with the Cadarache von Kárman dynamo experiment in liquid sodium or gallium (at $P_M \sim 10^{-6}$) (Marié et al., *MHD*, **38**, 163, 2002).

The flow is highly turbulent.

• It gives an experimental dynamo *(2006 onward: Cadarache, CEA Paris, ENS Lyon & Paris, …)*

Is there a lack of universality in MHD turbulence?

- Tool: a code which enforces symmetries
- Two runs, 512^3 grids, one enforcing the Taylor-Green symmetries, one a generic pseudo-spectral code

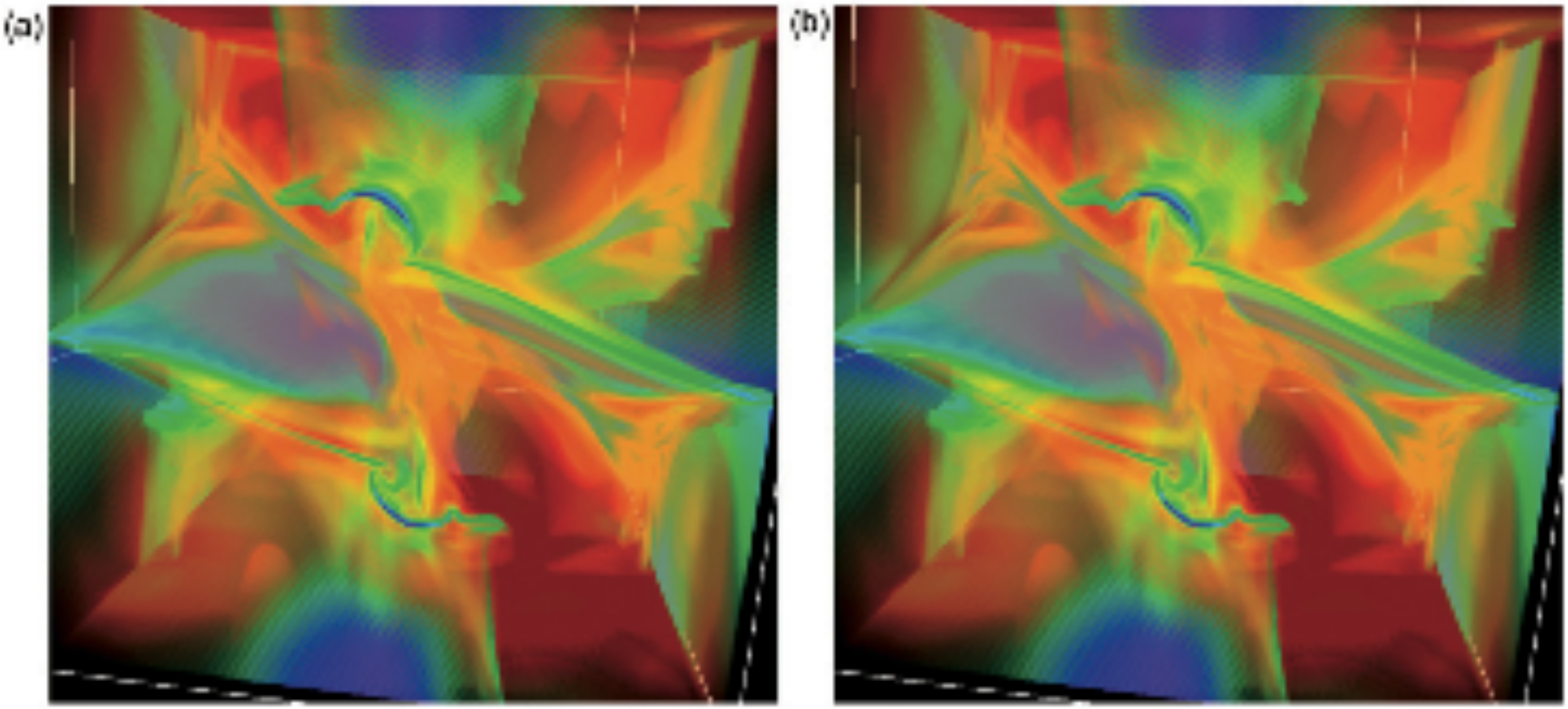

Pouquet et al. GAFD ***104****, 2010*

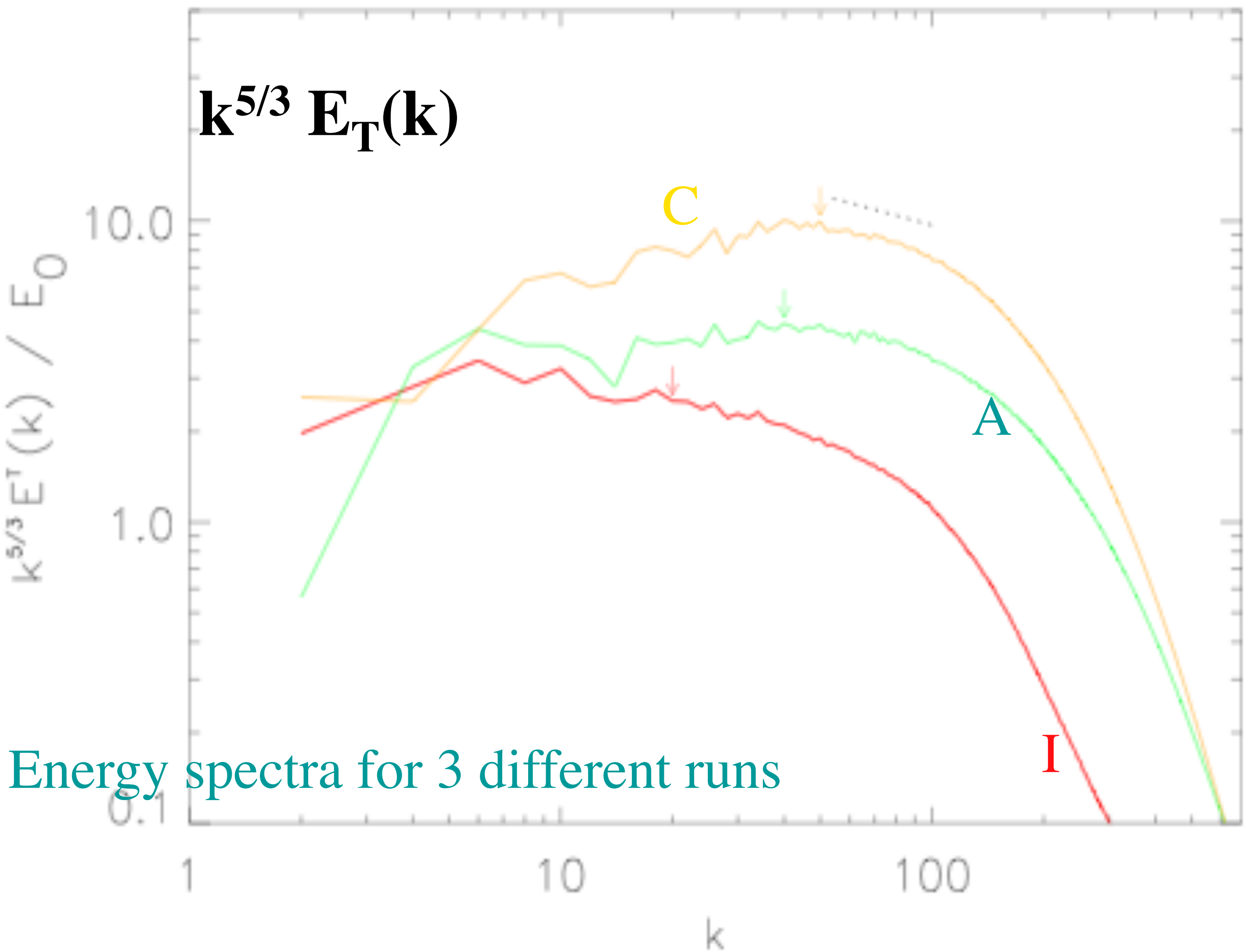

$B_0 = 0$,
$F = 0$

$E_v(t=0)=$
$E_M(t=0)=1$

$H_M(t=0)=0$
$H_C(t=0) \sim 0$

Symmetric MHD Taylor-Green 2048^3 equivalent res. $R_{lam} \sim 1300$, *Lee et al. 2010*

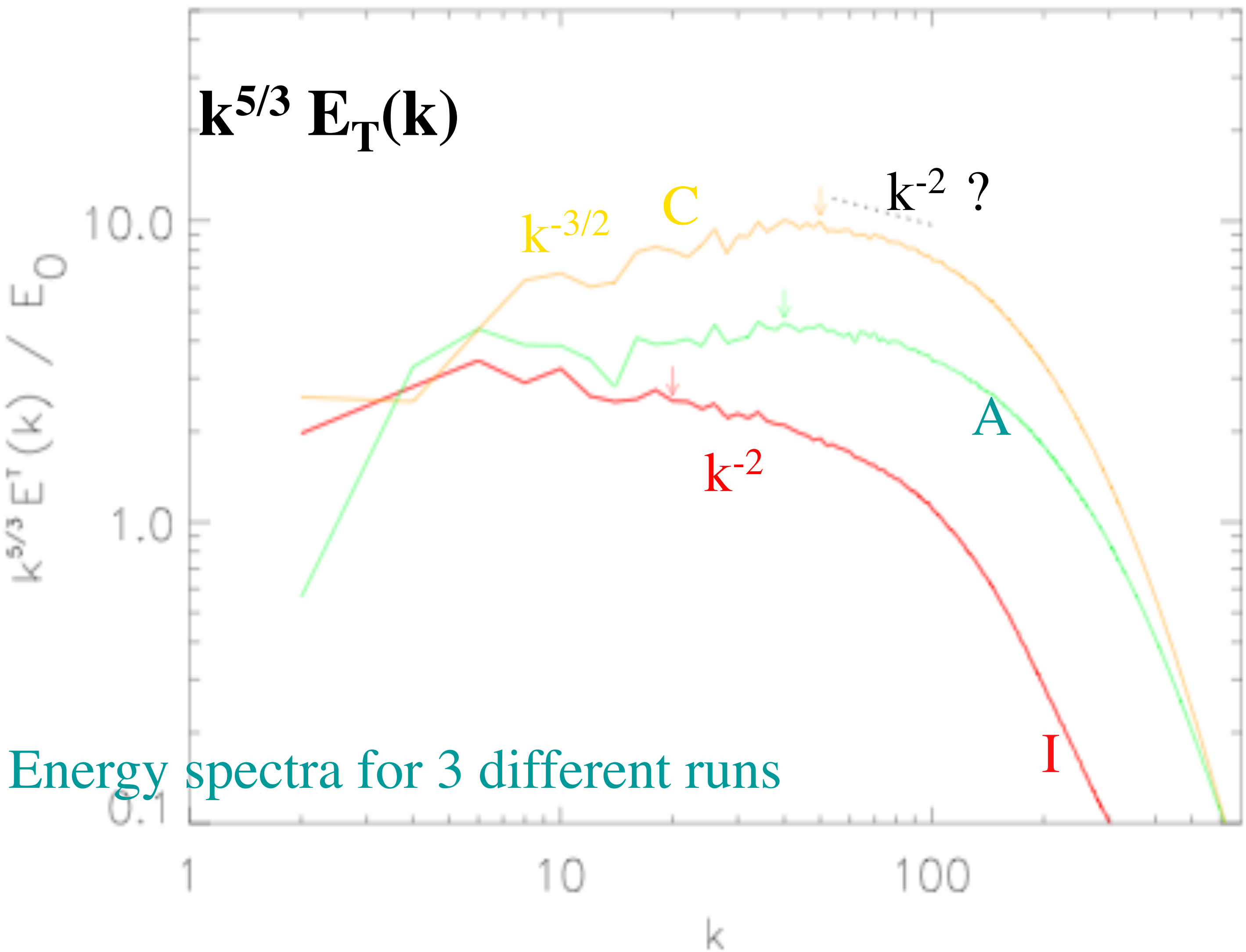

$B_0 = 0$,
$F = 0$

$E_v(t=0) =$
$E_M(t=0) = 1$

$H_M(t=0) = 0$
$H_C(t=0) \sim 0$

Symmetric MHD Taylor-Green 2048^3 equivalent res. $R_{lam} \sim 1300$, *Lee et al. 2010*

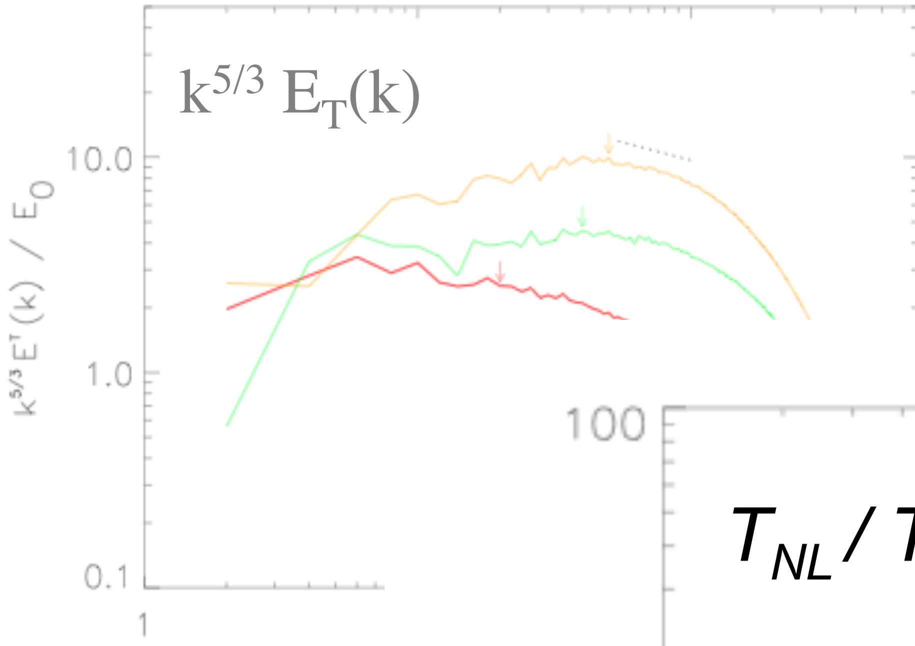

Energy spectra

B_0 = 0, F=0

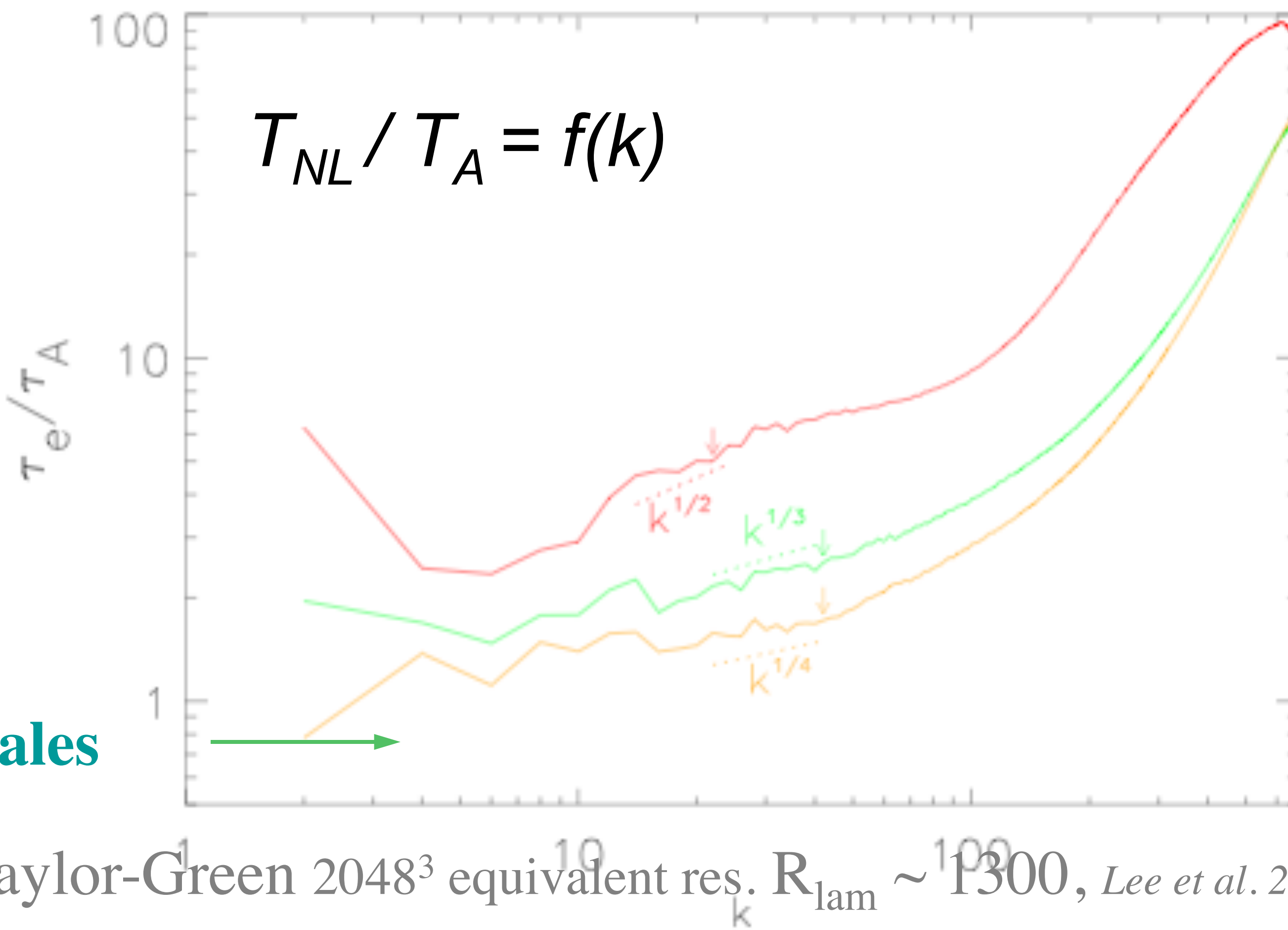

Ratio of time-scales

Symmetric MHD Taylor-Green 2048^3 equivalent res. $R_{lam} \sim 1300$, *Lee et al. 2010*

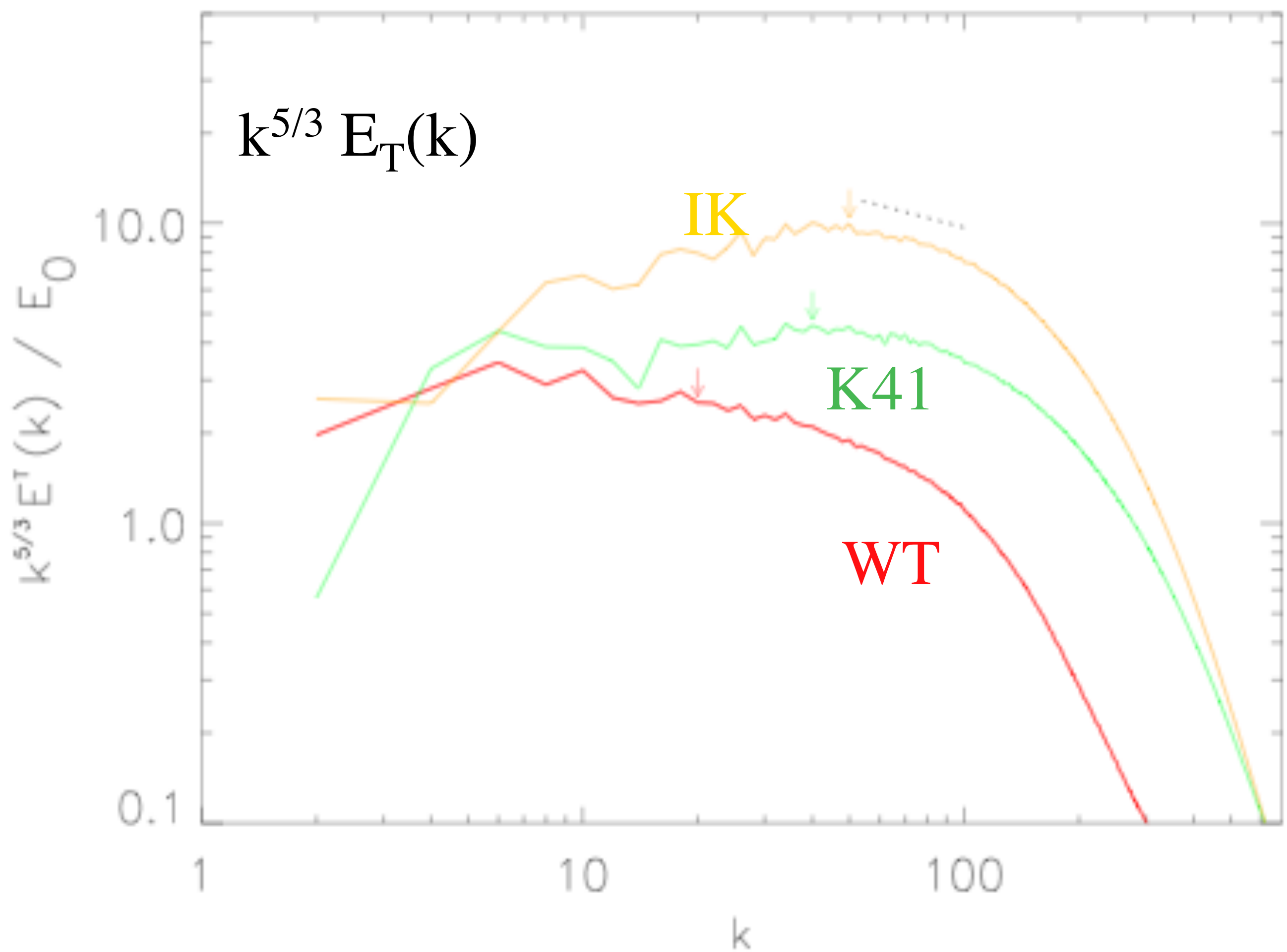

Lack of universality in MHD turbulence, B_0 = 0, F=0

- Do these spectral indices persist in time for a given flow?
- Would it be observed as well in the statistically steady state?

Symmetric MHD Taylor-Green 2048^3 equivalent res. $R_{lam} \sim 1300$, *Lee et al. 2010*

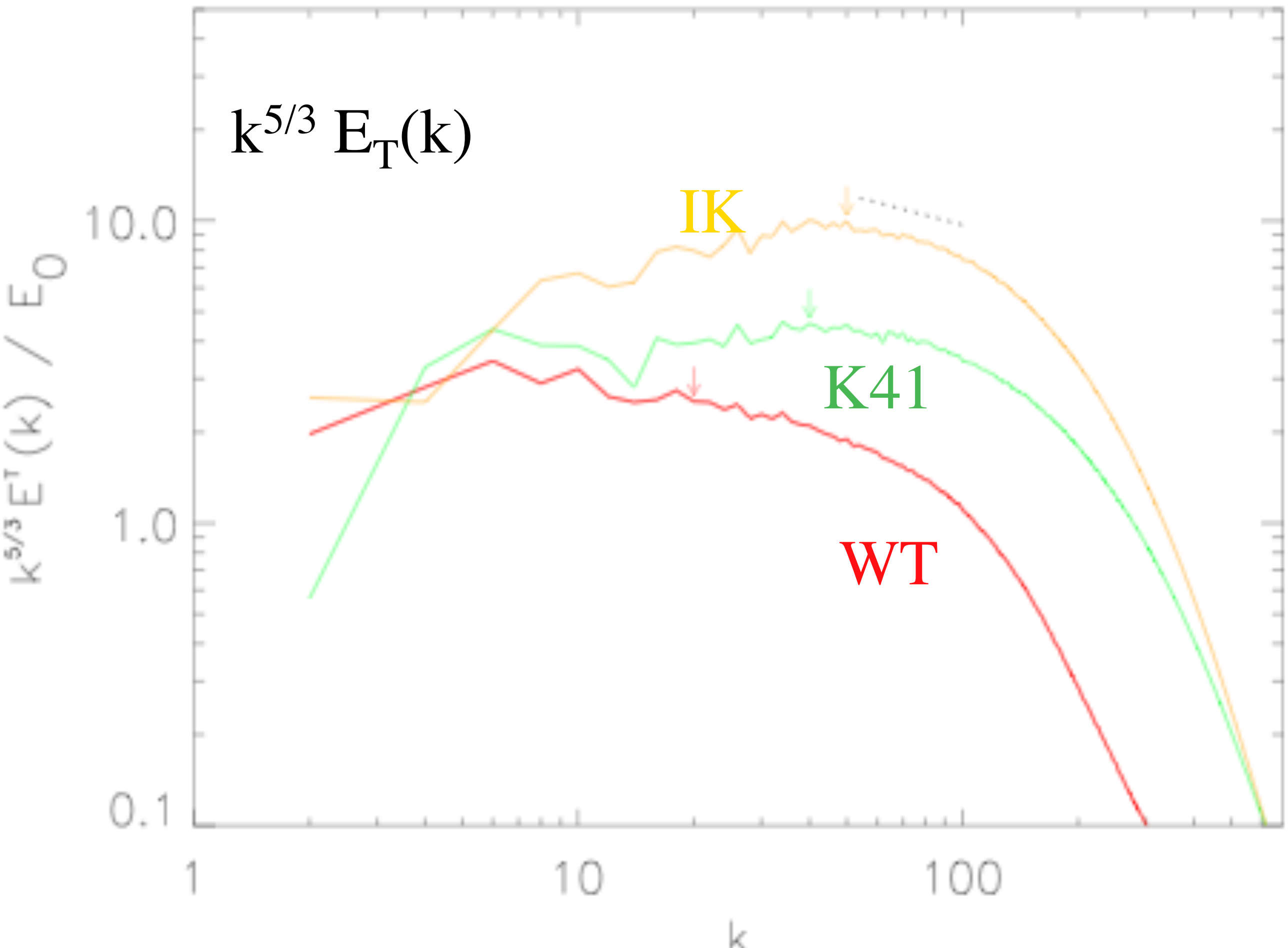

Lack of universality in MHD turbulence
B_0 = 0, F=0

- Do these spectral indices persist in time for a given flow?
- Would it be observed as well in the statistically steady state?

- Does the difference in indices persist at higher Reynolds number?
- Is there, in the IK case, a follow-up steeper spectrum?

Extreme events in the Solar Wind

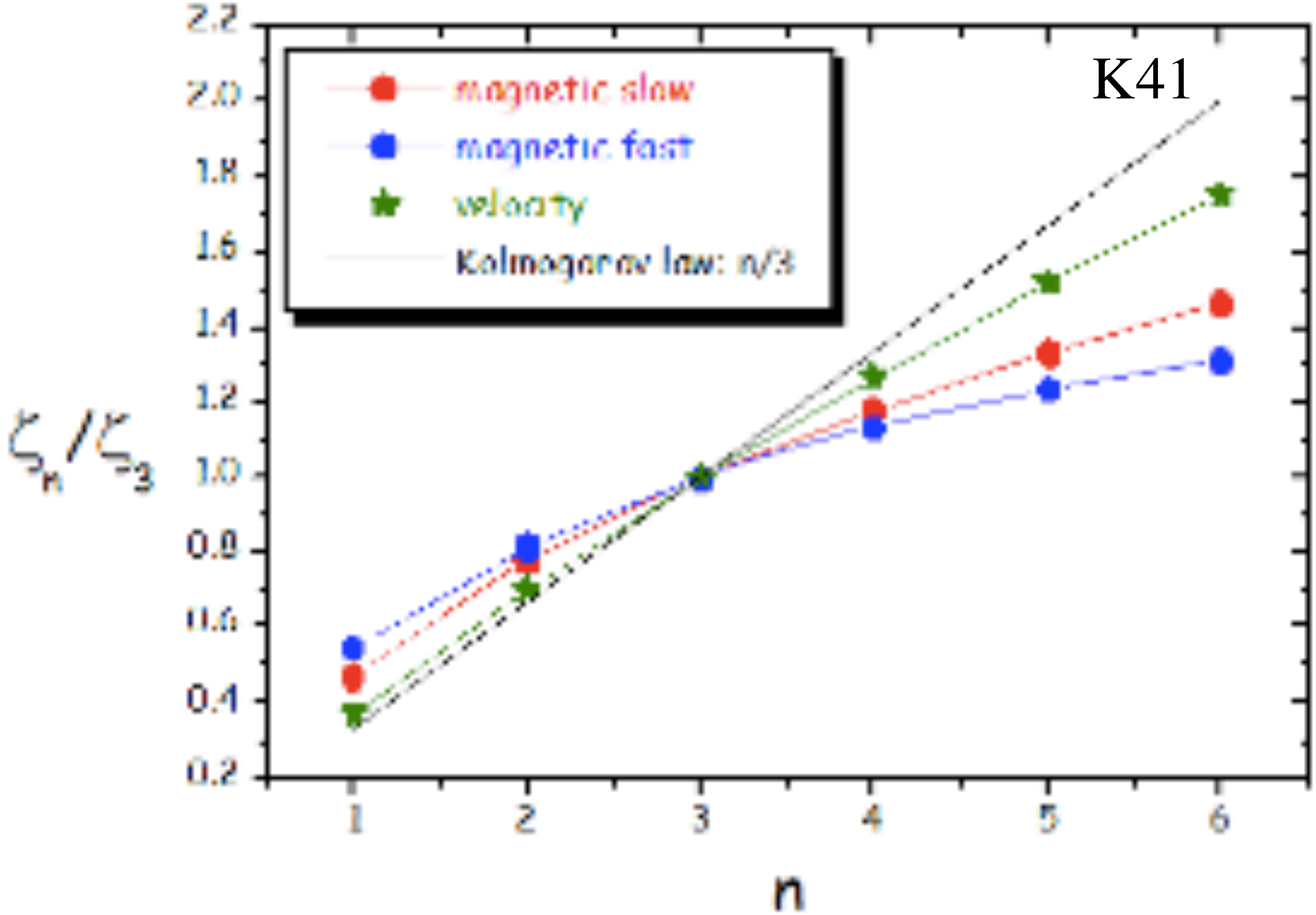

Fast vs. slow solar wind magnetic field,
and velocity data (Marino et al.)

Extreme events

in solar active regions

(Abramenko, review, 2007)

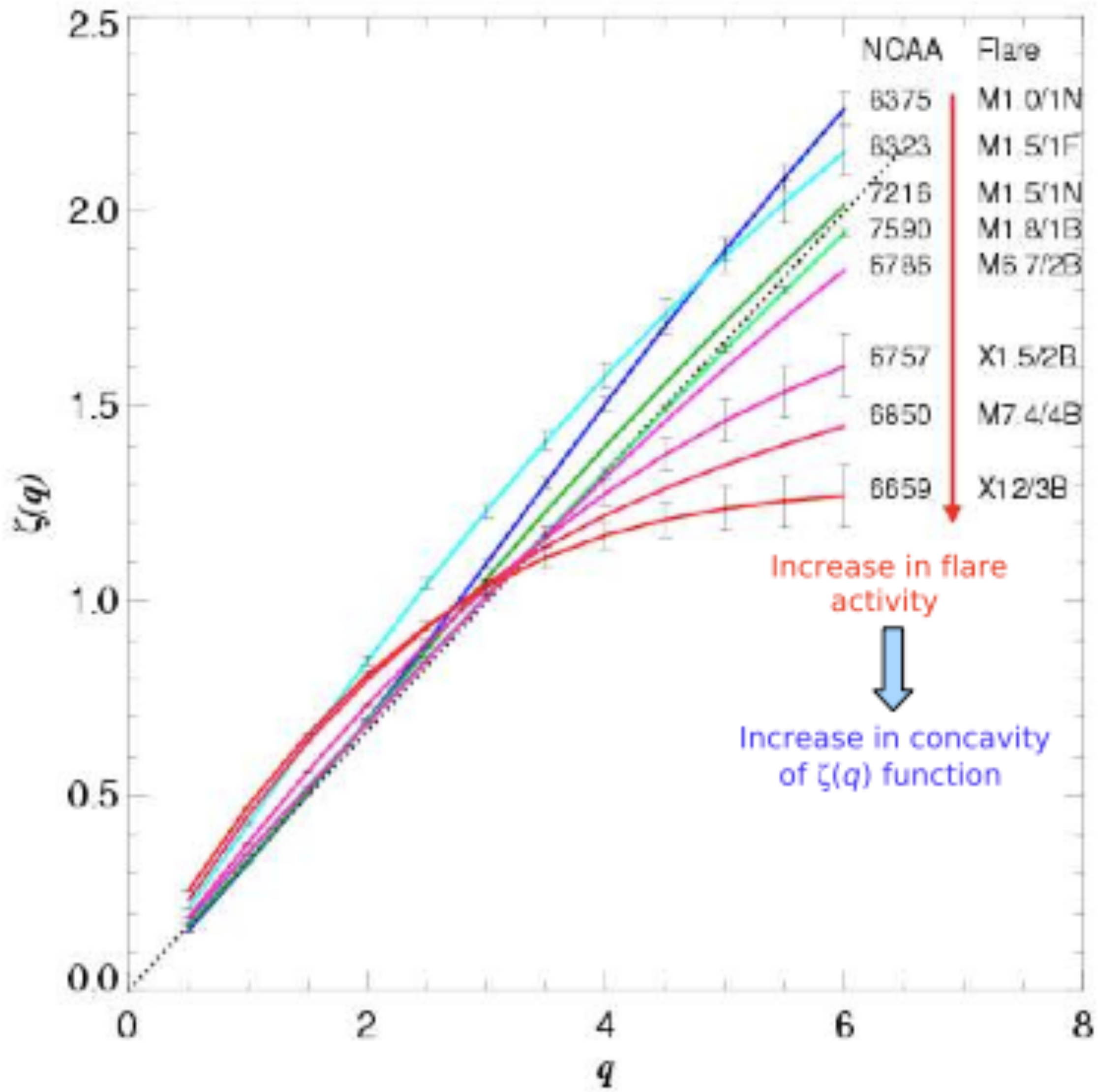

Figure 16: Scaling exponents $\zeta(q)$ of structure functions of order q calculated for eight active regions by Abramenko et al. (2002). The straight dotted line has a slope of $1/3$ and refers to the state of Kolmogorov turbulence. The NOAA number and the strongest flare (X-ray class/optical class) of each active region is shown. Increase of the flaring activity of active regions (from the top down to the bottom) is accompanied by general increase in concavity of $\zeta(q)$ functions.

Extreme events in numerical 3D MHD

- Scaling exponents, 512^3 DNS with varying B_0:
- As B_0 increases, so does the intermittency, i.e. the departure from a straight line

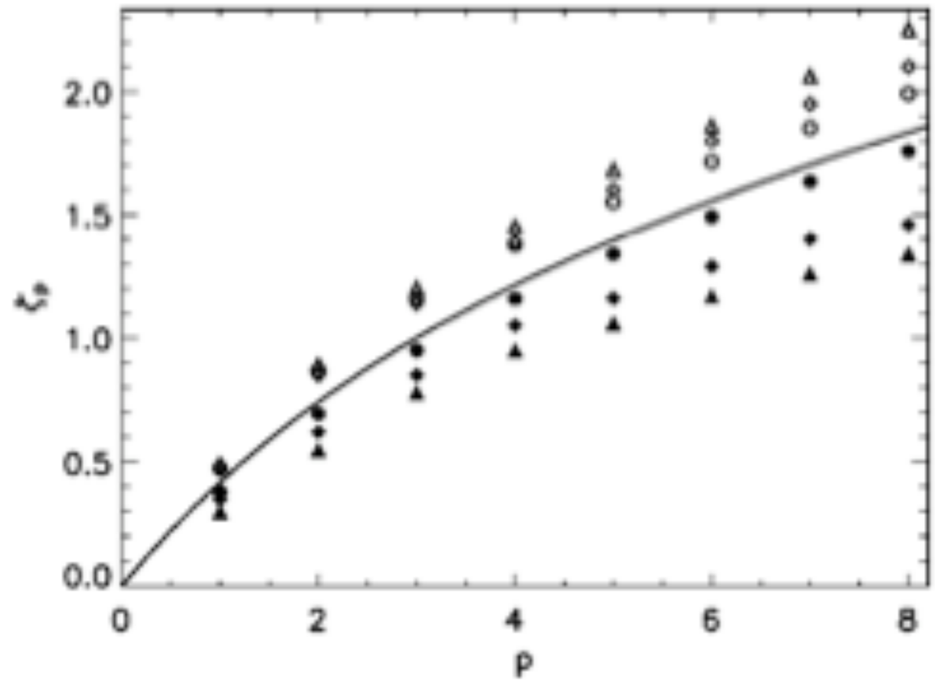

FIG. 1. Scaling exponents ζ_p of perpendicular (filled symbols) and parallel (open symbols) structure functions $S_p(\ell)=\langle|\delta z_\ell|^p\rangle$ for $B_0=0,5,10$ (circles, diamonds, triangles) together with isotropic

Müller & Biskamp, PRE 67 (2003)

Solar observation (Abramenkova et al.) MDI line of sight high res. magnetograms

- .6 x .6 arc sec., B> 17G, with 400 X 270 pixels and for long time series (up to 500 magnetograms)

- Is this a manifestation of weak MHD turbulence in the presence of a strong B?

The inertial slopes α measured
 from 3 to 10 Mm
(larger scale: sunspots) vary from
α=-2.3 (X-flare with index 130),
To α below 2.0 (flare index of 18),
To α=-1.6 (flare index of 0)

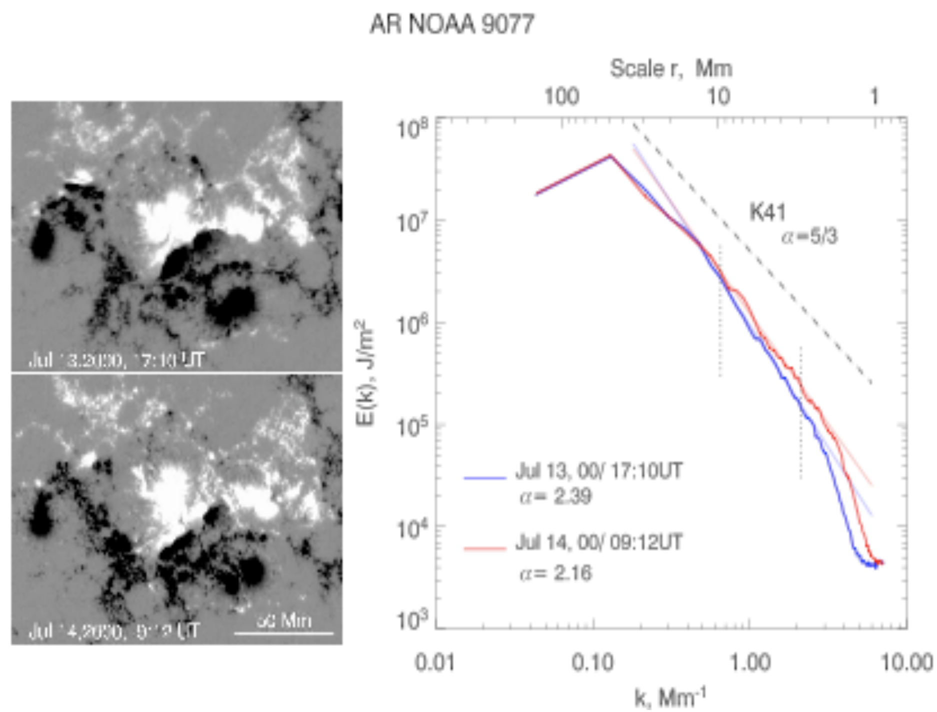

Solar observations (Abramenko et al.)
MDI - line of sight high res. magnetograms

Temporal variation of inertial index α in **dark black line**,

and flux in thin grey line

Kolmogorov 1941

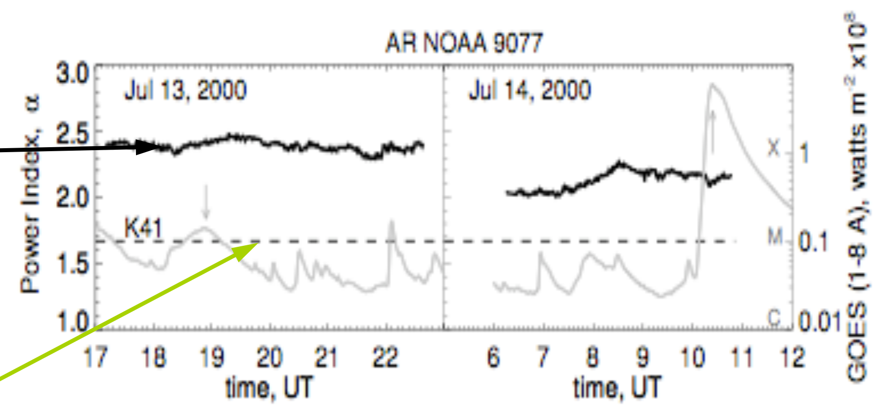

Fig. 2.— Time variations of the power index calculated for active region NOAA 9077 (left axis is valid for both panels). State of Kolmogorov turbulence is shown by *black dashed line*. GOES 1-8Å X-ray flux (right axis) is shown by *gray lines*. The arrows mark the X-ray flux peaks related to flares occurred in the active region under study.

Very active region with 37 flares (13 M, 3 X class)

Solar observations (Abramenko, 2005)

- *Temporal variation of **inertial index α** in dark black line, and flux in grey line*
- Or is it a manifestation of something else (like non-universal RMHD behavior)?

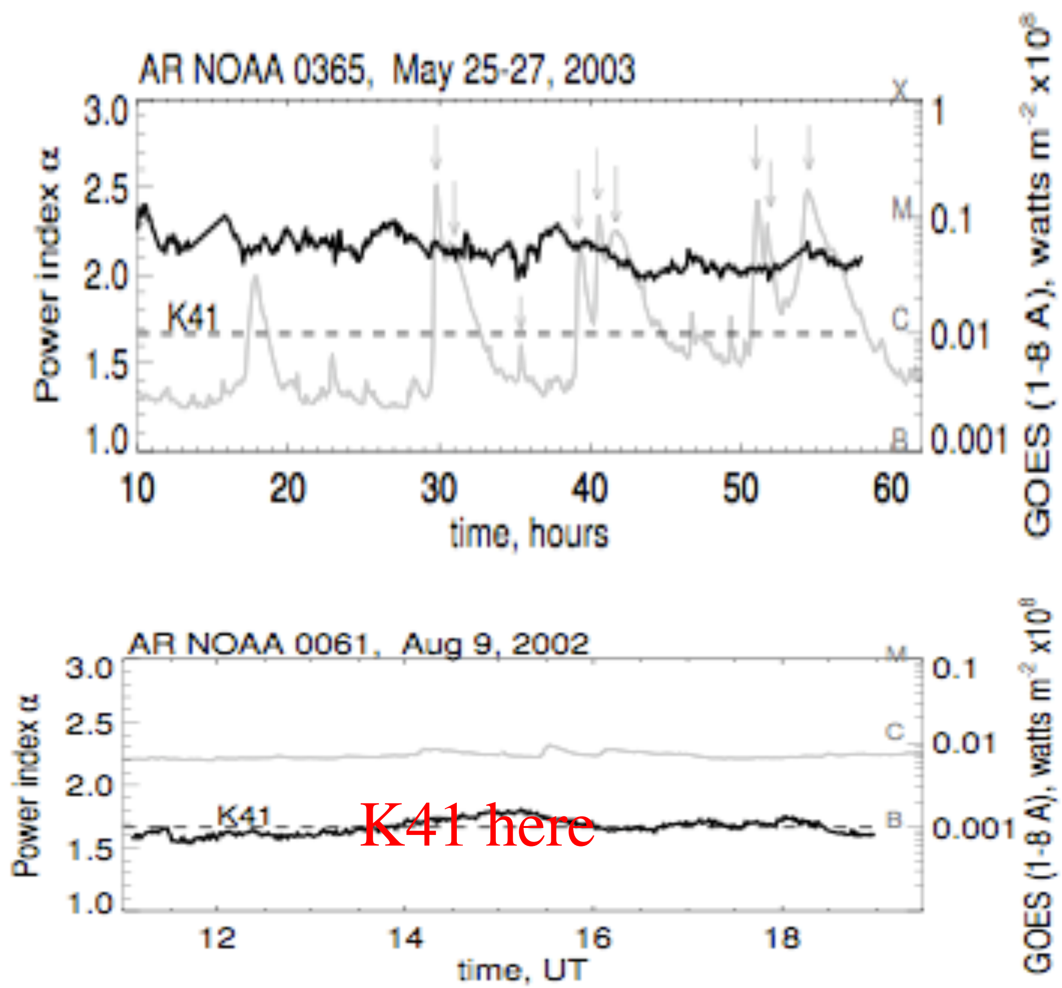

Do quiet regions follow Kolmogorov law?

But where is the intermittency?

Solar observations (Abramenko, 2005)

Variation of inertial index α **with flare type**

Stationarity (quiet) *vs.* bursty (chaotic, catastrophic) behavior?

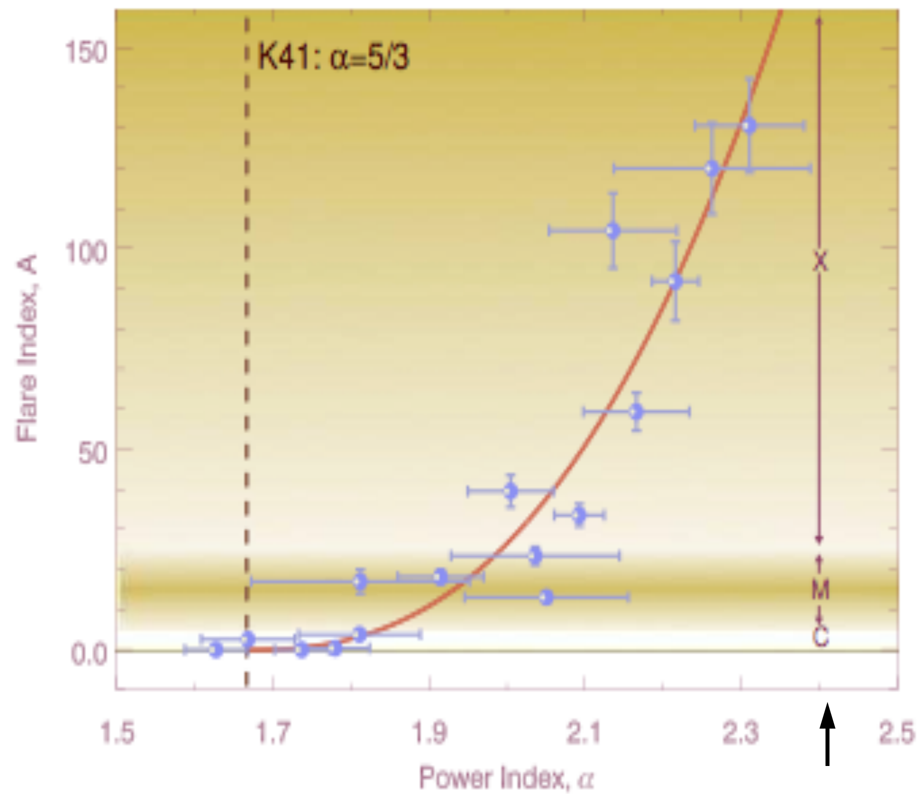

Flare type

Dmitruk, Gomez and Matthaeus, PoF 2003

Reduced MHD
Numerical data

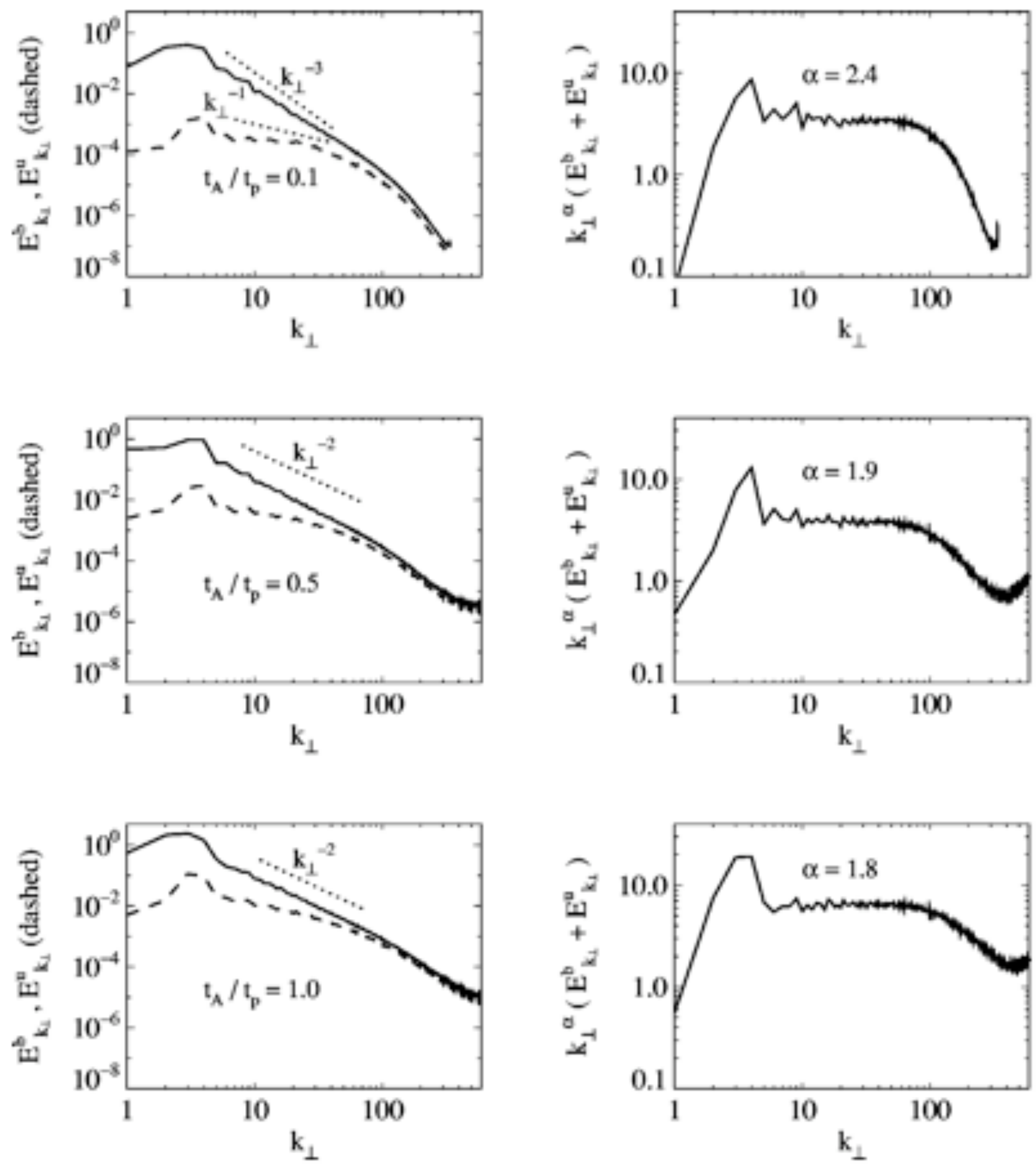

Rapazzo et al., 2008

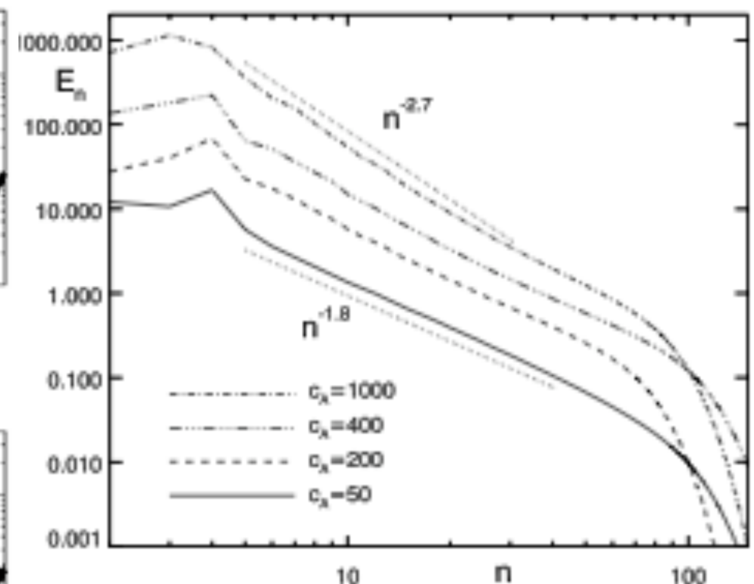

FIG. 8.—: Total energy spectra as a function of the wavenumber n for simulations F, G, H and I. To higher values of $c_{\mathcal{A}} = v_{\mathcal{A}}/u_{ph}$, the ratio between the Alfvén and photospheric velocities, correspond steeper spectra, with spectral index respectively 1.8, 2, 2.3 and 2.7.

Dmitruk, Gomez and Matthaeus, PoP

Reduced MHD
Numerical data

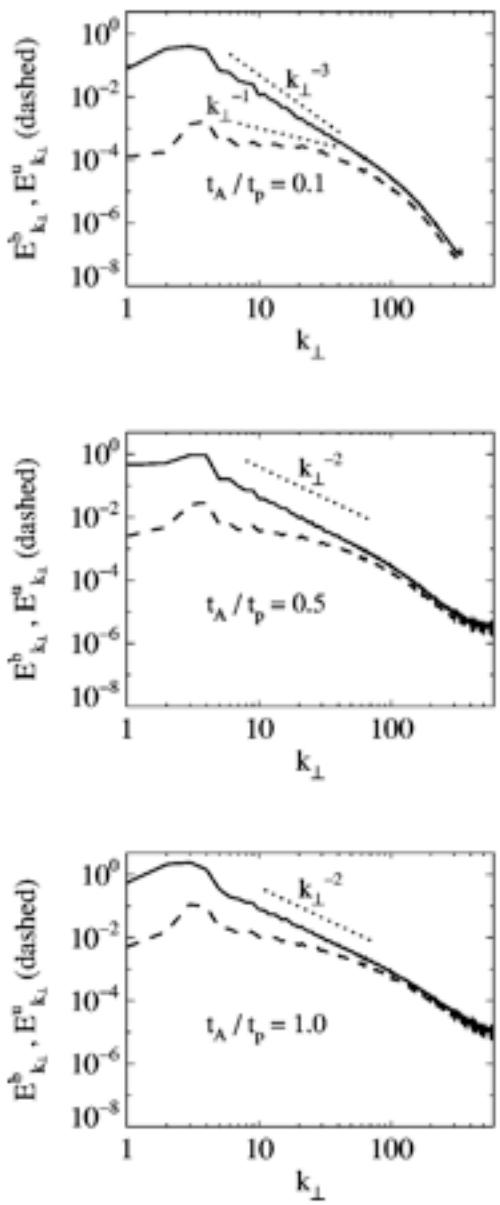

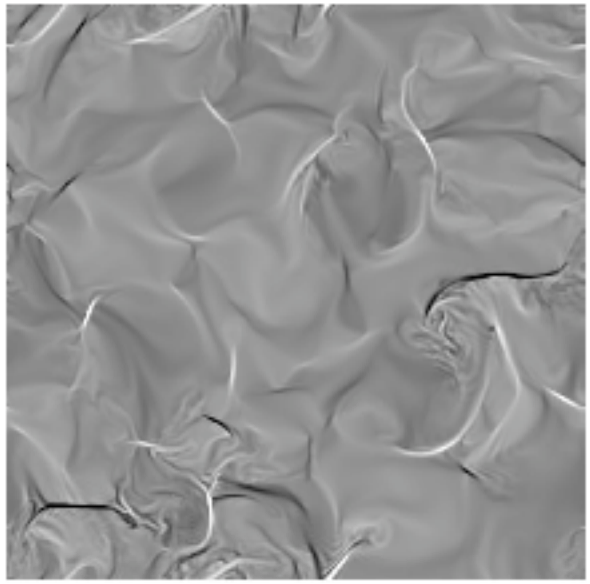

$t_A/t_p=0.5$

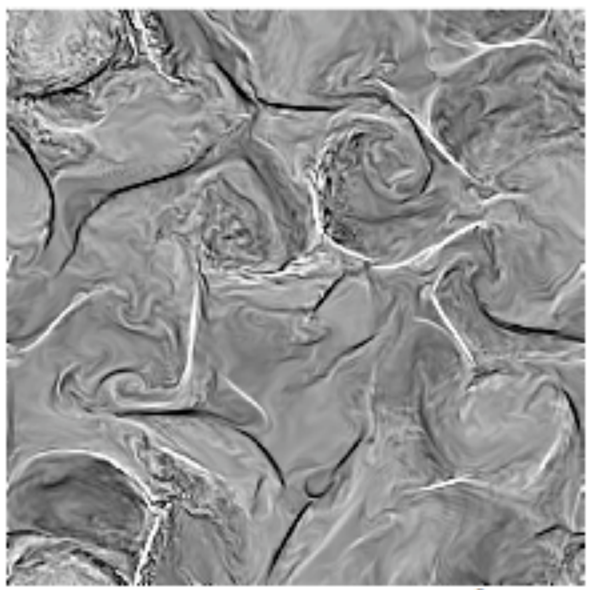

Rapazzo et al., 2008

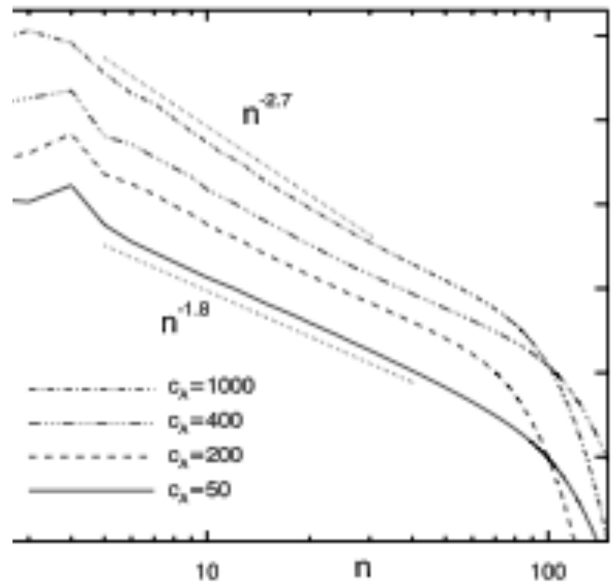

: Total energy spectra as a function of the er n for simulations F, G, H and I. To higher $_A = v_A/u_{ph}$, the ratio between the Alfvén and ric velocities, correspond steeper spectra, with dex respectively 1.8, 2, 2.3 and 2.7.

Grqppin Mueller PRL 2005

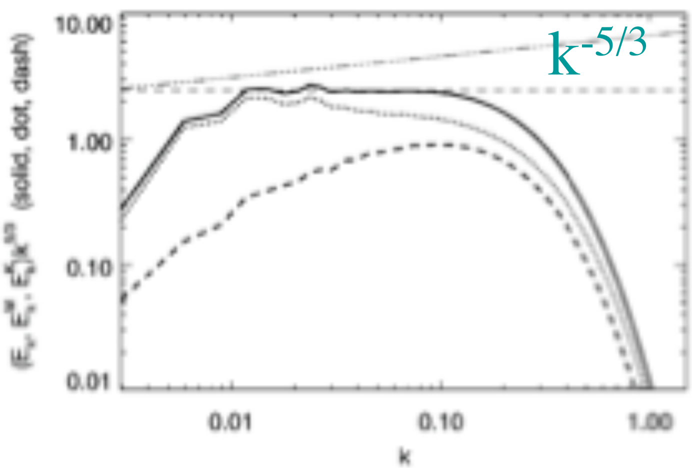

FIG. 1. Total (solid line), kinetic (dashed line), and magnetic (dotted line) energy spectra in 1024^3 case I simulation (normalized, time-averaged, and compensated). Dash-dotted line: $k^{-3/2}$ scaling.

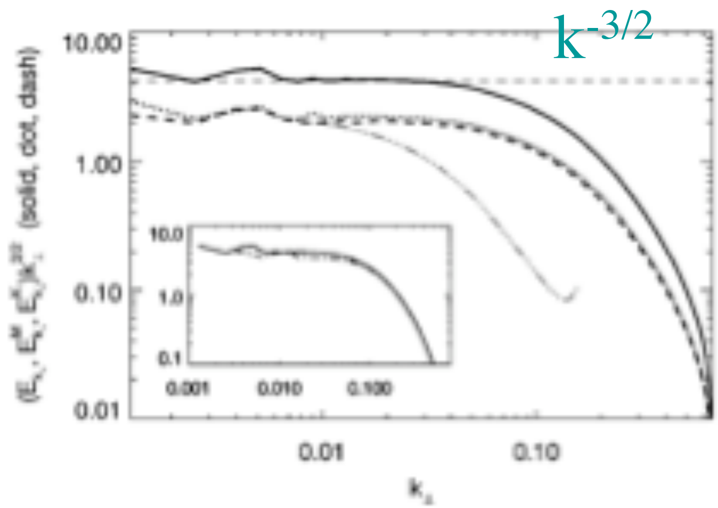

FIG. 2. Field-perpendicular total (solid line), kinetic (dashed line), and magnetic (dotted line) energy spectra (normalized, time-averaged, and compensated) in $1024^2 \times 256$ case II simulation with $b_0 = 5$. Dash-dotted curve: high-k part of field-parallel total energy spectrum. Inset: perpendicular total energy spectrum for resolutions of $512^2 \times 256$ (dash-dotted line) to $1024^2 \times 256$ (solid line).

Free decay, k0=4, EM=EV, PM=1
R=2700, HC~HM~0
1024^3, 9 T*

Forced, fixed energy up to k=2,
P_M=1,
R=2300, HC~0.15, HM~0.2 ,
B0=5, $b_{rms}=v_{rms}=1$,
1024^2 X 256,

Also: Maron et al, 2008: $k_{perp}^{-3/2}$

Going **beyond**, using models of turbulence

- Are spectral indices universal or do they change
  - with Rossby number, *at fixed Reynolds number?*
  - with Reynolds number, *at fixed Rossby number?*

Large Eddy Simulation (LES) with spectral modeling of turbulent flows *(Chollet & Lesieur, 1981)* but implementing:

- A dynamical fit to the computed energy spectrum instead of imposing Kolmogorov law
- Inclusion of helicity in both the eddy viscosity and the eddy noise
- (somewhat phase-preserving) eddy noise reconstruction

Numerical modeling

Direct Numerical Simulations
(DNS)

versus

Large Eddy Simulations
(LES)

* Resolve all scales
vs.
* Model (many) small scales

3D space & Spectral space

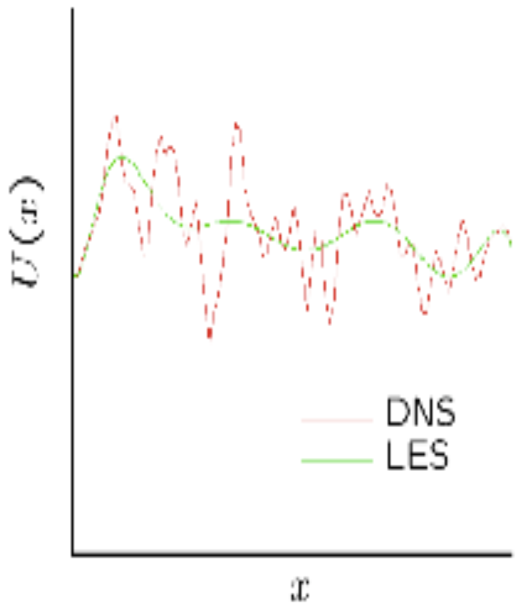

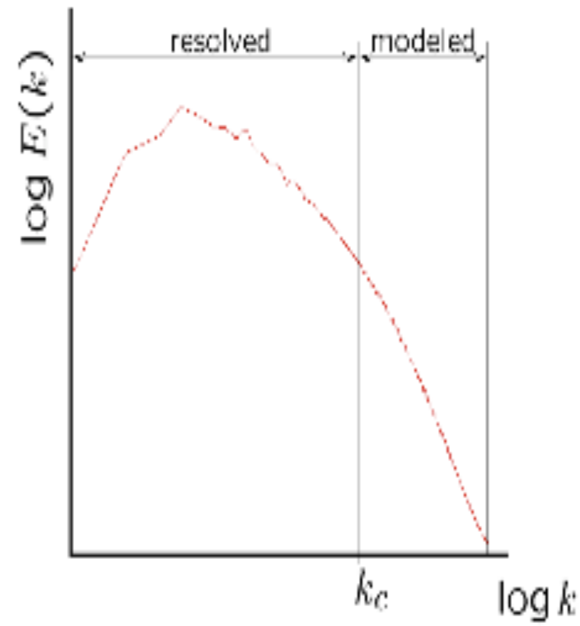

Slide from Comte, Cargese Summer school on turbulence, July 2007

Ratio of time scales: not constant in inertial range

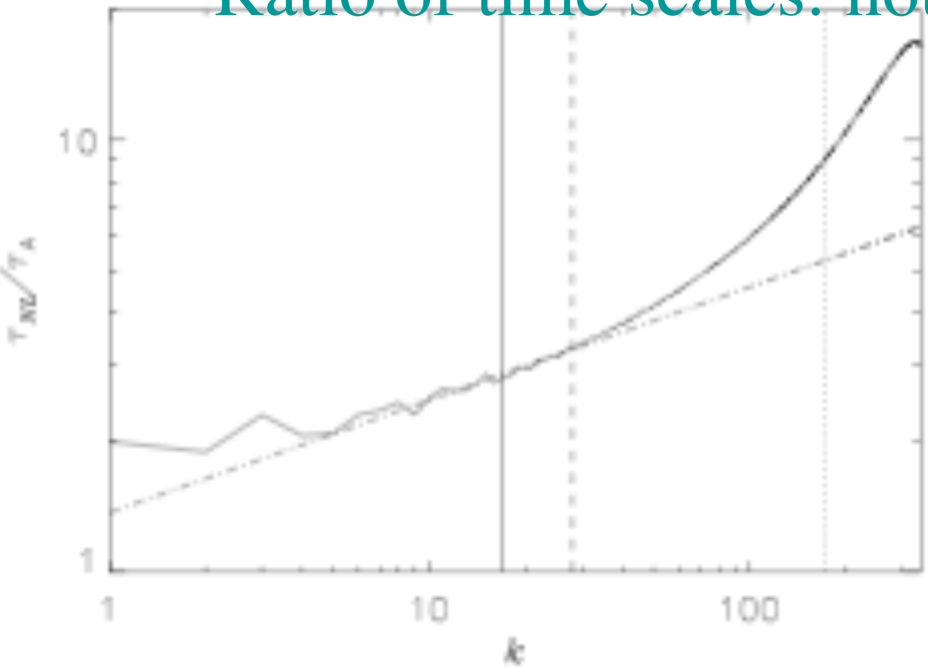

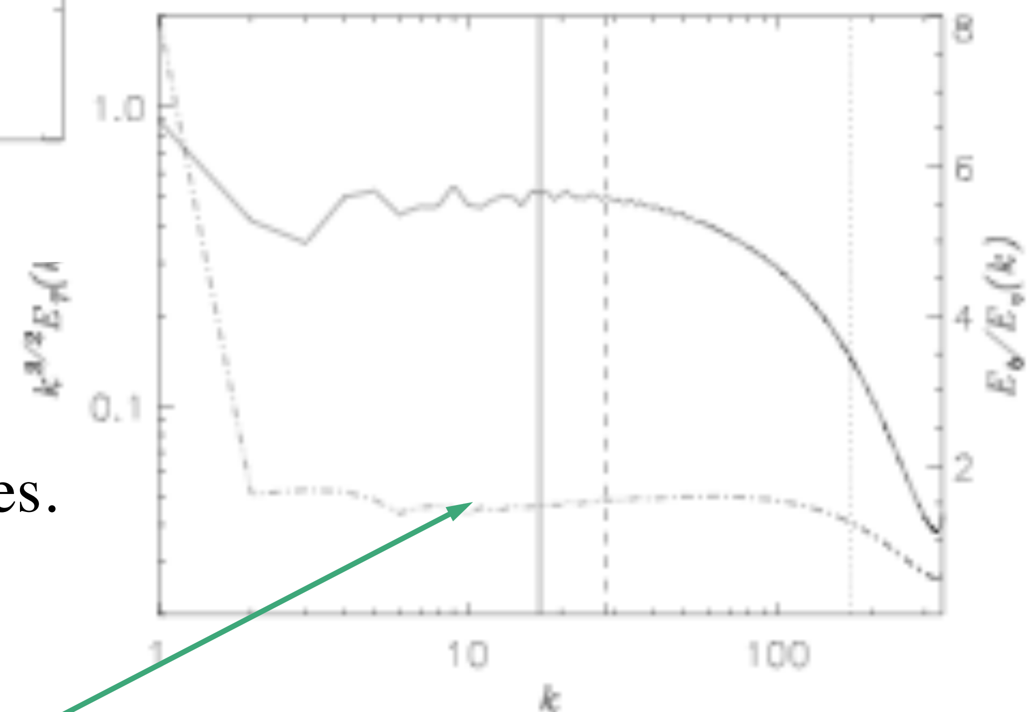

Lagrangian model, 6000^3 equiv. res.

Ratio $E_M(k)/E_V(k)$: constant in inertial range

Ratio of time scales: not constant in inertial range

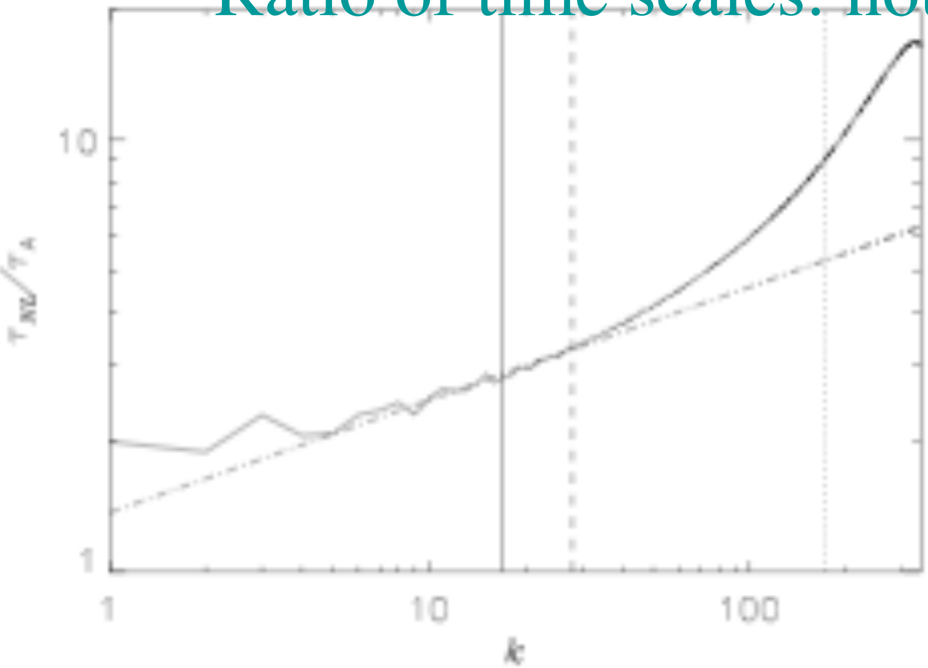

Lagrangian model, 6000^3 equiv. res.

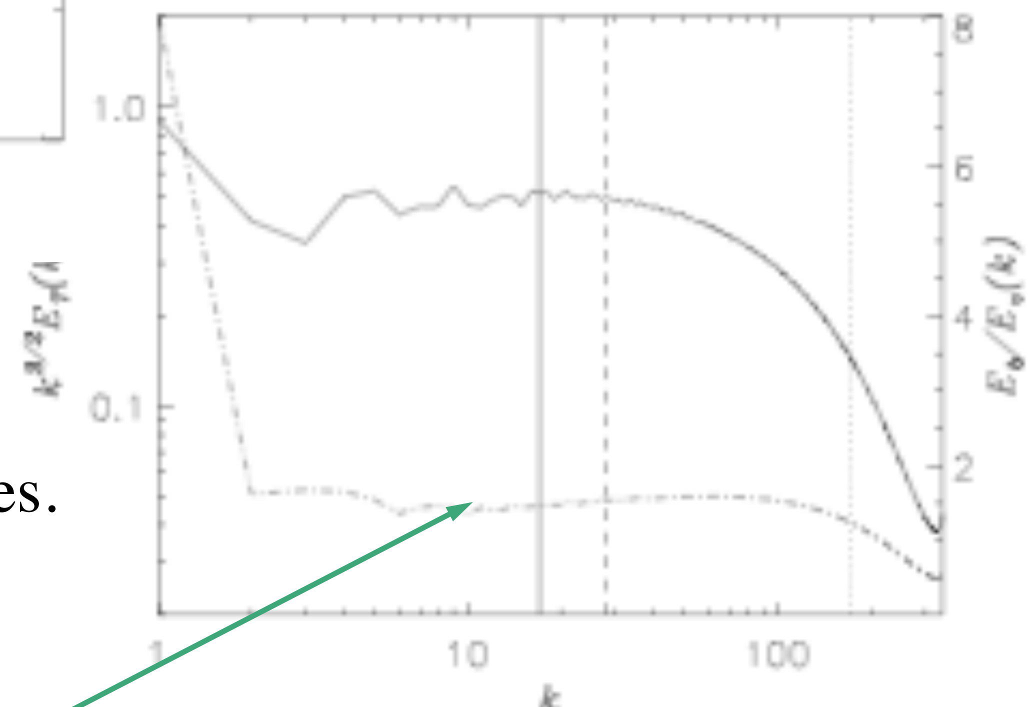

Ratio $E_M(k)/E_V(k)$, constant in inertial range: new paradigm?

Lagrangian-averaged (or alpha) Model for Navier-Stokes and MHD (LAMHD):

the velocity & induction are smoothed on lengths α_V & α_M, but not their sources (vorticity & current)

$$\mathbf{v} = \mathbf{u_s} + \delta\mathbf{v}, \ \mathbf{B} = \mathbf{B_s} + \delta\mathbf{B},$$

$$G_\alpha(\mathbf{r}, t) = \exp[-r/\alpha]/4\pi\alpha^2 r.$$

$$\mathbf{u_s} = G_{\alpha_V} \otimes \mathbf{v}, \ \mathbf{B_s} = G_{\alpha_M} \otimes \mathbf{B},$$

$$\mathbf{v} = (1 - \alpha_V^2 \nabla^2) \ \mathbf{u_s} \ \text{and} \ \mathbf{B} = (1 - \alpha_M^2 \nabla^2) \ \mathbf{B_s}$$

Equations preserve invariants (in modified - filtered L_2 --> H_1 form)

McIntyre (mid '70s), Holm (2002), Marsden, Titi, …, Montgomery & AP (2002)

Lagrangian-averaged NS & MHD Model Equations for the **ideal** case

Invariants of the MHD-alpha equations in two space dimensions

$$E = \frac{1}{2}\int d^2\mathrm{x}\,(\mathrm{u_s}\cdot\mathrm{v} + \mathrm{B_s}\cdot\mathrm{B})\ ,$$

$$H_C = \frac{1}{2}\int d^2\mathrm{x}\ \mathrm{v}\cdot\mathrm{B_s}\ ,$$

$$\mathcal{A} = \frac{1}{2}\int d^2\mathrm{x}\ A^2_{s_z}\ .$$

- The invariants, to which the usual Kolmogorov -like phenomenology will apply, involve **BOTH** the smoothed fields and the raw ones (H_1 norm instead of L_2)
- In 3D, replace A by magnetic helicity

Lagrangian-averaged NS & MHD **dissipative** Model Equations

- Advection by smooth velocity field
- The velocity equation involves both the smooth and rough fields
- The induction equation involves only smooth fields, except for dissipation which, in terms of B_s, is hyperdiffusive

(remember: $v_k \sim (1- \alpha^2_v k^2)\, u_{s,k}$, $B_k \sim (1- \alpha^2_m k^2)\, B_{s,k}$)

Scientific framework

- In the MHD, understanding the processes by which energy is distributed and dissipated down to kinetic scales, and the role of nonlinear interactions and turbulence in the Sun and for space weather
- Modeling of turbulent flows with magnetic fields in three dimensions, taking into account long-range interactions between eddies and waves, and the geometrical shape of small-scale eddies
- Understanding Cluster observations in preparation for a new remote sensing NASA mission (MMS: Magnetospheric Multi-Scale)

Cancellation Exponent

Rapid change of sign of fields of zero mean (& derivatives)

Ott *et al.*, 1992: sign-singular measure $\mu_i(l)$ as the difference of two probabilities, for disjoint subsets $Q_i(l)$ of size l covering $Q(L)$

$$\mu_i(l) = \frac{1}{\int_{Q(L)} d\boldsymbol{r}\, |f(\boldsymbol{r})|} \int_{Q_i(l)} d\boldsymbol{r}\, f(\boldsymbol{r}) \qquad (1)$$

As l grows, cancellations between structures of opposite signs occur

$$\chi(l) = \sum_{Q_i(l)} |\mu_i(l)| \sim l^{-\kappa} \qquad (2)$$

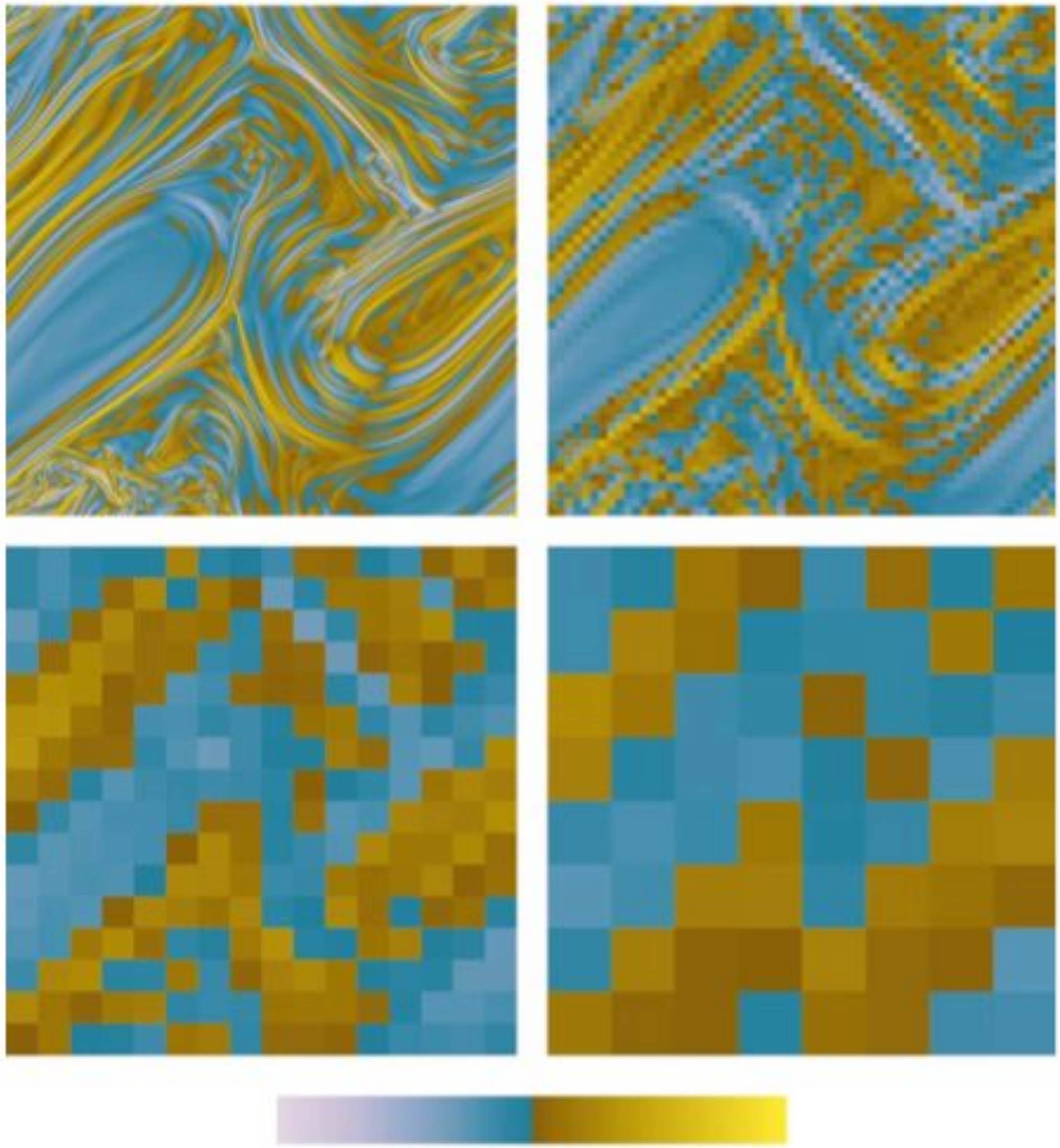

FIG. 3. (Color) The coarse-grained signed measure of the current J at time $t=7.3$ for four different box sizes, namely $l/L=0.001$, $l/L=0.016$, $l/L=0.059$, $l/L=0.12$, from top to bottom. Colors range from cyan for negative J values to yellow for positive ones, going through blue and brown. Cancellations at large scales are responsible for the decrease in magnitude of the measure.

Sorriso-Valvo et al., PoP **9** (2002)

Cancellation exponent κ *(upper curve)* and magnetic dissipation (lower curve): comparison of DNS and LAMHD

*Graham et al., PRE **72**, 2005*

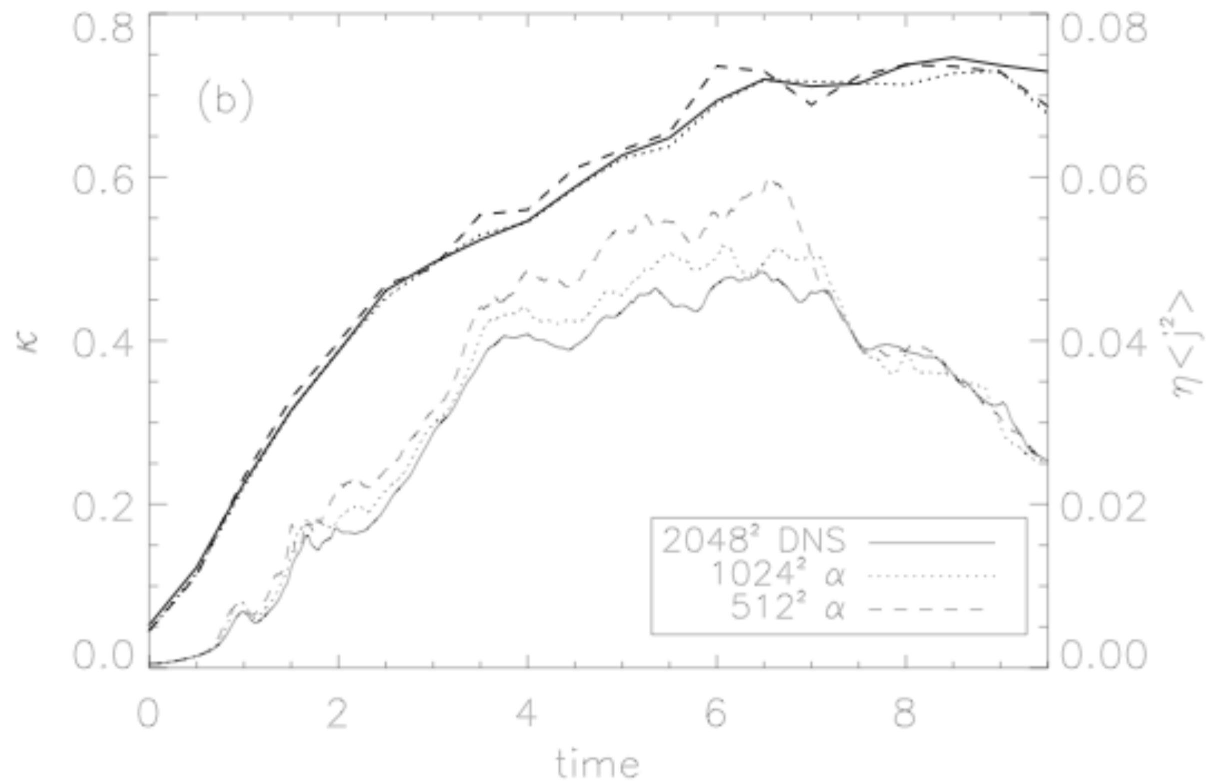

$\varkappa = [\mathrm{d} - d_F]/2$ *(see Sorriso-Valvo et al. PoP, 2002)*

Variation of correlation with scale

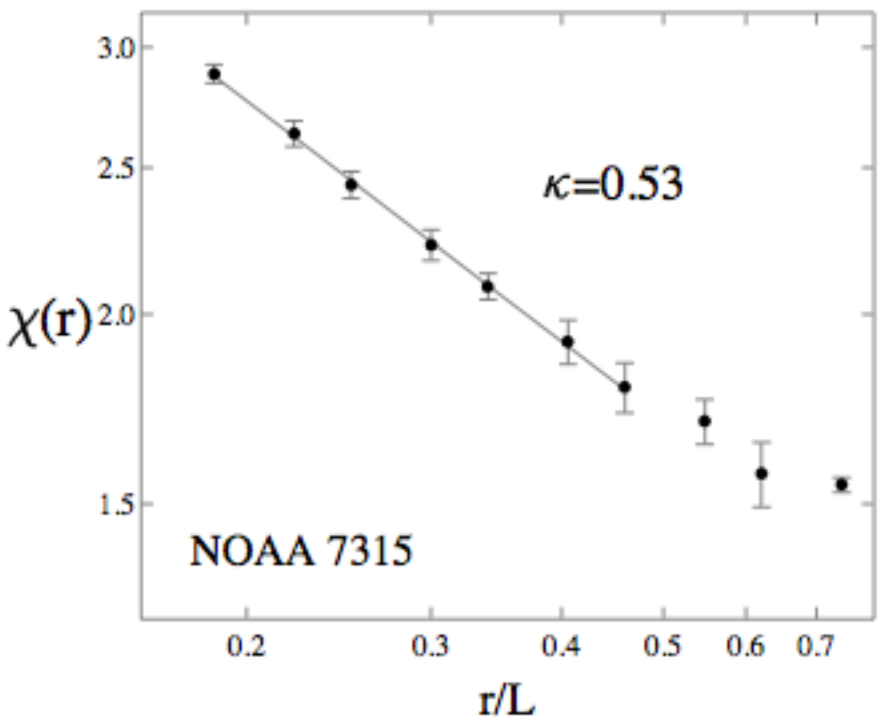

- Solar data,

active region

2D-MHD

- Three invariants:
  - Total energy $E_T = \langle v^2/2 + b^2/2 \rangle$
  - Cross-helicity $\mathbf{H_c = \langle v.b \rangle}$
  - Magnetic potential $\mathbf{E_A = \langle a^2 \rangle}$, b = **curl** a

- These invariants have different physical dimensions: E_A is more ``large-scale'' than E_T and H_c

- Statistical equilibria: possibility of an inverse cascade of E_A together with **direct cascades of E_T** and of H_c (all observed numerically), like in 3D.

- Is H_c ``more'' or ``less'' invariant than E_T?
  W**hat happens to the ratio H_c / E_T**? (selective decay)

Cascades in forced 2D-MHD

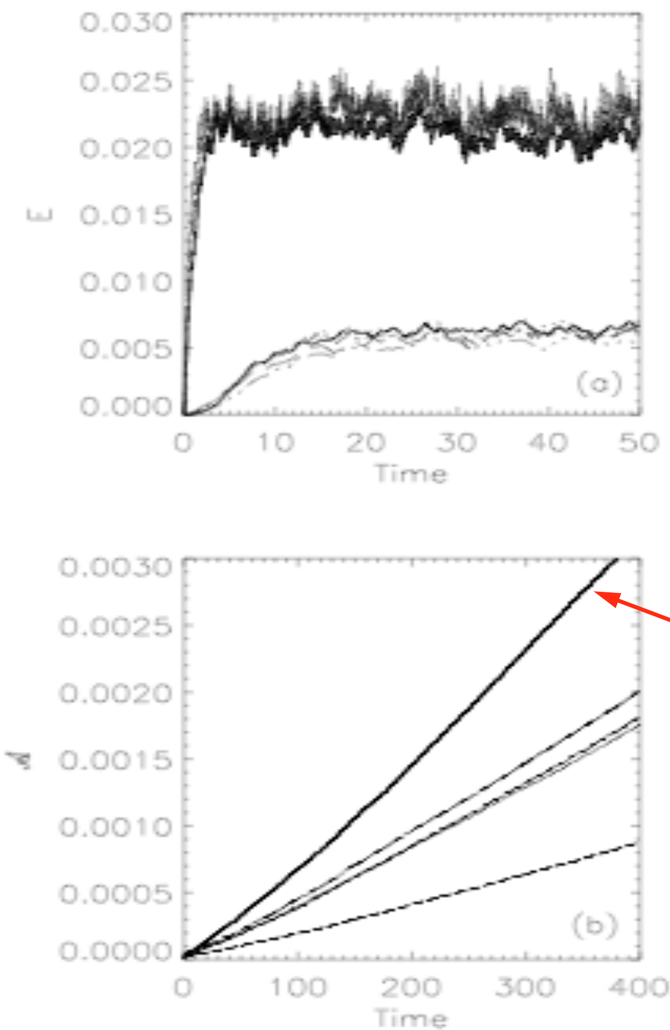

- **Energies** (top: magnetic; bottom: kinetic} as a function of time are correctly represented in the model
- However, the growth of squared magnetic potential due to the inverse cascade is always smaller than for DNS *(solid line)*
- Negative resistivity instability which involves the small scales

  where the filtering occurs

Inverse Cascade of Magnetic Potential

Normalized energy difference

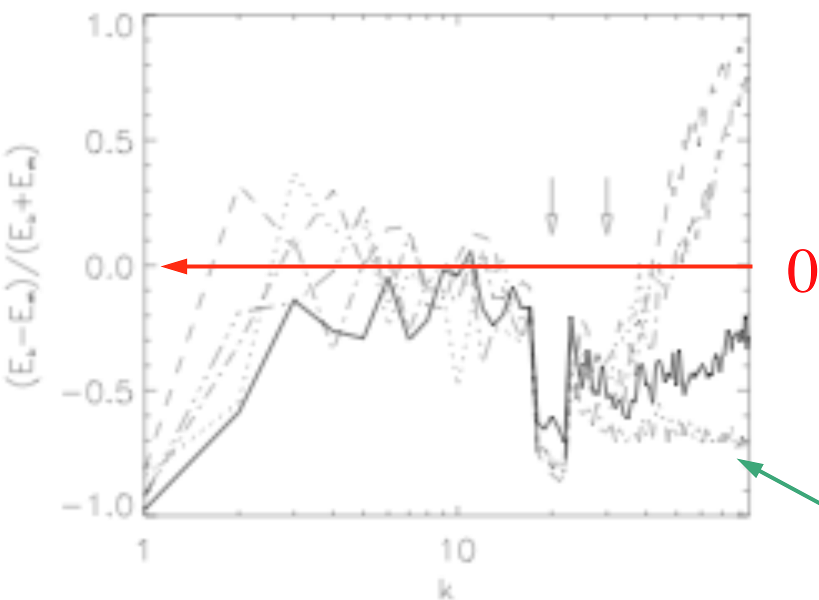

- Turbulent magnetic resistivity
  $\eta_{turb} \sim E_V - E_M$ in the small scales
  is <0 when $E_M > E_V$, and is responsible for the inverse cascade
  (*AP*, JFM 1978; turbulence closure result)

Solid line: DNS; other lines: α runs
(arrows indicate values of alpha)

- Change of sign of η_{turb} in small scales for α runs
  (except for the one with α_m*=0)*

- In conclusion:

- The LAMHD model works up to the cut-off length α
- The errors are smaller than for under-resolved runs
- The growth rate of large-scale instabilities is OK in 3D

The model allows for computations in regimes of turbulence never explored before at a known given Reynolds number

Phys. Fluids 17, 035112; and 18, 045106 and 20, 035107; Phys Rev E 76, 056310

Validation of LES: temporal evolution of total energy

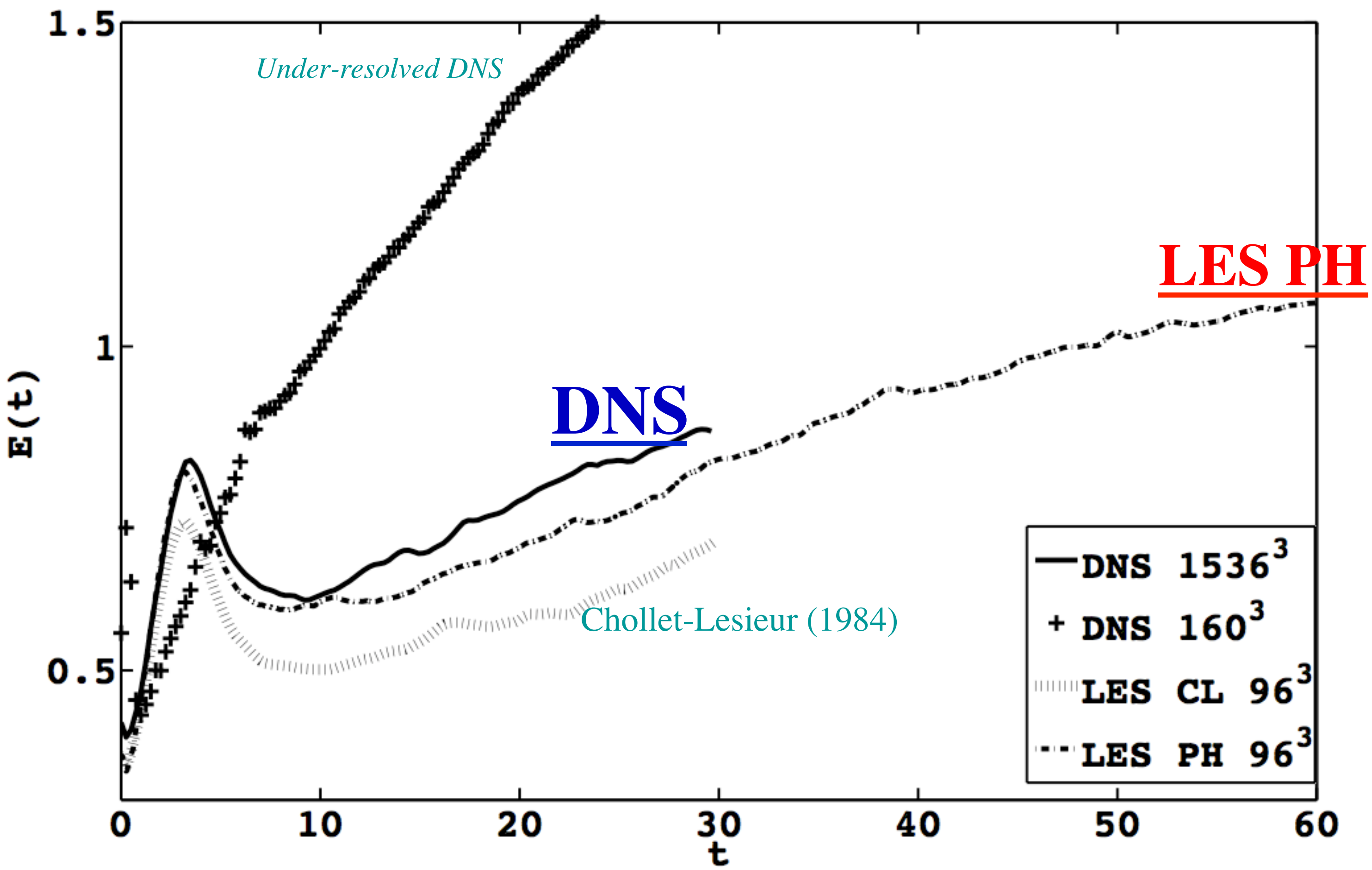

Savings in CPU : 0.5*[1536/96]^4 ~ 30,000 *(also for memory)*

Validation of LES, energy spectrum

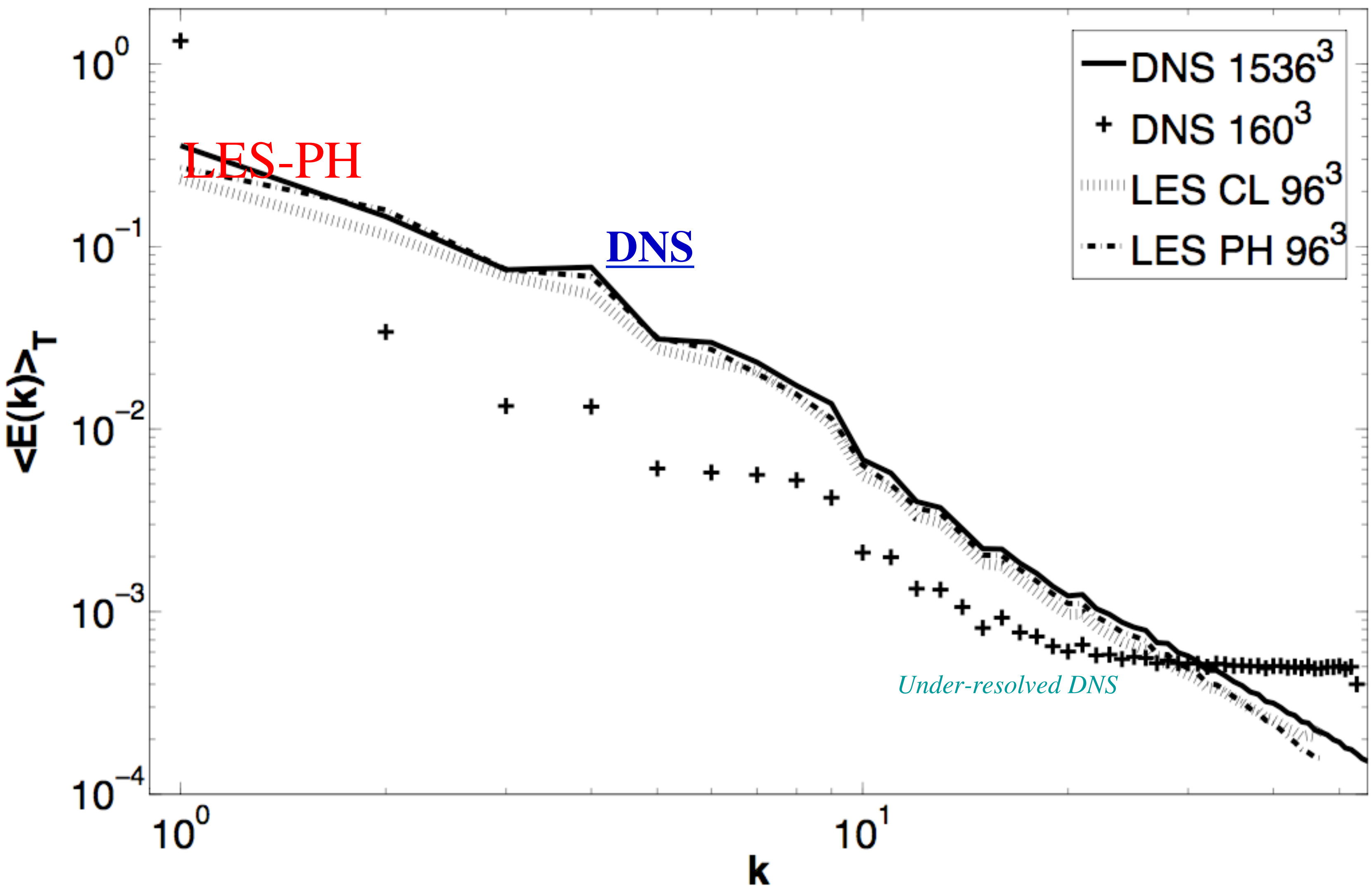

Validation of LES, Helicity spectrum

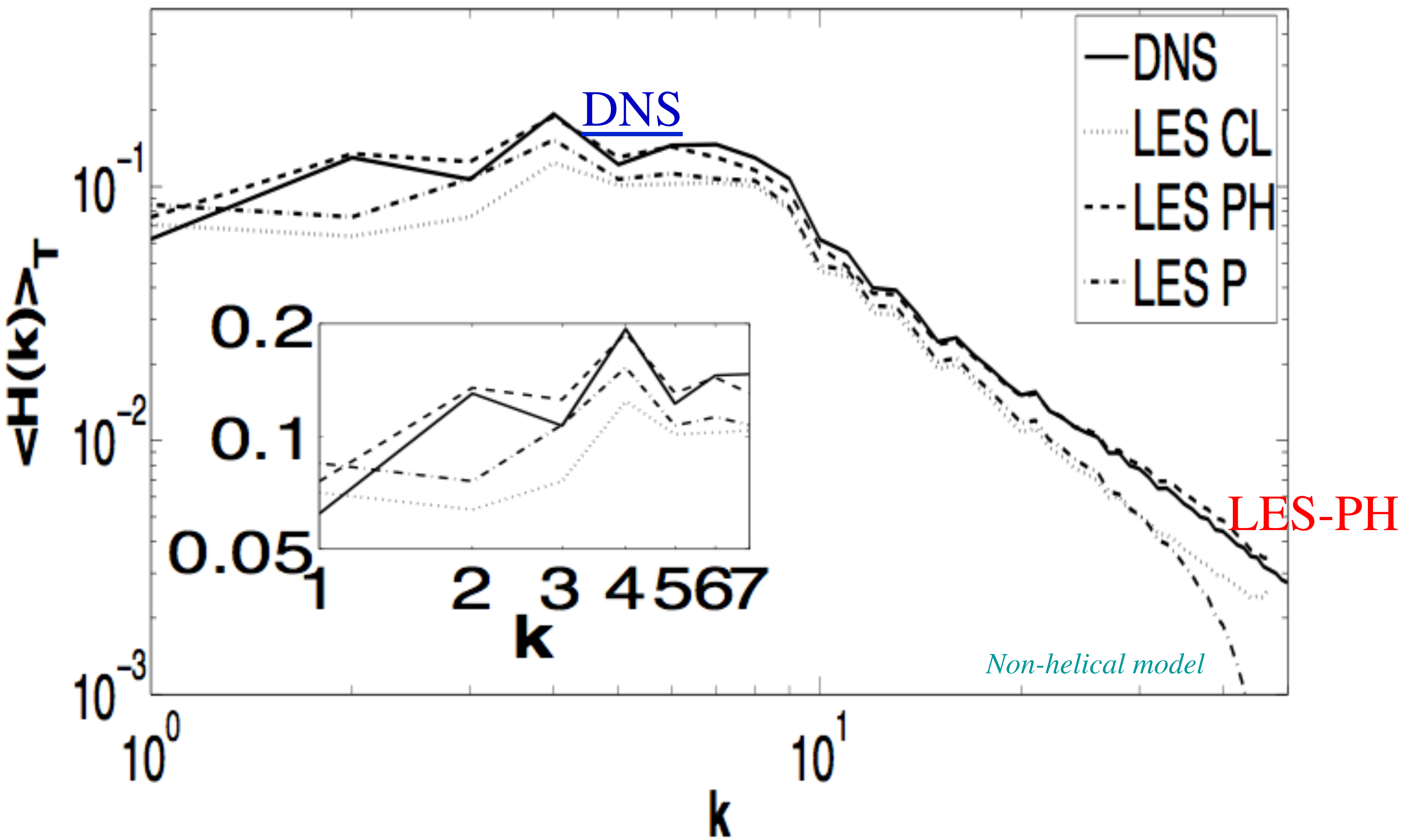

Phenomenologies for MHD turbulence

- *MHD could be like* ***fluids*** → *Kolmogorov spectrum* $E_{K41}(k) \sim k^{-5/3}$

Or

- ***Slowing-down*** *of energy transfer to small scales because of Alfvén waves propagation along a (quasi)-uniform field* B_0: $E_{IK}(k) \sim (\varepsilon^T B_0)^{1/2} k^{-3/2}$

  (Iroshnikov - Kraichnan (IK), mid '60s)

  $T_{transfer} \sim T_{NL} * [T_{NL}/T_A]$, *or 3-wave interactions but still with isotropy.*
  Eddy turn-over time $T_{NL} \sim l/u_l$ *and wave (Alfvén) time* $T_A \sim l/B_0$

And

- **Weak turbulence** theory for MHD *(Galtier et al PoP 2000)*: anisotropy develops and the exact spectrum is: $E_{WT}(k) = C_w\, k_{perp}^{-2} f(k_{//})$

  Note: WT is IK -compatible when isotropy ($k_{//} \sim k_{perp}$) *is assumed:* $T_{NL} \sim l_{perp}/u_l$ *and* $T_A \sim l_{//}/B_0$

Or $k_{perp}^{-5/3}$ *(Goldreich Sridhar, APJ '95)* ? Or $k_{perp}^{-3/2}$ *(Nakayama '99; Boldyrev '06, Yoshida '07)* ?

Another way to go to higher Reynolds numbers …

Moore's law: Doubling of speed of processors every 18 months implies doubling of resolution for DNS in 3D every 6 years …

* *Develop models of turbulent flows (Large Eddy Simulations, closures, Lagrangian-averaged, …)*
* Improve numerical techniques

* Be patient

- Is Adaptive Mesh Refinement (AMR) a solution?

- *If so, how do we adapt? How much accuracy do we need?*

The need for Adaptive Mesh Refinement

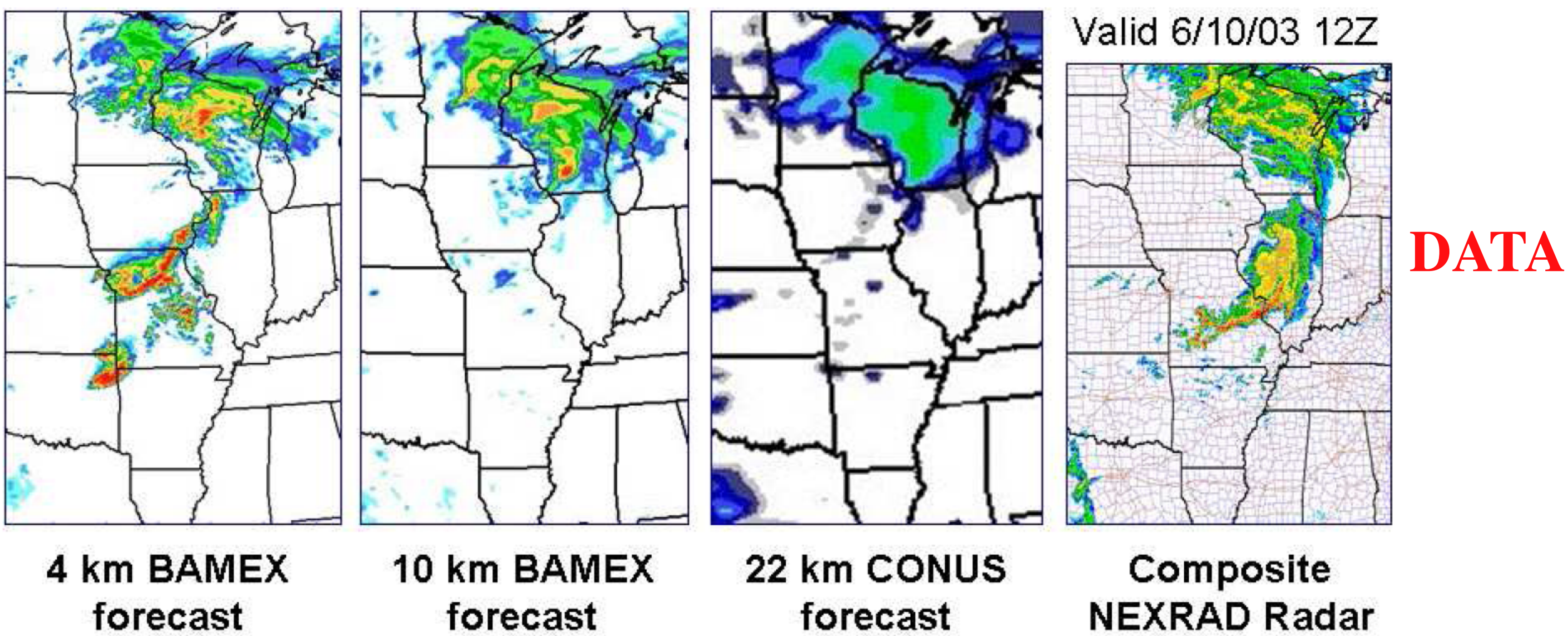

Figure 1: From Bill Skamarock, showing the lack of convergence with model resolution.

AMR on 2D Navier-Stokes

Rosenberg et al., JCP 2006;
Aimé Fournier et al., 2008

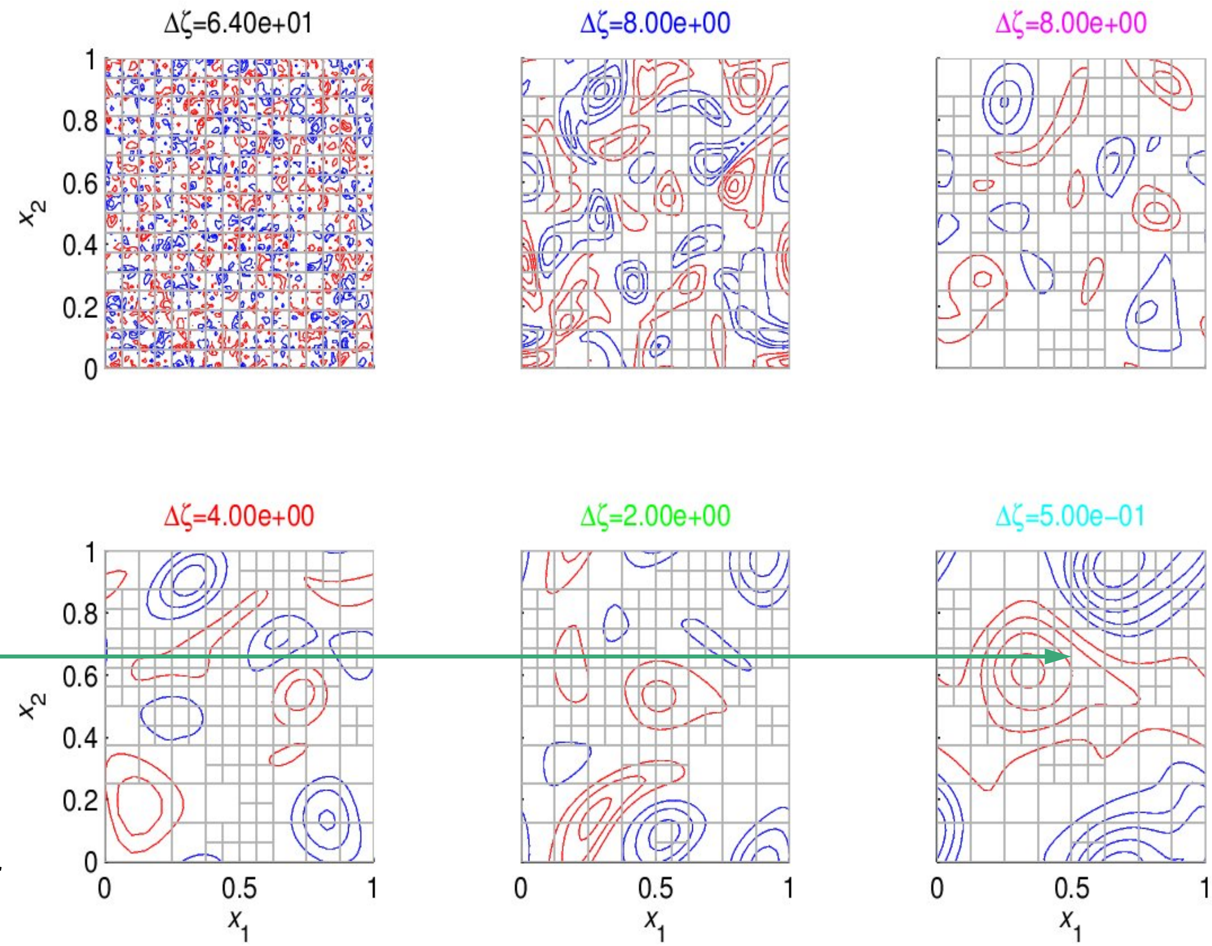

- Decay for long times (incompressible)
- Formation of dipolar vortex structures
- Lesser number of degrees of freedom (~ 1/4) with AMR, compared to an equivalent pseudo-spectral code (periodic boundary conditions)

(but ….)

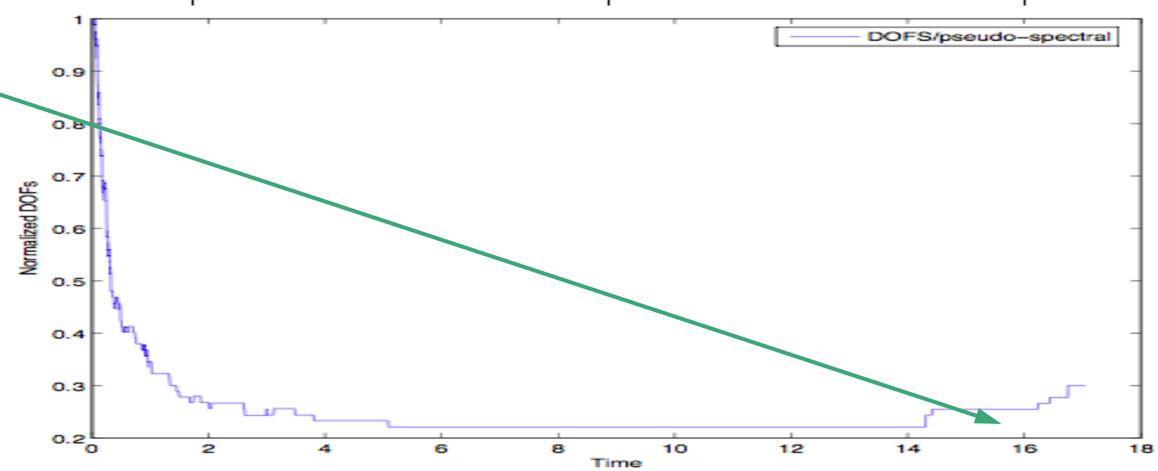

AMR in incompressible 2D - MHD turbulence at R~1000

- AMR using spectral elements of **different orders, P;**
- DNS is in black
- No noticeable differences when using the L_2 norms (energy and its dissipation)
- But **accuracy matters** when looking at Max norms, here the current

Rosenberg et al., New J. Phys., 2007

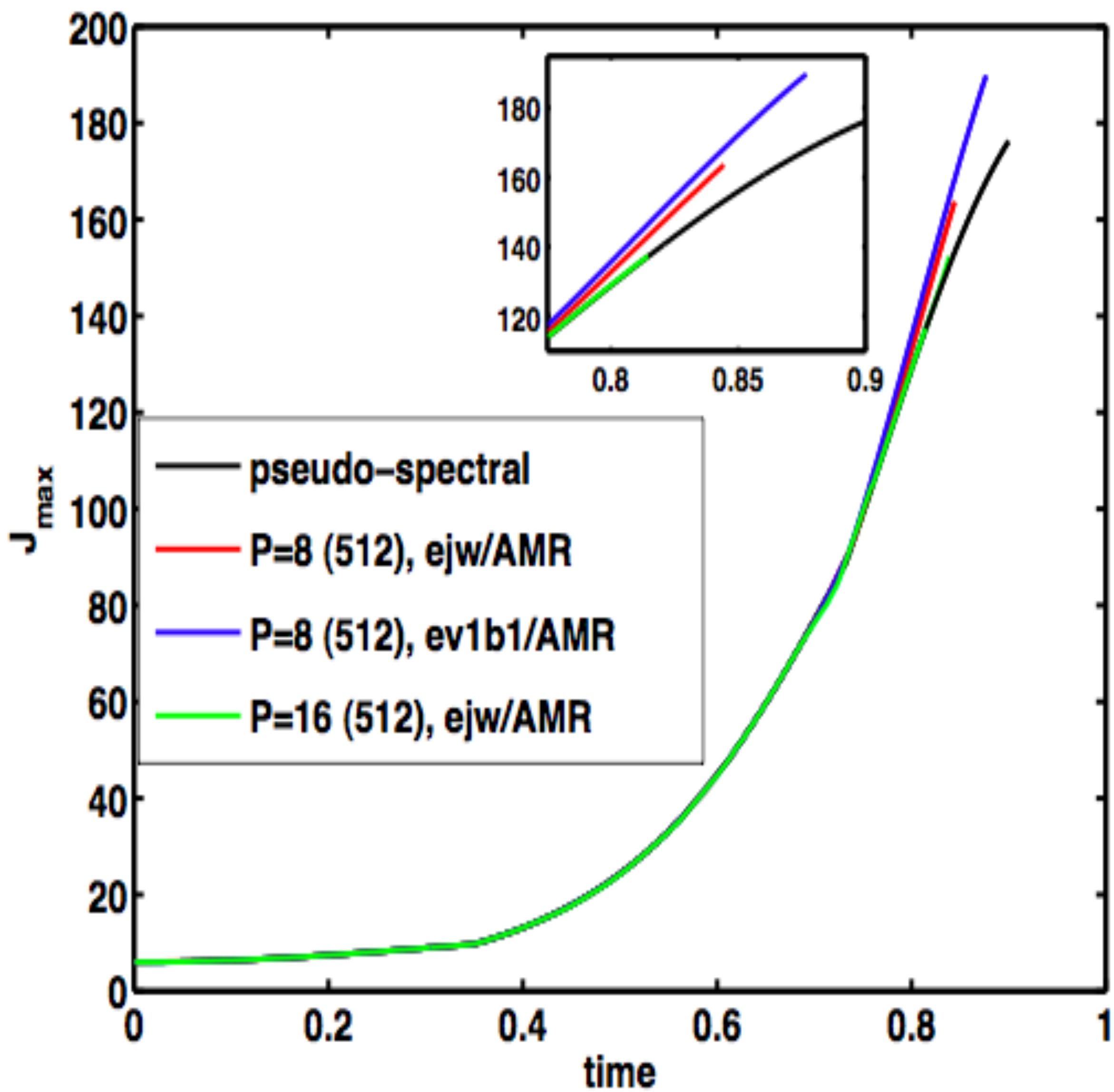

AMR in 2D - MHD turbulence

- Magnetic X-point configuration in 2D
- Temporal variation of:

  Dissipation

  J_{max}

  Degrees of freedom

normalized by the number of modes in a pseudo-spectral code at the same R_v,

~33%

Refinement and coarsening criteria …

Rosenberg et al., New J. Phys. 2007

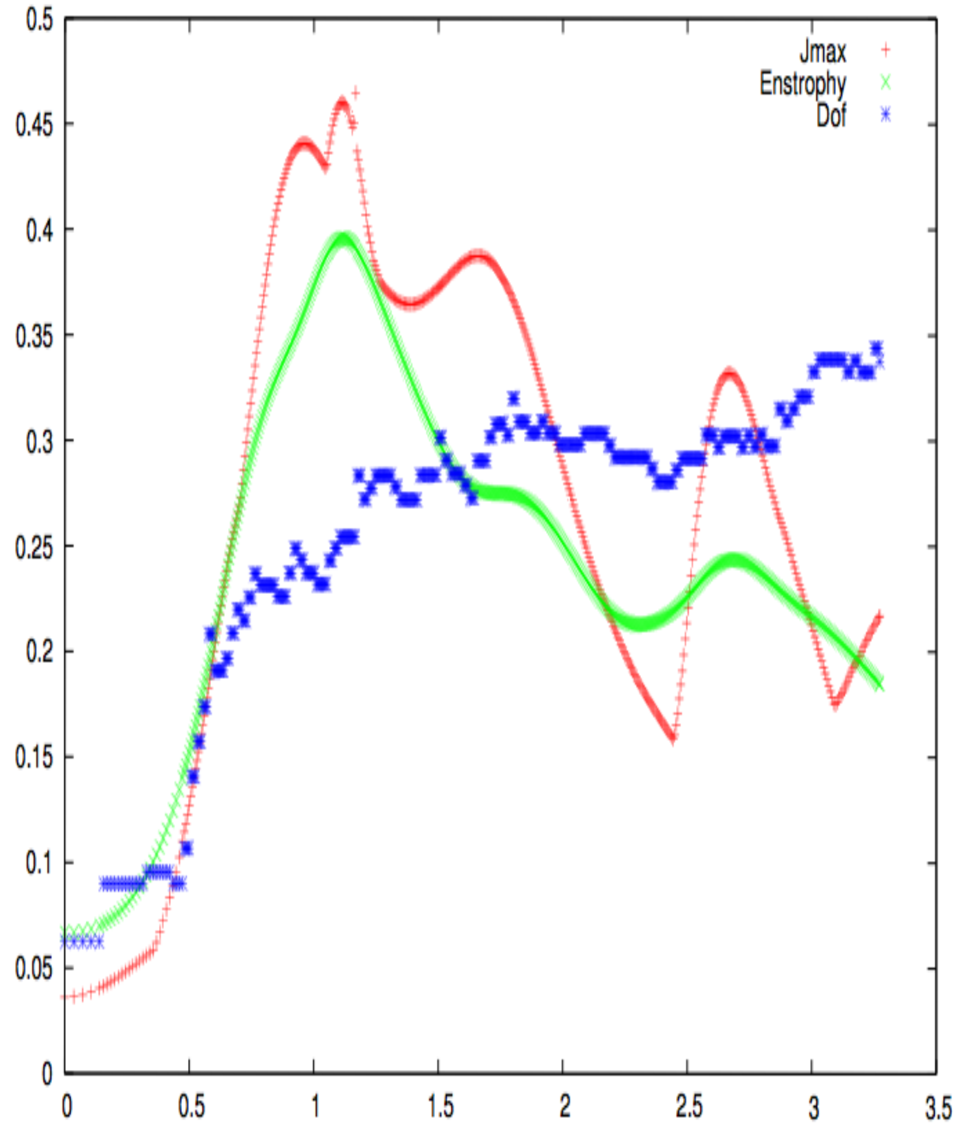

2D -MHD Orszag-Tang vortex with AMR

- **Error** in temporal derivative of total energy (compared to dissipation)

  is ~ 10^{-3}

  (computed every 10 time steps)

- Error in ∇.v is ~ 10^{-5} *(controlled by a code parameter)*

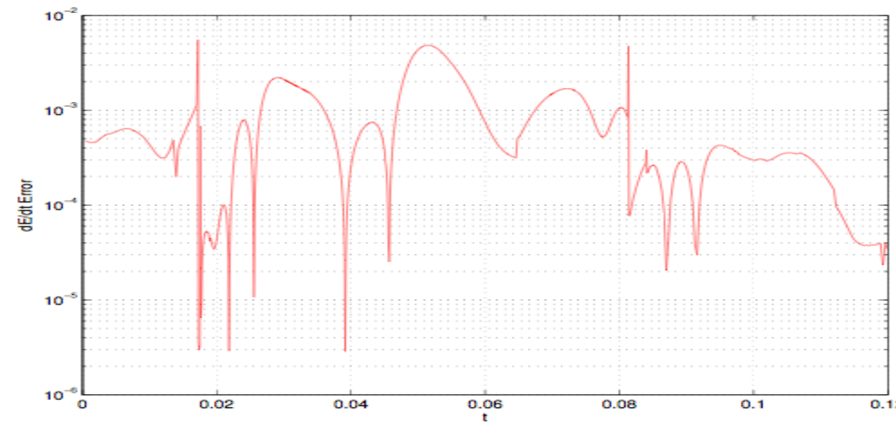

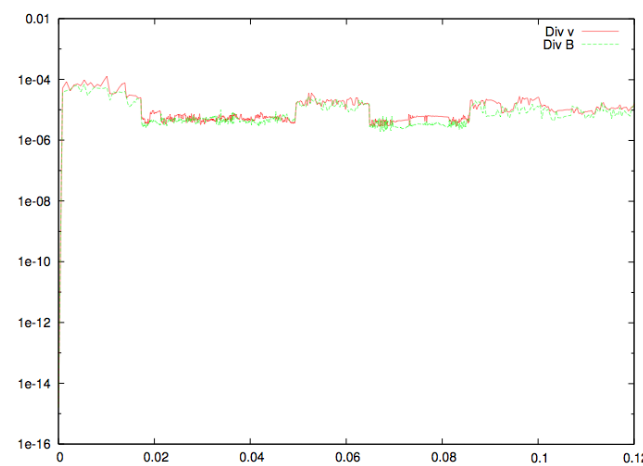

Rosenberg et al., New J. Phys. 2007

Examples of AMR

Parallel flux tubes in 3D, ideal run with effective resolution up to 4096^3

Grauer Marliani PRL 84 (2000)

Hairpin vortex, Euler case

Grauer et al. PRL 80 (1998)

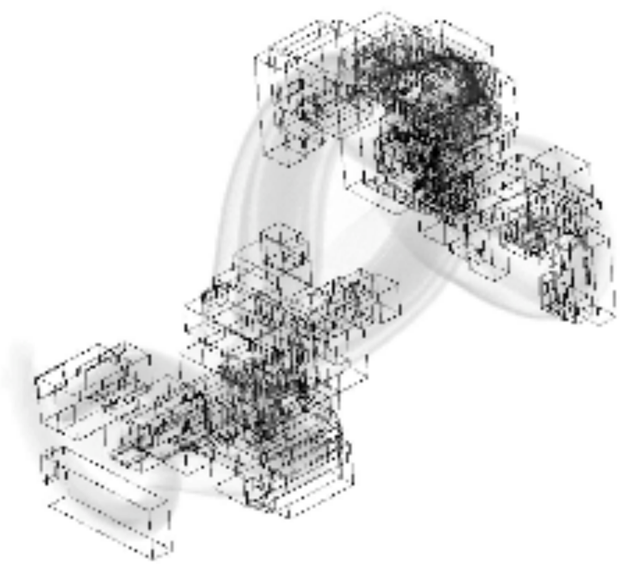

FIG. 4. Volume rendering of $|\omega|$ at time 1.32. Only level 3, 4, and 5 grids are shown.

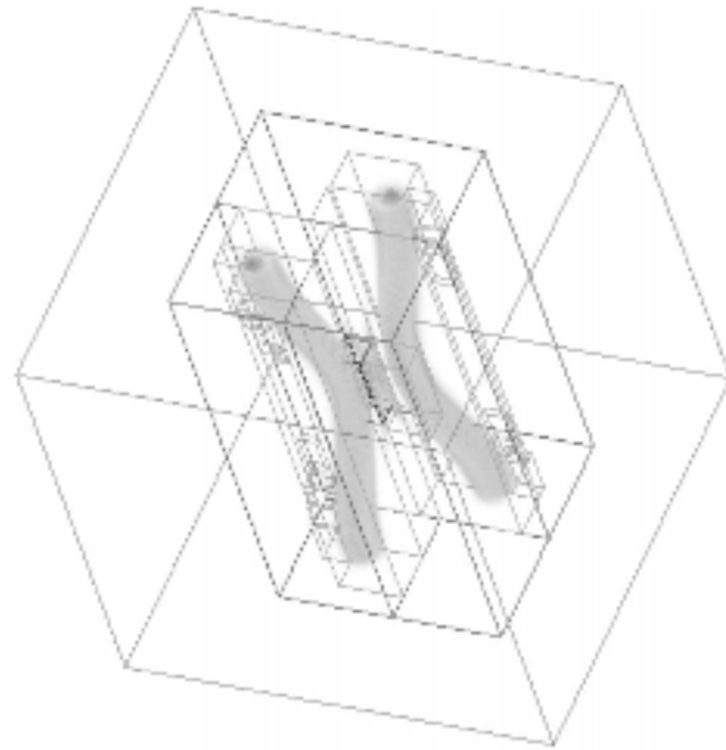

FIG. 4. Volume rendering of $|j|$ at time 0.42.

Thank you for your attention!